

# **Adenylyl cyclase membrane anchors: novel receptor function**

## **Dissertation**

der Mathematisch-Naturwissenschaftlichen Fakultät  
der Eberhard Karls Universität Tübingen  
zur Erlangung des Grades eines  
Doktors der Naturwissenschaften  
(Dr. rer. nat.)

vorgelegt von  
Sherif Elsabbagh  
aus Kairo, Ägypten

Tübingen  
2024

Gedruckt mit Genehmigung der Mathematisch-Naturwissenschaftlichen Fakultät der  
Eberhard Karls Universität Tübingen.

Tag der mündlichen Qualifikation:

05.07.2024

Dekan:

Prof. Dr. Thilo Stehle

1. Berichterstatter/-in:

Prof. Dr. Joachim Schultz

2. Berichterstatter/-in:

Prof. Dr. Peter Ruth

To my family...THANK YOU!

To my wife...I Love You!

## Acknowledgement

I am grateful to my advisor, Prof. Dr. Joachim Schultz whose guidance, support, and expertise have been invaluable throughout my doctoral journey. You provided not only academic mentorship but also encouragement and inspiration. I will always remember, “Be curious” and “Always ask questions”. Your dedication and commitment were truly inspiring to me.

I want to thank Prof. Dr. Andrei Lupas for his continuous support to our group and all provocative discussions and questions during group meetings.

I would like to thank Prof. Dr. Peter Ruth for being my second supervisor and for the fruitful discussions during TAC meetings.

I am thankful to Prof. Dr. Doron Rapaport for being a member of the TAC committee and all beneficial discussions and questions.

I am thankful to Prof. Dr. Harald Gross for his help and collaboration. You were a key contributor in my PhD journey. Thank you for the time you spare to discuss about all analytical stuff which taught me alot.

Ms. Anita Schultz, thank you for being there and your continuous help while doing experiments. Most importantly, thank you for all the tea times which witnessed our discussions and chats. I will always remember you coming to our office at 4:00 o'clock saying “I prepare tea”.

I want to thank Ms. Ursula Kurz for the hard work she did in the lab and her continuous support. I will not forget our tea times and your attempts to speak with me in English, and sometimes Arabic. You were very kind and nice to me.

I would like to thank my colleague Marius Landaus. I found it easy and comfortable working with you. You were really kind, helpful, understanding and most importantly, I had the chance to talk to you about football.

Special thanks to my former colleagues, Dr. Anubha Seth, Dr. Julia Grischin and Dr. Manuel Finkbeiner. You made my life easier during my first PhD days and helped me a lot.

To my brothers, Ahmed and Ramy, thank you for being there. Thank you for supporting my back.

To my wife Aliaa, I love you. For me, your presence affected me positively. Thank you for being here, supporting me and bearing up all the stress with me. Thank you for being my life partner. I wish that the upcoming days, with you, will be better and better.

To mom and dad, without you, I would not be here. This PhD is for you. You took care of me for my whole life and continued to support me under any circumstances. You always encouraged me to be better and to fight for my dream. I had hard times where I told you that I want to stop. But you kept telling me “Stand up and raise your head. You can do it”. You are the reasons why I am still here. I hope that now you are proud of me.

Finally, I want to thank ME. You have always dreamed of this moment. You fought for it and here you are, you did it. Be proud of yourself. Your journey was full of ups and downs, joy, and sadness but you managed to get through all this. I am sure that you learned a lot and it is time for you now to say goodbye to this period of your life and prepare for your next step. Congratulations!! You did a great job!

# Table of contents

Abbreviations .....	1
Summary .....	2
Zusammenfassung .....	3
List of publications .....	5
<b>1. INTRODUCTION</b> .....	<b>6</b>
<b>1.1 cAMP-dependant pathway</b> .....	<b>6</b>
<b>1.2 Adenylyl cyclases</b> .....	<b>7</b>
<b>1.3 Mammalian Adenylyl cyclases</b> .....	<b>8</b>
<b>1.4 TM domains are orphan receptors</b> .....	<b>10</b>
<b>2. OBJECTIVE</b> .....	<b>13</b>
<b>3. RESULTS AND DISCUSSION</b> .....	<b>14</b>
<b>3.1 Publication I: Distinct glycerophospholipids potentiate Gs<math>\alpha</math>-activated adenylyl cyclase activity</b> .....	<b>14</b>
<b>3.2 Publication II Heme b inhibits class III adenylyl cyclases</b> .....	<b>31</b>
<b>3.3 Manuscript: A new class of receptors: the membrane anchors of mammalian adenylyl cyclases</b> .....	<b>52</b>
<b>4. DISCUSSION and OUTLOOK</b> .....	<b>99</b>
<b>5. REFERENCES</b> .....	<b>102</b>

## Abbreviations

AC	Adenylyl cyclase
CAI-1	Cholera autoinducer-1
CTE	Cyclase transducing element
CqsS	Cholera quorum sensing receptor
DHEA	Dehydroepiandrosterone
FBS	Fetal bovine serum
FBS <sub>sexo</sub>	Exosome-depleted fetal bovine serum
FSK	Forskolin
GPL	Glycerophospholipid
HD	Helical domain
mAC	Membrane-bound adenylyl cyclase
SDPA	1-stearoyl-2-docosaheptaenoyl-phosphatidic acid
TM	Transmembrane

## SUMMARY

**Nine membrane bound** mammalian isoforms of adenylyl cyclase (mACs) convert ATP into cAMP, an important second messenger in signal transduction. Previous data have supported the notion that mACs membrane anchors could be regarded as orphan receptors for unknown ligands that could establish a new way of regulating the activity of mACs. Herein, I describe the work been done attempting to isolate and identify a ligand that can modulate the activity of mACs via binding to its membrane domain.

**In the first study**, lipids -expected as ligands- were isolated from fetal bovine serum at different pH values. Lipidomic analysis identified glycerophospholipids (GPL) as major constituents. Surprisingly, 1-stearoyl-2-docosahexaenoyl-phosphatidic acid (SDPA) enhanced  $G_s\alpha$  activation of mAC3. Examining the specificity of the fatty acyl substituents and head group of phosphatidic acid demonstrated a notable specificity. We also showed the GPLs' capability to affect other mACs differently, indicating a modest specificity. Further data suggested SDPA binding to a cytosolic site. SDPA enhanced mAC activity in mouse brain cortical membranes indicating its physiological importance. Collectively, this study identified GPLs as intracellular effectors of mACs, settling a new way of regulating mAC activities, and opening the door to looking for other paths of mACs regulation.

**In the second study**, extraction and fractionation of bovine lung tissue identified heme b that attenuated  $G_s\alpha$ -stimulated activities of all mAC isoforms. Likewise, heme b attenuated class III bacterial ACs with similar efficacy to mACs. In addition, it decreased cAMP accumulation in HEK293 cells and attenuated  $G_s\alpha$ -stimulated AC activities in brain cortical membranes. Data suggested its direct binding to the catalytic dimer. The study adds a new facet to the distinct physiological and toxic actions played by heme b and evokes the possible linkage between the second messenger cAMP and pathological conditions where heme b levels are elevated.

**In the last study**, we identified aliphatic lipids as mACs potential ligands. Initially, oleic acid enhanced mAC2, 3, 7, and 9 activities with distinct efficacies. In a cellular context, it enhanced cAMP accumulation in HEK293-mAC3. Exploring the ligand space for those mACs identified other stimulating fatty acids with remarkable specificity. Further analysis revealed the attenuation of mAC1 and 4 by arachidonic acid and mAC5 and 6 by anandamide. To prove the specific ligand interaction with mAC membrane domains, we generated an mAC5<sub>TM</sub>-mAC3<sub>cat</sub> chimera which was not affected by oleic acid and attenuated by anandamide. The study validates a novel receptor role for mAC membrane anchors and establishes a new way of cAMP regulation; an interplay between rapid solute and tonic lipid signaling.

## Zusammenfassung

**Neun membrangebundene** Isoformen der Säugetier-Adenylylcyclase (mAC) wandeln ATP in cAMP um, einen wichtigen sekundären Botenstoff der Signaltransduktion. Frühere Daten haben die Annahme gestützt, dass die Membrananker der mACs als Waisenrezeptoren für unbekannte Liganden betrachtet werden könnten, die einen neuen Weg zur Regulierung der Aktivität von mACs etablieren könnten. Hier beschreibe ich die Isolierung und Identifikation eines Liganden, der die Aktivität von mACs durch Bindung an deren Membrandomäne modulieren kann.

**In der ersten Studie** wurden Lipide, die als Liganden dienen sollten, aus fötalem Kälberserum bei verschiedenen pH-Werten extrahiert. Eine Lipidomanalyse identifizierte Glycerophospholipide (GPL) als Hauptbestandteile. Überraschenderweise verstärkte 1-Stearoyl-2-docosahexaenoylphosphatidsäure (SDPA) die  $G_{\alpha}$ -Aktivierung von mAC3. Die Untersuchung der Spezifität der Acylsubstituenten und der Kopfgruppe der GPLs zeigte eine bemerkenswerte Spezifität. Wir haben auch gezeigt, dass die GPLs andere mACs unterschiedlich beeinflussen, was auf eine weniger ausgeprägte Isoform-Spezifität hinweist. Weitere Daten deuten darauf hin, dass SDPA an eine zytosolische Domäne bindet. SDPA verstärkte die mAC-Aktivität in kortikalen Membranen des Gehirns von Mäusen, was ihr eine physiologische Bedeutung verleiht. Zusammenfassend identifizierte diese Studie GPLs als intrazelluläre Effektoren von mACs, etablierte eine neue Art der Regulierung der mAC-Aktivität und öffnete die Tür für die Suche nach anderen Möglichkeiten der mAC-Regulierung.

**In der zweiten Studie** wurde durch Extraktion und Fraktionierung von Rinderlungengewebe Häm b identifiziert, welches die  $G_{\alpha}$ -stimulierten Aktivitäten aller mAC-Isoformen abschwächte. Ebenso schwächte Häm b bakterielle ACs der Klasse III mit ähnlicher Wirksamkeit ab. Darüber hinaus verringerte es die cAMP-Akkumulation in HEK293-Zellen und schwächte  $G_{\alpha}$ -stimulierte AC-Aktivitäten in den kortikalen Membranen des Gehirns von Mäusen ab. Die Daten deuten auf eine direkte Bindung mit dem katalytischen Dimer hin. Die Studie fügt den unterschiedlichen physiologischen und toxischen Wirkungen von Häm B eine neue Facette hinzu und weist auf einen möglichen Zusammenhang zwischen dem sekundären Botenstoff cAMP und pathologischen Zuständen hin, bei denen der Häm b-Spiegel erhöht ist.

**In der letzten Studie** haben wir aliphatische Lipide als potenzielle Liganden der mACs identifiziert. Ölsäure steigerte die Aktivitäten von mAC2, 3, 7 und 9 mit unterschiedlicher Wirksamkeit. *In vivo* steigerte es die cAMP-Akkumulation in HEK293-mAC3. Bei der Untersuchung des Ligandenraums für diese mACs wurden

andere stimulierende Fettsäuren mit beachtlicher Spezifität identifiziert. Weitere Tests ergaben die Abschwächung von mAC1 und 4 durch Arachidonsäure und mAC5 und 6 durch Anandamid. Um die spezifische Ligandeninteraktion mit den mAC-Membrandomänen nachzuweisen, haben wir eine mAC5<sub>TM</sub>-mAC3<sub>cat</sub>-Chimäre konstruiert, die nicht durch Ölsäure beeinflusst aber durch Anandamid abgeschwächt wurde. Die Studie validiert eine neuartige Rezeptorrolle für den mAC-Membrananker und etabliert eine neue Art der cAMP-Regulation; ein Zusammenspiel zwischen der schnellen Signalübertragung durch lösliche Stoffe und der tonischen (lipid-gesteuerten) Signalübertragung.

## List of publications dealt within this thesis

### *Publications*

Seth, A., Landau, M., Shevchenko, A., Traikov, S., Schultz, A., **Elsabbagh, S.**, & Schultz, J. E. (2022). Distinct glycerophospholipids potentiate G $\alpha$ -activated adenylyl cyclase activity. *Cellular signalling*, 97, 110396. <https://doi.org/10.1016/j.cellsig.2022.110396>

**Elsabbagh, S.**, Landau, M., Gross, H., Schultz, A., & Schultz, J. E. (2023). Heme b inhibits class III adenylyl cyclases. *Cellular signalling*, 103, 110568. <https://doi.org/10.1016/j.cellsig.2022.110568>

### *Submitted manuscript*

Landau, M., **Elsabbagh, S.**, Gross, H., Fischer, A., Schultz, A., Schultz, J. E. (2024). A new class of receptors: the membrane anchors of mammalian adenylyl cyclases.

# 1. INTRODUCTION

## 1.1 cAMP-dependent pathway

The cAMP-dependent pathway is a GPCR driven signaling pathway used in cell communication. In this cascade, GPCRs are cell membrane receptors that detect extracellular molecules and translate them into intracellular responses. About 2% of human genome encode GPCRs, representing the largest receptor family. GPCR family members regulate a wide range of key physiological functions, including neurotransmission, blood pressure, cardiac activity, glucose and lipid metabolism, sensory perception, etc. (Pierce, Premont and Lefkowitz 2002, Heldin, Lu et al. 2016). A group of membrane associated proteins, termed G-proteins, interacts with an effector enzyme, adenylyl cyclase (AC), thus transducing the ligand-receptor interaction into an intracellular response (Taylor 1990). G-proteins bind both GDP and GTP. GDP is bound in the inactive state, and when activated, G-proteins exchange GTP for GDP. G-proteins are known to be heterotrimers composed of three subunits,  $\alpha$ ,  $\beta$ , and  $\gamma$  that are structurally distinct.  $\beta$ , and  $\gamma$  subunits are associated together, acting as one functional unit. The  $\alpha$  subunit has a GTPase activity to terminate AC activation (Syrovatkina, Alegre et al. 2016).

Earl Sutherland's discovery more than 60 years ago that hormone-induced glycogen breakdown in the liver is mediated by cAMP resulted in the formulation of the core idea of the intracellular second messenger (Sutherland and Rall 1958). cAMP signals are transmitted into action by various effector proteins mainly, but not exclusively protein kinase A (Walsh, Perkins and Krebs 1968), the exchange protein directly activated by cAMP (de Rooij, Rehmann et al. 2000), and cyclic nucleotide-gated ion channels (Fesenko, Kolesnikov and Lyubarsky 1985). Many biological processes, such as hormone secretion, glycogen breakdown (Hardman, Robison and Sutherland 1971), smooth muscle relaxation (Andersson and Nilsson 1972), cardiac contraction (Post, Hammond and Insel 1999, Okumura, Kawabe et al. 2003) are implicated in the functions of cAMP, according to biochemical and genetic data. In bacteria, cAMP activates catabolite activator protein, regulating metabolism (Gancedo 2013). Protein secretion, virulence and phototaxis are further cAMP dependant responses (Iseki, Matsunaga et al. 2002, McDonough and Rodriguez 2011).

## 1.2 Adenylyl Cyclases

Despite having a similar function, ACs don't descend from the same ancestor. Instead, they are split into six distinct classes, of which five classes (I, II, IV, V, VI) haven't been subjected to extensive research mostly as they are confined to a narrow range of prokaryotic species (Linder and Schultz 2003, Bassler, Schultz and Lupas 2018). Class II ACs stand out among them because pathogenic bacteria such as *Bordetella pertussis* and *Bacillus anthracis* release them as toxins that disrupt the levels of cAMP in their hosts (Rogel, Schultz et al. 1989, Barzu and Danchin 1994, Paccani, Finetti et al. 2011). Class III is the most numerous structurally, functionally diversified, and pharmacologically significant AC class and it is the only class that is present in animals. The conserved catalytic domain defines this family and shares similarities with the bacterial diguanylate cyclases' catalytic GGDEF domain (Pei and Grishin 2001). Class III ACs are further subdivided into four subclasses termed IIIa-III d based on sequence similarity between homologous catalytic subunits (Figure 1) (Linder and Schultz 2003).

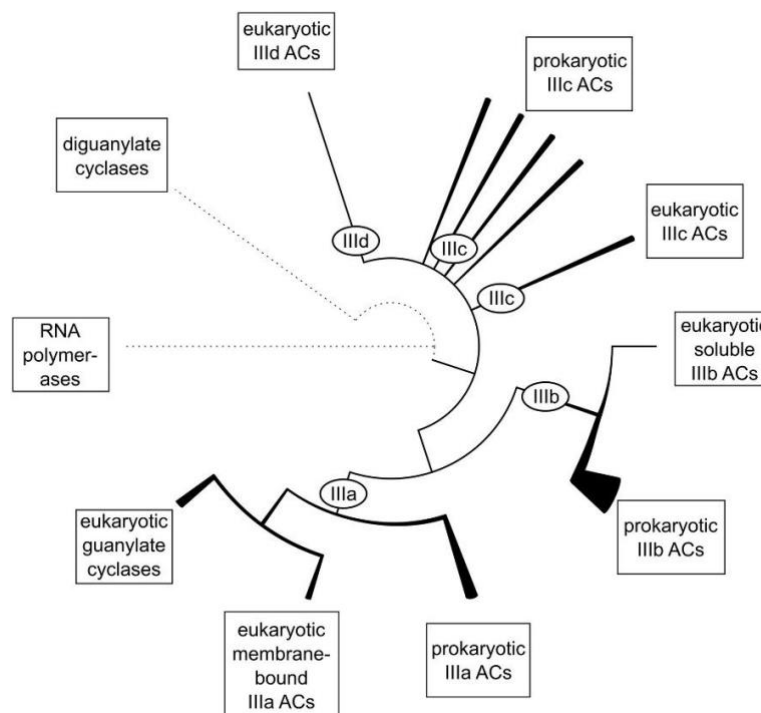


**Figure 1. Evolutionary relationships between class III ACs' catalytic domains.** Major subdivisions' relations are shown as solid lines. Line thickness depicts the divergence of domain architectures within a branch. Remote homology is indicated by dotted lines. (From (Bassler, Schultz and Lupas 2018)).

Dimerization is necessary for class III AC activity. At the subunit interface, two catalytic centers are formed by bacterial AC homodimers. In eukaryotic ACs, the so-called pseudo heterodimers are made up of two complementary catalytic units linked together to create a single catalytic centre at the interface. Biochemical and structural studies have clarified the catalytic mechanism (Tesmer and Sprang 1998). Three pairs of residues are crucial: A divalent metal cofactor,  $Mn^{2+}$  or  $Mg^{2+}$ , is coordinated by a pair of aspartate residues to allow a nucleophilic attack of the ribose 3'-hydroxyl group on the  $\alpha$ -phosphate of ATP. One arginine and one asparagine side chains stabilize the resultant transition state. The third pair of residues, aspartate and lysine are important for substrate specificity. Eukaryotic ACs have relatively little structural variation, and the domain architectures of these structures are usually preserved across major clades. For instance, two architectural types of ACs and three types of guanylate cyclases were found in all animal species. Some of these, like the mACs have experienced considerable lineage-specific expansion, resulting in several genetic copies of the same kind (mACs 1-9;). Later, it was shown that the membrane domains of mACs 1, 3, and 8, as well as isoforms 2, 4, and 7, and 5 and 6, have commonalities. mAC9's membrane anchor domains are unique compared to all others (Bassler, Schultz and Lupas 2018).

### **1.3 Mammalian Adenylyl Cyclases**

Mammalian ACs belong to class III, with nine membrane bound isoforms which participate in GPCR signaling pathway and one soluble AC (termed AC10) that is not directly linked to GPCR (Khannpnavar, Mehta et al. 2020). mACs share similar architecture (Figure 2), having two repeats of a membrane-spanning domain (TM domain), two linkers of about 80 residues containing a stretch of 19 amino acids that form a cyclase transducing element (CTE) (Ziegler, Bassler et al. 2017) , termed by others as helical domains (HD) ,that connect the TM domains to two conserved catalytic domains and a variable N-terminus in common (Sadana and Dessauer 2009). The two cytoplasmic domains (C1 and C2) both contain a region with around 230 amino acid residues that are similar, which causes pseudosymmetry (C1a and C2a). At their interface, they combine to create a catalytic dimer. The N and C-termini of C1 and C2 domains, known as C1b and C2b are the most variable among the various isoforms (Sadana and Dessauer 2009). A substrate-binding site and a corresponding

forskolin (FSK) site are created along the domain interface by the pseudosymmetry. Based on their regulatory characteristics, mACs are frequently classified into four main types. Group I is made up of  $\text{Ca}^{2+}$ -stimulated mAC1, 3, and 8, group II includes  $\text{G}\beta\gamma$ -stimulated mAC2, 4, and 7, group III involves  $\text{G}\alpha/\text{Ca}^{2+}$ -inhibited mAC5 and 6, and group IV is the FSK-insensitive mAC9 (Sadana and Dessauer 2009).

The topic of why different mAC isoforms are required and what functional tasks are regulated by each isoform emerged. The specificity shown in mAC function is mostly defined by tissue distribution. Most of the data for tissue distribution rely on PCR or Northern blotting due to the low abundance of mAC expression and the poor quality of the available antibodies. Nonetheless, it is evident that most cells express two or more mAC isoforms, and the brain expresses almost all of them (Sadana and Dessauer 2009). It has been shown that mACs play important roles in mammalian physiology. For example, mAC1 and 8 have been linked to learning and memory. mAC3 has been implicated in diabetes and obesity. mAC5 and 6 have been extensively studied in relation to cardiac function (Dessauer, Watts et al. 2017).

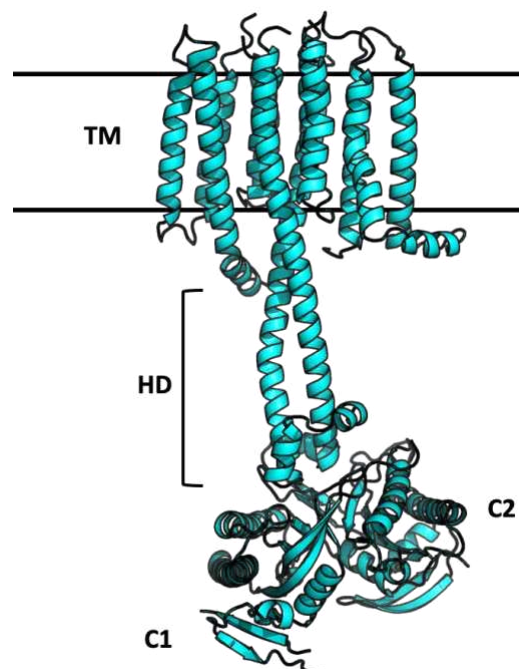


**Figure 2. Structure of bovine AC9** (Qi, Sorrentino et al. 2019) **depicting general ACs architecture.** TM; Transmembrane domain, HD; Helical domain, C1 and C2; Catalytic domains 1 and 2, respectively.

## 1.4 TM domains are orphan receptors.

Two related C1 and C2 domains and two different membrane anchors, TM1 and TM2, were found in the initial amino acid sequence of a mammalian AC (Krupinski, Coussen et al. 1989). TM domains were thought to have channel- or transporter-like capabilities; however, these claims were never proven (Krupinski, Coussen et al. 1989). The surprising finding that the independently expressed C1/C2 catalytic domains are regulated by  $G_s\alpha$  has been employed in the majority of biochemical experiments, i.e. the membrane anchoring appeared unnecessary for catalysis and regulation (Tang and Gilman 1995). Why then do we need 2x6 TM spans when just 1 or 2 would have been enough to bind into the membrane? Searching for a physiological role other than membrane-anchoring can be justified by the evolutionary conservation of the membrane domains for more than half a billion years (Beltz, Bassler and Schultz 2016, Ziegler, Bassler et al. 2017, Bassler, Schultz and Lupas 2018). In addition, the size of the TM domains exceeds 30% of the whole protein size which surpasses the demand for just membrane attachment. Notably, TM1 and TM2 are different and alignment between these domains failed owing to low conservation. Besides, lack of conservation among the membrane anchors of different mACs was observed regardless of their classification to similarly regulated groups (Seebacher, Linder and Schultz 2001). However, TM domains of an individual mAC isoform are highly conserved among different species (Schultz 2022). Random mutations within the membrane domains were shown to attenuate or even abrogate mAC activity (Levin and Reed 1995). All these deliberations would raise the question of whether the role of the mAC TM domains is only limited to the protein anchoring or not.

Previously, the hexahelical cholera quorum-sensing receptor CqsS from *Vibrio* was substituted for the mycobacterial Rv1625c 6TM domain to create the CqsS-Rv1625c chimera (Beltz, Bassler and Schultz 2016). Cholera auto inducer-1 (CAI-1), the CqsS ligand, enhanced the chimera activity. A family of CTEs that are essential for signal transduction were also characterized (Ziegler, Bassler et al. 2017). The fact that they are isoform-specifically conserved in mACs reinforced the idea that the mAC membrane domains might serve as ligand receptors. Further information provided a proof-of-concept experiment to show how a 2x6 anchor domain can control the activity of mAC2 catalytic dimer (Seth, Finkbeiner et al. 2020). Prospective ligands were expected to be present in the body extracellular fluid. Indeed, data showed that human

serum substantially and concentration-dependently attenuated the activity of mAC2 stimulated by  $G_s\alpha$ . Fetal bovine serum (FBS) had no effect on the basal and  $G_s\alpha$ -stimulated activities of CqsS-mAC2 chimera ruling out the possibility of serum having an impact on the catalytic domains or its activation by  $G_s\alpha$  and indicated that the observed effect was dependent on the presence of the mAC2 membrane anchor. Data demonstrated a new level of mAC regulation, through the TM domains, that is spatially distinct from the catalytic dimer. Moreover, regulatory input via the membrane domains readily suggested a possible explanation for their remarkable evolutionary conservation in an isoform-specific manner (Bassler, Schultz and Lupas 2018). The receptor function of mACs TM domains is further supported by the recently solved cryo-EM structures for mAC5, 8, 9, and the mycobacterial AC Rv1625c/Cya featuring an extracellular cavity at the TMs interface that differs in size and electrostatic potential among the aforementioned structures, suggesting possible interactions with potential ligands i.e. small molecules, ions, peptides, lipids (Figure 3) (Qi, Sorrentino et al. 2019, Mehta, Khanppnavar et al. 2022, Khanppnavar, Schuster et al. 2024, Yen, Li et al. 2024).

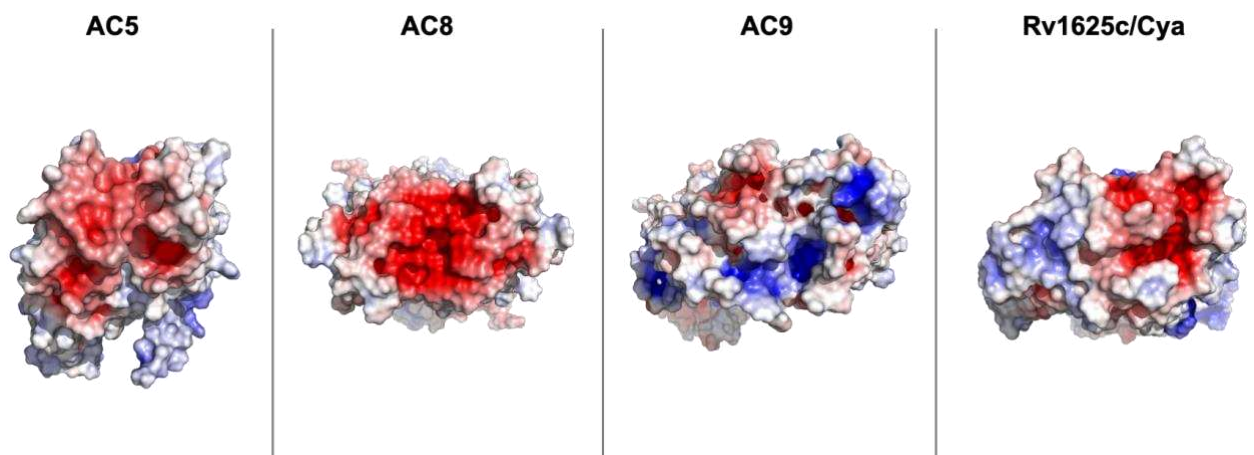


**Figure 3. Top view of TM domains of AC5, 8, 9, and Rv1625c/Cya revealing putative extracellular ligand binding sites.** Structures are shown in surface representation, coloured based on the electrostatic potential.

In 2020, a three-state model for mAC regulation was hypothesized (Seth, Finkbeiner et al. 2020). At equilibrium, there are three different ground states of mAC: state A (inactive), state B (inactive), and state C (active) (Figure 4). State A and state B differ in the conformational flexibility of the C1/C2 catalytic domains. In state A, the catalytic domains are structurally restricted and unable to form an active dimer. In state

B, the catalytic domains are structurally unconstrained but rarely collapse into active dimers (state C) due to their low affinity for each other. The 'C' state is responsible for the very low basal activity observed in all mACs. Restricting conformational flexibility by binding ligands outside the cell shifts the equilibrium to the inactive 'A' state, attenuating basal and Gs $\alpha$ -stimulated activities of mAC. The 'C' state is further stabilized by Gs $\alpha$  binding to cytosolic dimers, activating mAC. The proposed model offers the possibility that ligands may be binding at the membrane anchors. In this binding, membrane anchors act as receptors, relaying extracellular signals across the cell membrane to catalytic dimer. In this way, each mAC isoform is individually targeted by extracellular ligands and primed for physiologically measured GPCR/Gs $\alpha$  responses. Such a regulatory network would explain the mystery why multiple Gs $\alpha$ -stimulated mAC isoforms are often expressed in a single cell.

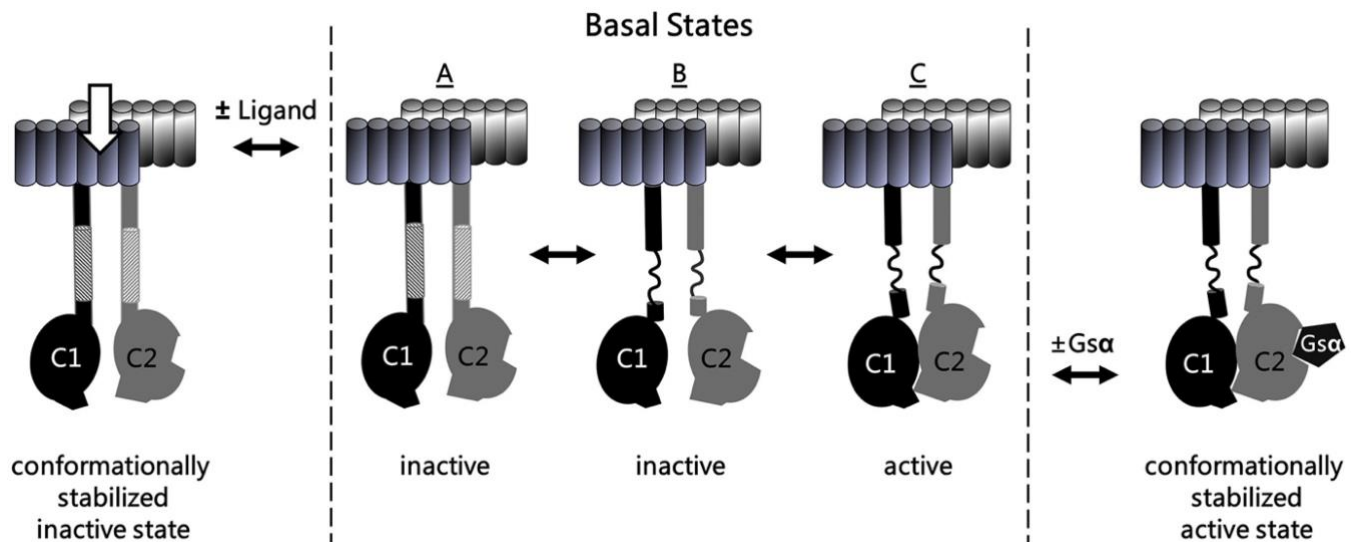


**Figure 4. Three-state model of mAC regulation.** (From (Seth, Finkbeiner et al. 2020)).

## 2. OBJECTIVE

The role played by the TM domain of membrane bound ACs apart from anchoring is not yet clear. Data generated by our group supported a hypothesis that they could be regarded as orphan receptors for unknown ligands.

In this context, searching for ligands that bind to mACs membrane anchors has become a major query that needs to be addressed. First, we need to determine a potential source of these ligands. Is the serum the only source? Then, the chemical nature of the ligands must be identified (protein, lipid). Studying how a certain ligand regulates various mAC isoforms and the degree of its specificity is important. Proving that an identified ligand exerts its action by interacting with the mAC membrane domains is of utmost importance. Additionally, probing for the effect of the prospective ligands *in vivo*, thereby indicating its physiological relevance is crucial.

To address these aspects, various analytical (Lipidomics, Chromatography, GC-MS, NMR) approaches have been utilized in conjunction with biochemical assays. This led to the identification of lipid compounds that were found to regulate mAC activity. This work establishes a new perspective towards direct mACs regulation along with the indirect regulation by GPCR.

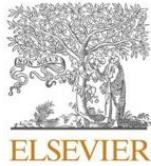
### 3. RESULTS AND DISCUSSION

#### 3.1 Publication I:

Seth, A., Landau, M., Shevchenko, A., Traikov, S., Schultz, A., **Elsabbagh, S.**, & Schultz, J. E. (2022). Distinct glycerophospholipids potentiate Gs $\alpha$ -activated adenylyl cyclase activity. *Cellular signalling*, 97,110396.  
<https://doi.org/10.1016/j.cellsig.2022.110396>

**Position in list of authors:** 6

**Author contributions:** I helped in experimental investigation, especially transfection, maintenance of HEK293 cells overexpressing mAC isoforms for prospective membrane and intact cell assays. I performed intact cell assay of SDPA against mAC3. I contributed to manuscript revising and editing (with all authors). I estimate my contribution by 15%.



## Distinct glycerophospholipids potentiate G $\alpha$ -activated adenylyl cyclase activity

Anubha Seth<sup>a,1,2</sup>, Marius Landau<sup>b,1</sup>, Andrej Shevchenko<sup>c</sup>, Sofia Traikov<sup>c</sup>, Anita Schultz<sup>b</sup>, Sherif Elsabbagh<sup>b</sup>, Joachim E. Schultz<sup>b,\*</sup>

<sup>a</sup> Max-Planck-Institut für Biologie, Tübingen, Germany

<sup>b</sup> Pharmazeutisches Institut der Universität Tübingen, Tübingen, Germany

<sup>c</sup> Max-Planck-Institut für molekulare Zellbiologie und Genetik, Dresden, Germany

### ARTICLE INFO

#### Keywords:

Adenylyl cyclase  
Membrane anchor  
Receptor  
Glycerophospholipids  
Phosphatidic acid  
Cyclic AMP

### ABSTRACT

Nine mammalian adenylyl cyclases (AC) are pseudoheterodimers with two hexahelical membrane domains, which are isoform-specifically conserved. Previously we proposed that these membrane domains are orphan receptors (<https://doi.org/10.7554/eLife.13098>; <https://doi.org/10.1016/j.cellsig.2020.109538>). Lipids extracted from fetal bovine serum at pH 1 inhibited several mAC activities. Guided by a lipidomic analysis we tested glycerophospholipids as potential ligands. Contrary to expectations we surprisingly discovered that 1-stearoyl-2-docosahexaenoyl-phosphatidic acid (SDPA) potentiated G $\alpha$ -activated activity of human AC isoform 3 seven-fold. The specificity of fatty acyl esters at glycerol positions 1 and 2 was rather stringent. 1-Stearoyl-2-docosahexaenoyl-phosphatidylserine and 1-stearoyl-2-docosahexaenoyl-phosphatidylethanolamine significantly potentiated several G $\alpha$ -activated mAC isoforms to different extents. SDPA appears not interact with forskolin activation of AC isoform 3. SDPA enhanced G $\alpha$ -activated AC activities in membranes from mouse brain cortex. The action of SDPA was reversible. Unexpectedly, SDPA did not affect cAMP generation in HEK293 cells stimulated by isoproterenol, PGE<sub>2</sub> and adenosine, virtually excluding a role as an extracellular ligand and, instead, suggesting an intracellular role. In summary, we discovered a new dimension of intracellular AC regulation by chemically defined glycerophospholipids.

### 1. Introduction

cAMP is a universal regulator of numerous cellular processes [7,32,36,38]. Its biosynthesis is via adenylyl cyclases. This report deals with the nine mammalian, membrane-bound pseudoheterodimeric ACs (mACs; reviewed in [2,7,24,32]). Currently, a direct regulation of mACs does not exist. The accepted regulation is indirect and includes (i) the extracellular activation of G-protein-coupled receptors, (ii) intracellular release of the G $\alpha$  subunit from a trimeric G-protein and, (iii), as a last step mAC activation by the free  $\alpha$ -subunit [7,30]. Secondly, calmodulin, Ca<sup>2+</sup> ions, G $\beta\gamma$  and phosphorylation are cytosolic effectors. In contrast, we recently have assigned a direct regulatory role mediated by the membrane domains of mACs acting as receptors [3,34]. In this proposal, the mAC receptors are comprised of the two hexahelical

domains each connected to a cytosolic catalytic domain, C1 and C2, via highly conserved cyclase transducing elements [7,34,46]. These transducing elements, also termed helical domains, are perfectly suited to mediate signal transduction between membrane anchors and the catalytic dimer as shown by the cryo-EM structure of AC9 holoenzyme [27]. The proposal for a receptor function is based on: (i) the evolutionary conservation of the membrane anchors in an isoform-specific manner for >0.5 billion years [2], (ii) on highly conserved cyclase-transducing-elements [46], and (iii) on catalytic domains conserved from cyanobacteria to mammals [2,16,18,34], (iv) on a most recent cryo-EM structure of the mycobacterial cyclase Cya at 3.6Å resolution in which a potential intramembrane binding pocket for lipophilic compounds was identified (Metha et al. 2022; <https://doi.org/10.1101/2021.12.01.470738>).

**Abbreviations:** mAC, membrane-delimited adenylyl cyclase; GPL, glycerophospholipid; SDPA, 1-stearoyl-2-docosahexaenoyl-phosphatidic acid.

\* Corresponding author at: Pharmazeutisches Institut der Universität Tübingen, Auf der Morgenstelle 8, 72076 Tübingen, Germany.

E-mail address: [joachim.schultz@uni-tuebingen.de](mailto:joachim.schultz@uni-tuebingen.de) (J.E. Schultz).

<sup>1</sup> Both contributed equally.

<sup>2</sup> Present address: Dept. of Pharmacology, Yale University School of Medicine, 333 Cedar Street, New Haven, CT 06520–8066, USA.

<https://doi.org/10.1016/j.cellsig.2022.110396>

Received 6 June 2022; Received in revised form 27 June 2022; Accepted 28 June 2022

Available online 2 July 2022

0898-6568/© 2022 The Author(s). Published by Elsevier Inc. This is an open access article under the CC BY-NC-ND license (<http://creativecommons.org/licenses/by-nc-nd/4.0/>).

Recently we reported ligand-mediated inhibition of a G $\alpha$ -activated mAC2 in a chimera in which the AC membrane domains were replaced by the hexahelical quorum-sensing receptor CqsS from *Vibrio* sp. that has a known lipophilic ligand, cholera-auto-inducer-1 [3,22,34]. In an initial approach to identify ligands for the mAC receptors we used fetal bovine serum (FBS) which had been shown to contain inhibitory components [34]. Eliminating peptides or proteins as possible ligands we fractionated lipids by extraction with chloroform/methanol at different pH values [4]. Expecting to isolate inhibitory components we report the most surprising discovery that 1-stearoyl-2-docosahexaenoyl-phosphatidic acid (SDPA) potentiated G $\alpha$ -activated mAC3 activity up to 7-fold. The actions of SDPA resemble, to a limited extent, those of the plant diterpene forskolin [7]. The data establish a new layer of direct mAC regulation and emphasize the importance of glycerophospholipids (GPLs) in regulation of intracellular cAMP generation.

## 2. Materials and methods

### 2.1. Reagents and materials

The genes of the human AC isoforms 1–9 cloned into the expression plasmid pcDNA3.1+/C-(K)-DYK were purchased from GenScript and contained a C-terminal flag-tag. Creatine kinase was purchased from Sigma, restriction enzymes from New England Biolabs or Roche Molecular. All chemicals were from Avanti Lipids and Sigma-Merck. \_ENREF\_24The constitutively active G $\alpha$ Q227L point mutant was expressed and purified as described earlier [8,10,11]. Forskolin was a gift from Hoechst, Frankfurt, Germany. Human serum (catalog # 4522 from human male AB plasma) and fetal bovine serum were from Gibco, Life Technologies, Darmstadt, Germany (catalog #: 10270; lot number: 42Q8269K).

### 2.2. Plasmid construction and protein expression

AC1C1-AC1C2 was generated in pQE60 with *NcoI/HindIII* restrictions sites according to Tang et al. [39]. The construct boundaries were: MRGSH<sub>6</sub>-HA-hAC1-C1<sub>M268-R482</sub>-AAAGGMPPAAAGGM -hAC2-C<sub>2R822-S1091</sub>. HEK293 cells were maintained in Dulbecco's modified Eagle's medium (DMEM) containing 10% fetal bovine serum at 37 °C with 5% CO<sub>2</sub>. Transfection of HEK293 cells with single mAC plasmids was with PolyJet (SignaGen, Frederick, MD, USA). Permanent cell lines were generated by selection for 7 days with G418 (600  $\mu$ g/mL) and maintained with 300  $\mu$ g/mL G418 [1,6,37]. Clonal selection was omitted. For membrane preparation cells were trypsinized and collected by centrifugation (3000  $\times$ g, 5 min). Cells were lysed and homogenized in 20 mM HEPES, pH 7.5, 1 mM EDTA, 2 mM MgCl<sub>2</sub>, 1 mM DTT, and one tablet of cComplete, EDTA-free (for 50 mL), 250 mM sucrose by 20 strokes in a potter homogenizer. Debris was removed by centrifugation for 5 min at 1000  $\times$ g, membranes were then collected by centrifugation at 100,000  $\times$ g for 60 min at 0 °C, resuspended and stored at –80 °C in 20 mM MOPS, pH 7.5, 0.5 mM EDTA, 2 mM MgCl<sub>2</sub>. Expression was checked by Western blotting.

Membrane preparation from mouse brain cortex was according to [33,34]. For each preparation three cerebral cortices were dissected and homogenized in 4.5 mL cold 48 mM Tris-HCl, pH 7.4, 12 mM MgCl<sub>2</sub>, and 0.1 mM EGTA with a Polytron hand disperser (Kinematica AG, Switzerland). The homogenate was centrifuged for 15 min at 12,000 g at 4 °C and the pellet was washed once with 5 mL 1 mM potassium bicarbonate. The final suspension in 2 mL 1 mM KHCO<sub>3</sub> was stored in aliquots at –80 °C.

### 2.3. Adenylyl cyclase assay

AC activities were determined in a volume of 10  $\mu$ l using 1 mM ATP, 2 mM MgCl<sub>2</sub>, 3 mM creatine phosphate, 60  $\mu$ g/mL creatine kinase, 50 mM MOPS, pH 7.5. Ca<sup>2+</sup>, usually present at low  $\mu$ M concentrations, was

**Table 1**

Lipid extraction of FBS with chloroform/methanol.

% G $\alpha$ activated Adenylyl Cyclase Activity	pH		
	14	6	1
hAC1	99 $\pm$ 5	91 $\pm$ 5	25 $\pm$ 1
hAC2	176 $\pm$ 8	158 $\pm$ 4	149 $\pm$ 9
hAC3	183 $\pm$ 40	175 $\pm$ 41	31 $\pm$ 11
hAC5	98 $\pm$ 7	123 $\pm$ 12	50 $\pm$ 7
hAC6	91 $\pm$ 4	89 $\pm$ 2	57 $\pm$ 4
hAC7	140 $\pm$ 6	131 $\pm$ 4	79 $\pm$ 6
hAC8	192 $\pm$ 11	193 $\pm$ 7	115 $\pm$ 4
hAC9	201 $\pm$ 22	251 $\pm$ 12	140 $\pm$ 12

2 mL FBS were extracted with chloroform/methanol (1:2) according to [4]. The organic phase was evaporated, and the residue was dissolved in 35  $\mu$ l DMSO. Adenylyl cyclases were activated by 600 nM G $\alpha$  and 33 nl of the DMSO extracts were added. Basal AC activities were in the order of the table: 0.11, 0.43, 0.02, 0.4, 0.16, 0.02, 0.33, and 0.04 nmol cAMP $\cdot$ mg<sup>-1</sup> $\cdot$ min<sup>-1</sup>, respectively. 600 nM G $\alpha$ -activated activities were 0.49, 1.31, 0.36, 2.23, 0.71, 0.25, 3.16 and 1.67 nmol cAMP $\cdot$ mg<sup>-1</sup> $\cdot$ min<sup>-1</sup>.  $n = 4$ –12.

not complexed by EGTA. The cAMP assay kit from Cisbio (Codolet, France) was used according to the supplier's instructions. For each assay a cAMP standard curve was established [34]. Lipids were dissolved in 100% ethanol or DMSO at high concentrations and acutely diluted in 20 mM MOPS pH 7.5 at concentrations, which limited organic solvent in the assay at maximally 1%. Up to 2% neither ethanol nor DMSO had any effect on AC activity.

### 2.4. Lipidomic analysis

Lipids were extracted from MonoQ purified aqueous fractions by methyl-*tert*-butyl ether/methanol as described [21] after adjusting their pH to 1.0 and 6.0, respectively. The collected extracts were dried under vacuum, and re-dissolved in 500  $\mu$ l of water/acetonitrile 1:1 (v/v). Lipids were analyzed by LC-MS/MS on a Xevo G2-S QTof (Waters) mass spectrometer interfaced to Agilent 1200 liquid chromatograph. Lipids were separated on a Cortecs C18 2.7  $\mu$ m beads; 2.1 mm ID  $\times$  100 mm (Waters) using a mobile phase gradient: solvent A: 50% aqueous acetonitrile; solvent B: 25% of acetonitrile in isopropanol; both A and B contained 0.1% formic acid (v/v) and 10 mM ammonium formate. The linear gradient was delivered with flow rate of 300  $\mu$ l/min in 0 min to 12 min from 20% to 100% B; from 12 min to 17 min maintained at 100% B, and from 17 min to 25 min at 20% B. Mass spectra were acquired within the range of  $m/z$  50 to  $m/z$  1200 at the mass resolution of 20,000 (FWHM). The chromatogram was searched against web-accessible XCMS compound database at [https://xcmsonline.scripps.edu/landing\\_page.php?pgcontent=mainPage](https://xcmsonline.scripps.edu/landing_page.php?pgcontent=mainPage). Lipids were quantified using Skyline 21.1.0.278 software using synthetic lipid standards [42] spiked into the analyzed fractions prior lipid extraction.

### 2.5. Data analysis and statistical analysis

All incubations were in duplicates or triplicates. For easier presentation, data were normalized to respective controls and S.E.M values are indicated. Data analysis was with GraphPad prism 8.1.2 using a two-tailed *t*-test.

## 3. Results

### 3.1. Lipids as possible mAC effectors

In exploratory experiments, we extracted lipids from FBS with chloroform/methanol at pH 1, pH 6, and pH 14 [4]. After evaporation of solvent the solid residues were dissolved in DMSO and tested against human mAC isoforms 1, 2, 3, 5, 6, 7, 8, and 9 in membrane preparations from HEK293 cells transfected with the respective ACs (Table 1). The

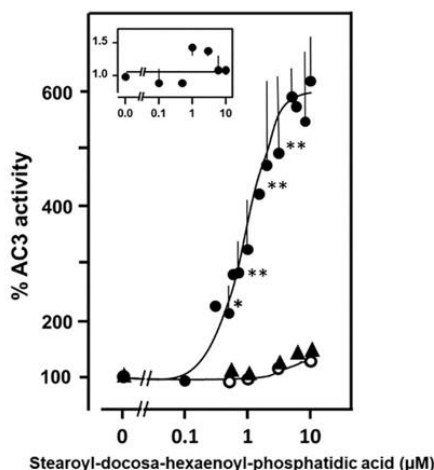


**Fig. 1.** 1-Stearoyl-2-docosahexaenoyl-phosphatidic acid concentration-dependently potentiates mAC3 activated by 600 nM  $G\alpha$  (filled circles). 100%  $G\alpha$ -activated mAC3 activity corresponded to  $707 \pm 187$  pmoles  $cAMP \cdot mg^{-1} \cdot min^{-1}$ . Basal mAC3 activity is not significantly affected by SDPA (open circles; 100% basal activity corresponds to 34 pmoles  $cAMP \cdot mg^{-1} \cdot min^{-1}$ ). Triangles: Effect of SDPA on the C1-C2 soluble AC construct activated by 600 nM  $G\alpha$  (Basal activity was 12 pmol  $cAMP \cdot mg^{-1} \cdot min^{-1}$ . 600 nM  $G\alpha$  activated activity was 150 pmol  $cAMP \cdot mg^{-1} \cdot min^{-1}$  corresponding to 100%). Insert: Activity of the mycobacterial AC Rv1625c is unaffected by SDPA (activity was 23 nmoles  $cAMP \cdot mg^{-1} \cdot min^{-1}$ ). Data were normalized to respective 100% activities. Significances in a two-tailed *t*-test: \*;  $p < 0.05$ ; \*\*;  $p < 0.01$  compared to 100% activity. For clarity, not all significances are marked.  $N = 4-6$ ; error bars denote S.E.M.'s.

pH 1 extract inhibited  $G\alpha$ -activated AC 1, 2, 5, 6, and 7 to different extents. The pH 6 and pH 14 extracts appeared to enhance  $G\alpha$ -activated AC isoforms 2, 3, 8, and 9 (Table 1).

We then carried out a lipidomic analysis with the pH 1 and the pH 6 fractions [21,42]. Based on previous data we expected ligands which inhibit  $G\alpha$ -activated mAC activities [34]. Therefore, we concentrated on lipids present in the pH 1 fraction. Apart from several. Based on previous data we expected potential ligands which inhibit  $G\alpha$ -activated mAC activities and concentrated on lipids present in the pH 1 fraction [34]. Apart from several minor constituents from different lipid classes the major constituents in the acidic fraction were phosphatidic acids, phosphatidylcholine, phosphatidylethanolamine and phosphatidylserines (see Appendix Fig. 1 and 2). Next, we examined the effect of commercially available bulk lipids on  $G\alpha$ -activated mACs. Egg phosphatidic acids significantly stimulated, whereas other bulk lipids such as egg and liver phosphatidylcholine, brain gangliosides, sulfatides and cerebrosides had no significant effects.

The lipidomic analysis showed that highly unsaturated fatty acids such as arachidonic acid and docosahexaenoic acid are prominent acyl substituents in phosphatidic acids (Appendix Fig. 2). These acyl residues are only minor components in the tested egg or liver phosphatidic acids. Therefore, we assayed commercially available synthetic GPLs containing polyunsaturated fatty acids as acyl substituents. The general structure of glycerophospholipids is shown below (see Appendix Table 1 for a complete list of lipids examined in this study).

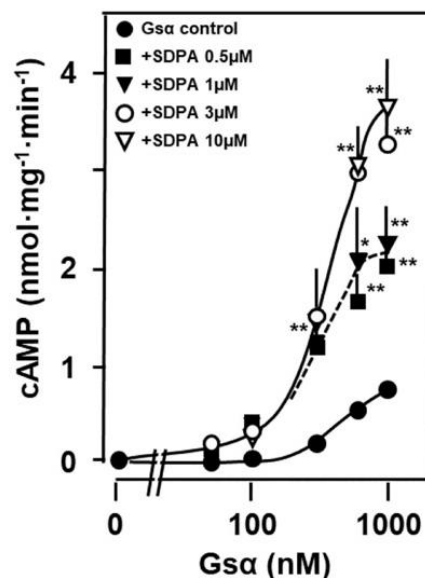
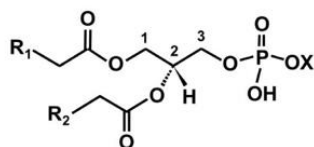


**Fig. 2.** SDPA increases the affinity of mAC3 for  $G\alpha$ . The  $EC_{50}$  concentration for  $G\alpha$  in the absence of SDPA was 518 nM and in the presence it was  $336 \pm 29$  nM ( $p < 0.02$ ;  $n = 5-6$ ). Basal AC3 activity was  $27 \pm 21$  pmoles  $cAMP \cdot mg^{-1} \cdot min^{-1}$ ; 1000 nM  $G\alpha$  increased mAC3 activity to  $791 \pm 128$  pmoles  $cAMP \cdot mg^{-1} \cdot min^{-1}$ . Significances: \*;  $p < 0.05$ ; \*\*;  $p < 0.01$  compared to corresponding activities without SDPA.  $n = 5-6$ ; error bars denote S.E.M. Often error bars did not exceed the symbol size.

Basic structure of glycerophospholipids:  $R_1$  and  $R_2$  are fatty acyl residues esterified at glycerol positions 1 and 2; X can be a proton  $H^+$  as in phosphatidic acid, choline (phosphatidylcholine), serine (phosphatidylserine), glycerol (phosphatidylglycerol), or ethanolamine (phosphatidylethanolamine).

The assays used membranes containing human mAC isoforms expressed in HEK293 cells. The mACs were activated by 600 nM of a constitutively active  $G\alpha$  (Q227L, here termed  $G\alpha$ ) because we expected to characterize an inhibitory input [11,34]. Most surprisingly, we discovered that 1-stearoyl-2-docosahexaenoyl-phosphatidic acid (SDPA) potentiated mAC3 up to 7-fold above the 16-fold activation already exerted by 600 nM  $G\alpha$  alone (Fig. 1). The  $EC_{50}$  of SDPA was 0.9  $\mu M$ . In the absence of  $G\alpha$  10  $\mu M$  SDPA had no significant effect (Fig. 1). As far as the synergism between  $G\alpha$ -activated mAC3 is concerned, the effect of SDPA was reminiscent of the known cooperativity between forskolin and  $G\alpha$  activated mACs [7].

Does the action of SDPA require a membrane-anchored AC holoenzyme or is the activity of a  $G\alpha$ -activated C1/C2 catalytic dimer potentiated as well? We produced a soluble active AC construct connecting the catalytic C1 domain of mAC1 and the C2 domain of mAC2 by a flexible linker [39] [39]. The construct was expressed in *E. coli* and purified via its His<sub>6</sub>-tag. It was activated 12-fold by  $G\alpha$  (from 12 to 150 pmol  $cAMP \cdot mg^{-1} \cdot min^{-1}$ ). SDPA up to 10  $\mu M$  did not affect basal activity and failed to significantly enhance  $G\alpha$ -activated activity of the chimera. We tentatively conclude that the SDPA action requires membrane anchoring of mACs.

We investigated whether SDPA affects the activity of a  $G\alpha$ -insensitive membrane-bound bacterial AC. We used the mycobacterial AC Rv1625c, a monomeric progenitor of mammalian mACs, which has a hexahelical membrane domain and is active as a dimer [12] [12]. The activity of the Rv1625c holoenzyme was unaffected by SDPA (Fig. 1 insert). The particular intrinsic properties of the mammalian membrane domains in conjunction with  $G\alpha$ -activation may be required to confer SDPA sensitivity.

Next, we examined which kinetic parameters are affected by SDPA.

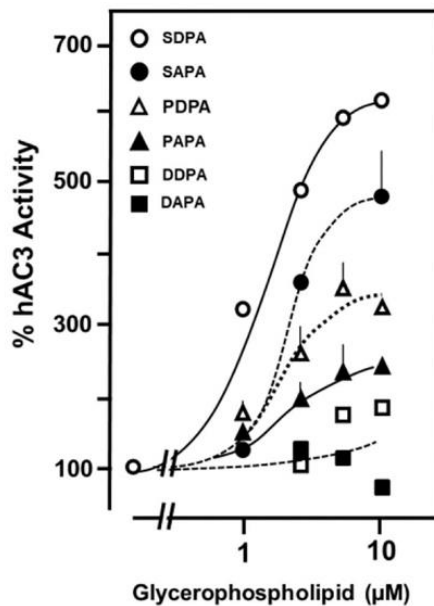


**Fig. 3.** Specificity of fatty acyl esters in phosphatidic acids for potentiation of  $G\alpha$ -activated mAC3. 600 nM  $G\alpha$ -activated activity (100%) was 446 pmol  $cAMP \cdot mg^{-1} \cdot min^{-1}$  (basal mAC3 activity was 15.2 pmol  $cAMP \cdot mg^{-1} \cdot min^{-1}$ ). Abbreviations: SAPA, 1-stearoyl-2-arachidonoyl-phosphatidic acid; PDPA, 1-palmitoyl-2-docosahexaenoyl-phosphatidic acid; PAPA, 1-palmitoyl-2-arachidonoyl-phosphatidic acid; DDPA, di-docosahexaenoyl-phosphatidic acid; DAPA, di-arachidonoyl-phosphatidic acid. The  $EC_{50}$  concentrations were 4.8, 1.3, and 1.4  $\mu M$ , for SAPA, PDPA, and DDPA, respectively (differences not significant;  $n = 3$ ). Error bars denote S.E.M. For comparison, a curve presenting SDPA is included.

For mAC3, the enzymatic reaction rates  $\pm$  SDPA were linear with respect to protein concentration and time up to 30 min. The  $K_m$  for substrate ATP (0.1 mM) was unaffected. The most striking effect of SDPA was the increase in  $V_{max}$  (from 4 to 8 nmol  $cAMP \cdot mg^{-1} \cdot min^{-1}$ ). Concentration-response curves for  $G\alpha$  in the presence of different SDPA concentrations showed that the affinity of mAC3 for  $G\alpha$  was significantly increased (Fig. 2). Most likely,  $G\alpha$  and SDPA act at distinct sites of the protein and potentiation by SDPA is due to concerted structural interactions, reminiscent of the cooperativity between  $G\alpha$  and forskolin [7].

### 3.2. Specificity of 1- and 2-acyl substituents in phosphatidic acid

Phosphatidic acid is the simplest GPL consisting of a glycerol backbone to which two fatty acids and phosphoric acid are esterified. At physiological pH it carries about 1.5 negative charges. Generally, at positions 1 and 2 of glycerol a variety of fatty acyl residues have been identified. We examined the biochemical specificity of the fatty acyl substituents in phosphatidic acid (Fig. 3).

10  $\mu M$  1-Stearoyl-2-arachidonoyl-phosphatidic acid (SAPA) potentiated  $G\alpha$ -activated mAC3 about 5-fold ( $EC_{50} = 4.8 \mu M$ ; Fig. 3). Exchanging the stearic acid at position 1 by a palmitic acid, i.e. 1-palmitoyl-2-docosahexaenoyl-phosphatidic acid (PDPA) reduced activity by about 50% compared to SDPA ( $EC_{50} = 1.3 \mu M$ ). Strikingly, the corresponding 1-palmitoyl-2-arachidonoyl-phosphatidic acid (PAPA) lost about 70% of activity compared to SDPA (Fig. 3), highlighting the structural contribution of the 1-fatty acyl substituent to biochemical activity. The importance of the substituent at position 1 was further emphasized when assaying 1, 2-di-docosahexaenoyl-phosphatidic acid (DDPA). The efficiency was reduced by 80% compared to SDPA (Fig. 3). The  $EC_{50}$  for DDPA was 1.4  $\mu M$ . Even more drastic was the absence of an

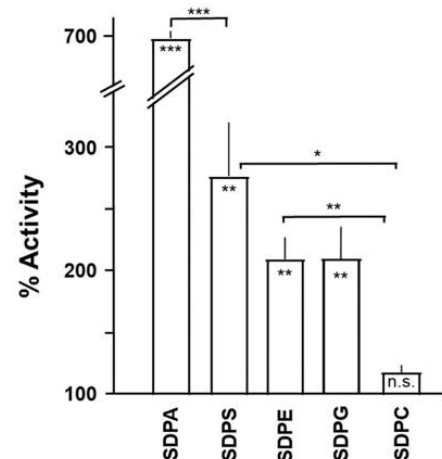


**Fig. 4.** Head group specificity of glycerophospholipids enhancing  $G\alpha$ -activated mAC3 activity. Basal mAC3 activity was 0.03.  $G\alpha$ -stimulated activity was 0.56 nmol  $cAMP \cdot mg^{-1} \cdot min^{-1}$  (corresponding to 100%). Concentration of lipids was 10  $\mu M$ . Error bars denote S.E.M. Significances: \*:  $p < 0.05$ ; \*\*:  $p < 0.01$ ; \*\*\*:  $p < 0.001$ ;  $n = 3-9$ .

effect using 1, 2-di-arachidonoyl-phosphatidic acid (DAPA; Fig. 3). Expectedly then, 1-stearoyl-2-linoleoyl-phosphatidic acid was inactive (not shown). The data show a remarkable positional specificity for the 1- and 2-acyl substituents of the glycerol backbone and indicate a specific and concerted interaction between the fatty acyl esters. The specificity of fatty acyl-substitution also strongly indicated that SDPA is not acting in its property as a general membrane GPL because other phosphatidic acids should be equally suitable as membrane lipids. Further, the peculiar biochemical properties of SDPA in its relation with AC isoforms suggest that the negative charges of phosphatidic acid are not sufficient to determine specificity, but that the lipid substitutions on position 1- as well as 2- probably are equally important.

### 3.3. Head group specificity of glycerophospholipids

The next question is whether 1-stearoyl-2-docosahexaenoyl-GPLs with different head groups might affect  $G\alpha$ -activated mAC3. First, we replaced the phosphate head group in SDPA by phosphoserine generating SDPS. This greatly reduced potentiation of  $G\alpha$ -activated mAC3 activity (2.8-fold potentiation; Fig. 4). A concentration-response curve of SDPS with mAC3 showed that the  $EC_{50}$  concentration was similar to that of SDPA (1.2 vs 0.9  $\mu M$ ;  $n = 6-9$ ; n.s.), but its efficacy is significantly lower suggesting that identical binding sites are involved.

We further used 1-stearoyl-2-docosahexaenoyl-ethanolamine (SDPE), 1-stearoyl-2-docosahexaenoyl-phosphatidylglycerol (SDPG) and 1-stearoyl-2-docosahexaenoyl-phosphatidylcholine (SDPC; Fig. 4). In this order, efficacy to enhance the  $G\alpha$ -activated mAC3 declined, with SDPC having no significant effect (Fig. 4). The surprising specificity of the 1- and 2-fatty acyl-substituents of the glycerol backbone was emphasized once again when we used 1-stearoyl-2-arachidonoyl-phosphatidyl-ethanolamine (SAPE) and 1-stearoyl-2-arachidonoyl-phosphatidylcholine. In both instances biochemical activity was lost (not shown). Consequently, we did not further probe GPLs with differing fatty acyl combinations at the glycerol 1- and 2-positions because, as demonstrated, changes in acyl substitutions resulted in considerable reduction or loss of biological activity (see Fig. 3).

### 3.4. Effect of glycerophospholipids on $G\alpha$ -activated adenylyl cyclase isoforms

So far, we examined only the mAC3 isoform that showed a

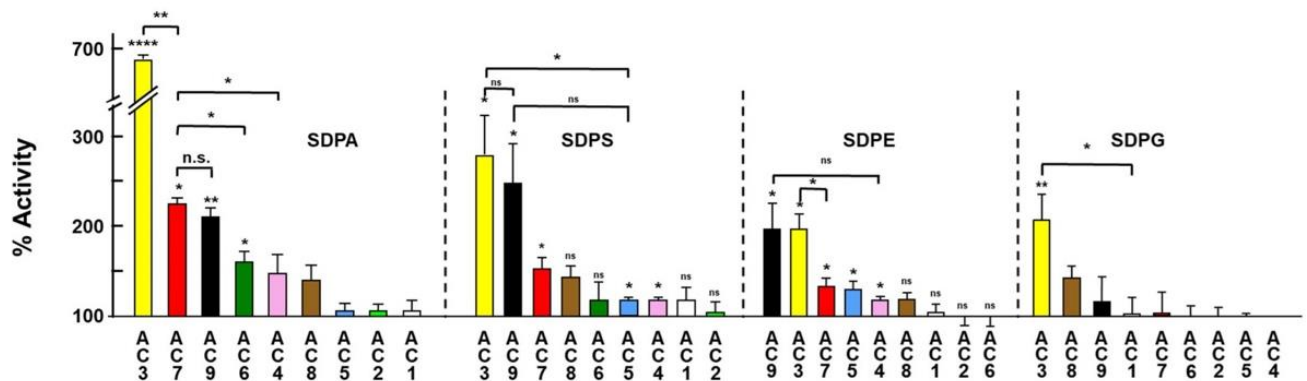


Fig. 5. Effect of 10  $\mu\text{M}$  of glycerophospholipids on various mAC isoforms activated by 600 nM  $\text{G}\alpha$ . Basal activities and  $\text{G}\alpha$ -activated activities are listed in Appendix Table 2). Error bars denote S.E.M. Significances: \*:  $p < 0.05$ ; \*\*:  $p < 0.01$ ; \*\*\*:  $p < 0.001$ ; \*\*\*\*:  $p < 0.0001$  compared to  $\text{G}\alpha$ -activated activity (set at 100%).  $n = 3-9$ .

particularly high synergism between  $\text{G}\alpha$  and SDPA. Does SDPA equally potentiate the  $\text{G}\alpha$ -activated activities of the other mAC isoforms? More generally, do GPLs display an mAC isoform specificity in the regulation of intracellular cAMP biosynthesis? We expressed the nine human mAC isoforms in HEK293 and, first, tested how SDPA affected the  $\text{G}\alpha$ -activated activities (Fig. 5).

Under identical experimental conditions 10  $\mu\text{M}$  SDPA significantly potentiated mAC7 (2.4-fold), mAC9 (2.1-fold) and mAC6 activities (1.5-fold). Concentration-response curves were carried for mACs 1, 2, 6, 7 and 9 (Appendix Fig. 3). The  $\text{EC}_{50}$  concentrations of SDPA for mAC6, 7 and 9 were 0.7  $\mu\text{M}$ , i.e. not significantly different from suggesting equal binding affinities. The other  $\text{G}\alpha$ -activated mAC isoforms were not significantly affected (Fig. 5 and Appendix Fig. 3). In summary, the data demonstrated that the mAC isoform specificity of SDPA was not absolutely stringent. The data then pose the question whether other GPLs may exert similar effects on mAC activities or display a different panel of isoform specificity. This was investigated using four more stearoyl-2-docosahexaenoyl-GPLs (Fig. 5). 10  $\mu\text{M}$  SDPS potentiated mAC3 and mAC9. Smaller, yet significant effects were measured with mACs 7, 8, 5, and 6 (Fig. 5). 10  $\mu\text{M}$  SDPE significantly potentiated  $\text{G}\alpha$ -activated mAC isoforms 9, 3, 7, 5, and 4 (in this order). 10  $\mu\text{M}$  SDPG significantly enhanced only mAC3 activity (Fig. 5). Compared to the seven-fold effect of SDPA on mAC3 these effects were small, yet, in mammalian biology such enhancements in mAC activity may well have profound physiological consequences. Up to 20  $\mu\text{M}$  SDPC which is a major constituent of the outer leaflet of membranes had no effect on any mAC isoform (not shown). Taken together, the data then demonstrate the capacity of chemically defined GPLs to enhance or potentiate the activation of  $\text{G}\alpha$ -activated mACs. We can virtually exclude coincidental and unspecific effects of the amphiphilic phospholipids because mAC isoforms were affected differentially. The results strongly suggest that a defined conformational space must exist at mACs that allows specific interactions with GPLs. Presently, the molecular details of the binding mode remain unknown.

### 3.5. Relationship between SDPA and forskolin

SDPA failed to activate basal mAC3 activity and only potentiates  $\text{G}\alpha$ -activated mAC3 activity (Fig. 1). The plant diterpene forskolin stimulates basal as well as  $\text{G}\alpha$ -activated mAC activities [7,41,44], i.e. the effects of SDPA and forskolin are only partly similar. Forskolin stimulates mACs expressed in Sf9 cells to rather different extents and with discrepant potencies, e.g. the  $\text{EC}_{50}$  concentrations for AC1 (0.7  $\mu\text{M}$ ) and AC2 (8.7  $\mu\text{M}$ ) differ >12-fold [25]. We established forskolin concentration-response curves for all mAC isoforms expressed in HEK293 cells under identical experimental conditions using  $\text{Mg}^{2+}$  as divalent cation, a comprehensive study which is lacking so far

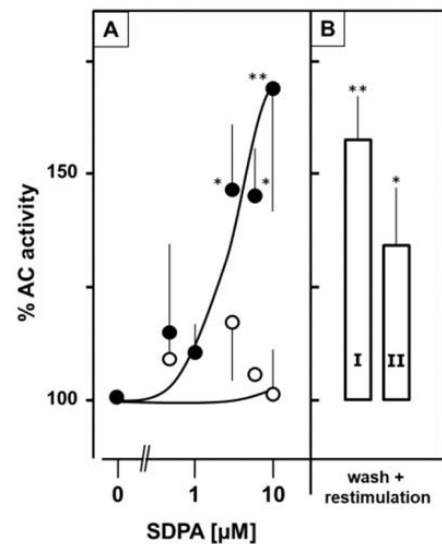


Fig. 6. 1-Stearoyl-2-docosahexaenoyl-phosphatidic acid (SDPA) concentration-dependently potentiates  $\text{G}\alpha$  activated adenylyl cyclase activity in brain cortical membranes from mouse. (A) 600 nM  $\text{G}\alpha$  was used to activate mACs in cortical membranes (solid circles: 100%  $\text{G}\alpha$ -activated activity is  $7.9 \pm 1.9 \text{ nmol cAMP}\cdot\text{mg}^{-1}\cdot\text{min}^{-1}$ ; open circles: basal activity (in absence of  $\text{G}\alpha$ ) is  $0.3 \pm 0.2 \text{ nmol cAMP}\cdot\text{mg}^{-1}\cdot\text{min}^{-1}$ .  $n = 6$ ). (B) Reversibility of SDPA action. Cortical brain membranes were incubated for 15 min without (I) and with (II) 10  $\mu\text{M}$  SDPA. Membranes were then collected by centrifugation, and re-assayed +600 nM  $\text{G}\alpha$  and 10  $\mu\text{M}$  SDPA. Error bars denote S.E.M., \*:  $p < 0.05$ ; \*\*:  $p < 0.01$  ( $n = 6$ ).

(Appendix Fig. 4).

Stimulations at 1 mM forskolin were between 3-fold for mAC1 and remarkable 42-fold for mAC3. The  $\text{EC}_{50}$  concentrations ranged from 2  $\mu\text{M}$  (mAC1) to 512  $\mu\text{M}$  forskolin (mAC7; Appendix Fig. 4). We also observed forskolin activation of mAC9 although the current consensus regarding this isoform is that it is forskolin insensitive. The latter conclusion is based on experiments with mAC9 expressed in insect Sf9 cells using  $\text{Mn}^{2+}$  as a cation [7]. Another report described a 2.3-fold forskolin activation of mAC9 when expressed in CMT cells [26], in line with our data (6-fold activation; appendix Fig. 4). We examined potential interactions between forskolin and SDPA using mAC3 activated by 600 nM  $\text{G}\alpha$ . Up to 10  $\mu\text{M}$ , SDPA did not significantly affect forskolin stimulation. We reason that the absence of interactions or cooperativity between forskolin and SDPA suggests that both agents affect mAC regions which exclude mutual cooperative interactions.

Nevertheless, considering the structural dissimilarity of forskolin and SDPA and the obvious lack of a molecular fit an identical binding site for both lipophilic agents is rather unlikely. On the other hand, both agents do interact with distantly binding  $G_{\alpha}$  in a cooperative manner.

### 3.6. SDPA enhances $G_{\alpha}$ -stimulated cAMP formation in mouse brain cortical membranes

Above we tested GPLs with individual mAC isoforms. Next, we asked whether SDPA would potentiate mAC activity in membranes isolated from mouse brain. In mouse brain cortex all mAC isoforms except for mAC4 are expressed [20,31]. We expected to measure at least some potentiation of the  $G_{\alpha}$ -activated AC activity by SDPA. The basal AC activity in cortical membranes of  $0.3 \text{ nmoles cAMP}\cdot\text{mg}^{-1}\cdot\text{min}^{-1}$  was unaffected by  $10 \mu\text{M}$  SDPA (Fig. 6A).  $600 \text{ nM}$   $G_{\alpha}$  stimulated AC activity 20-fold ( $7.9 \text{ nmoles cAMP}\cdot\text{mg}^{-1}\cdot\text{min}^{-1}$ ) and this was further enhanced 1.7-fold by  $10 \mu\text{M}$  SDPA ( $13.4 \text{ nmoles cAMP}\cdot\text{mg}^{-1}\cdot\text{min}^{-1}$ ). An SDPA concentration-response curve yielded an  $EC_{50}$  of  $1.2 \mu\text{M}$ , i.e. similar to those established in HEK293-expressed mAC isoforms (Fig. 6A; compare to Fig. 1 and Appendix Fig. 3). This demonstrated that the SDPA effect on mAC activities was not due to peculiar membrane properties of the HEK293 cells and supported the suggestion that the effects of GPLs may be of physiologically important.

Next, we asked whether SDPA acts directly via a membrane-receptor domain of hAC3 or is a cytosolic effector. We used HEK293 cells transfected with hAC3.  $2.5 \mu\text{M}$  isoproterenol increased cAMP levels from  $0.06$  to  $0.24 \text{ pmol}/10^4$  cells within 45 min (6-fold).  $10 \mu\text{M}$  SDPA did not affect isoproterenol stimulation. Addition of SDPA did not enhance intracellular cAMP generation (see Appendix Table 3). These unequivocal data virtually excluded that SDPA acted via extracellular binding sites (receptors) or via an efficient and rapid uptake system. In fact, although SDPA is a GPL, it is unlikely that it can pass into intact cells. First, the negatively charged headgroup of SDPA is dissociated at the pH of incubations. Second, SDPA might slide into the outer leaflet of the membrane, but it would require a flippase for incorporation into the inner leaflet and potential release into the cytosol. Considering the negative surface charge of the inner leaflet due to the predominance of phosphatidylserine we consider this as unlikely. Third, we did not observe significant incorporation of SDPA into brain cortical membranes (see below). Thus, the data tentatively suggest a cytosolic site for the action of GPLs.

### 3.7. Is SDPA a ligand?

GPLs are common building blocks of cell membranes. Major constituents of the inner leaflet are phosphatidylserines and phosphatidylethanolamines, whereas the outer leaflet contains predominantly phosphatidylcholine and sphingomyelin. In many tissues docosahexaenoic acid is a major substituent in membrane GPLs [14]. Phosphatidic acids are indispensable, yet minor membrane components [17]. The SDPA potentiation of  $G_{\alpha}$ -activated mAC3 could be due to a lack of SDPA. Added SDPA might be incorporated into the membrane close to mACs resulting in a reordering of mAC domains. Alternatively, SDPA may transiently bind to the cyclase. Under these latter circumstances the SDPA effect should be reversible. We attempted to dissect these possibilities. We incubated brain cortical membranes for 15 min at  $37^{\circ}\text{C}$  with  $10 \mu\text{M}$  SDPA. The membranes were then collected at  $100,000 \text{ g}$  and washed once. The membranes were susceptible to  $G_{\alpha}$  stimulation and potentiation by SDPA like naïve membranes (Fig. 6B). Furthermore, the supernatant of a  $50 \mu\text{M}$  SDPA preincubation potentiated the  $G_{\alpha}$  activation in naïve membranes, i.e., SDPA was not significantly incorporated into the membrane preparation. This supports the notion that SDPA, and most likely other GPLs, serve as intracellular effectors for mACs.

## 4. Discussion

Our results were contrary to the hypothesis at the outset because we expected to find an mAC inhibitory input. Most surprisingly we identified SDPA and other GPLs as positive effectors of mAC activities. Obviously, we have discovered a new system of intracellular mAC regulation. At this state our findings open more questions than can be answered with this initial report.

We used non-clonal HEK293 cells permanently transfected with mACs. HEK293 cells express considerable endogenous AC3 and 6 activities [37]. These endogenous mAC activities appear to be negligible in this context. First, upon transfection of mAC isoforms we observed very different basal AC activities virtually excluding that ‘contaminating’ endogenous AC activities affected our results (see Appendix Table 2 for a list of basal activities in transfected HEK293 cells). Second, we tested HEK293 cells in which mACs 3 and 6 were knocked out [37]. Upon mAC3 transfection SDPA similarly potentiated  $G_{\alpha}$ -activated mAC3 activity. Because these engineered cells proliferated rather slowly they were not used routinely.

Diacylglycerols and PA are lipid second messengers that regulate physiological and pathological processes, e.g. phosphatidic acids were reported to effect ion channel regulation and SDPA to act on the serotonin transporter in the brain [19,29,35]. So far, the specificity of fatty acyl residues and head groups in these lipids was not explored. Here, we observed a striking exclusivity of fatty-acyl esters at positions 1- and 2- of the glycerol backbone supporting a specific effector-mAC interaction. Usually, fatty acyl substitutions are regulated because they impart specific biophysical and biochemical properties [14]. We demonstrated that the combined fatty acyl ligands 1-stearoyl-2-docosahexaenoyl are more or less exclusive for the actions of SDPA. Even seemingly minor changes caused substantial changes in activity and efficacy, e.g., a change from stearoyl to palmitoyl at glycerol position 1 (Fig. 3). This argues for a specific steric interaction between the flexible stearoyl- and docosahexaenoyl carbon-chains. Acyl chain substitutions might then impair specific protein-ligand interactions, e.g. by a shrinkage of the binding surface. Apparently, such interactions are substantially diminished when only one of the two acyl residues is altered. Notably, didocosahexaenoyl- and di-arachidonoyl-phosphatidic acids (DDPA and DAPA) had mostly lost the capability to promote AC3 activity (Fig. 3). A particularly interesting point is the preference for 2-docosahexaenoyl acylation in the GPLs. Docosahexaenoic acid is an essential omega-3 fatty acid that cannot be synthesized at adequate quantities in infants or seniors [28]. Therefore it is widely sold as a nutraceutical and should be included into a balanced diet. Docosahexaenoic acid is particularly abundant in membrane lipids in the retina (about 60% of all lipids contain docosahexaenoic acid), testes, brain, heart and skeletal muscle [14]. A sodium-dependent symporter for uptake of this fatty acid, packaged as a lysophosphatidic acid, has been characterized and its structure was elucidated by cryo-EM [5,23,43]. Docosahexaenoic acid is needed for normal brain development and cognitive functions, a role in depression, aging and Alzheimer’s disease is discussed [9,13,14,23,45]. So far, mACs have not yet been noticed in metabolic disturbances caused by a lack of docosahexaenoic acid. The data presented here provides evidence that docosahexaenoic acid is involved in stimulating the cAMP generating system.

Examination of head group specificity displayed different patterns of mAC susceptibility and activity (Fig. 5). Notably, mAC isoforms 1 and 2 were not significantly affected by any of the GPLs assayed. This may be due to a general insensitivity for GPLs or that we did not identify the suitable bioactive GPLs. We did not examine the specificity of acyl substitution at the glycerol backbone in SDPS, SDPE, SDPG and SDPC because of the specificity of the stearic/docosahexaenoic acid couple in SDPA. We tested 1-stearoyl-2-arachidonoyl-phosphatidyl choline and the corresponding phosphatidyl-ethanolamine. Biological activity was absent with mACs 3, 5, 7, and 9, bolstering the assertion that fatty acyl specificity is stringent in these GPLs as well. Presently we cannot

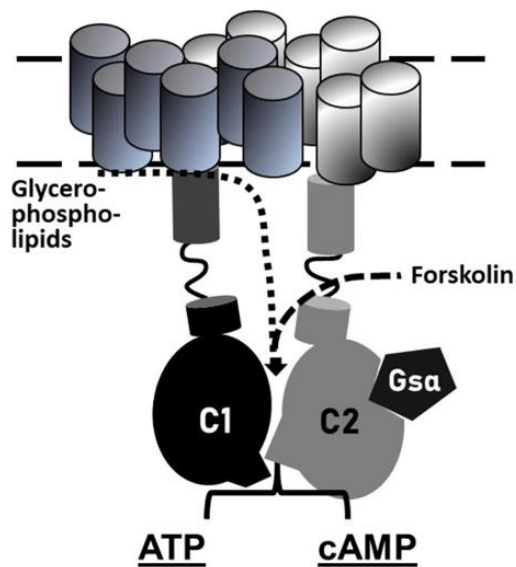


**Fig. 7.** Tentative scheme of a 2X6<sup>TM</sup>-adenylyl cyclase with regulatory input from G $\alpha$ , binding to the C2 catalytic domain, forskolin, binding to a degenerated second substrate-binding site [12,40], and glycerophospholipids, here proposed to enter and bind at the membrane anchor-receptor and extending towards the catalytic dimer.

completely exclude that GPLs acylated by different couples of acid substituents at the 1- and 2-positions might possess equal or better effector properties. In view of the large variety of GPLs this cannot be tested with a reasonable effort. Currently, we consider such a possibility as remote. We do not know how GPLs mechanistically potentiate AC activity in a synergistic interaction together with G $\alpha$ . The tentative scheme in Fig. 7 is intended to illustrate an approximation of potential interaction sites in relation to G $\alpha$  and forskolin. The precise nature of such interactions requires structural details (in progress).

Another question which is not answered in this study concerns the intracellular origin of GPLs, how their biosynthesis and release is regulated and tied into the cAMP regulatory system. Despite being water insoluble, an efficient traffic of phospholipids in cells exists, e.g. between locations of uptake and biosynthesis, to and from low-density-, high-density- and very low density lipoproteins, and the diversity of membrane-enclosed organelles such as mitochondria, nucleus, endoplasmic reticulum, endosomes, lysosomes, and the plasma membrane itself. Thus, lipid trafficking is a continuous cellular process connected to diverse signaling systems [14,35]. Part of the biosynthetic pathways for phosphatidic acid is the hydrolysis of GPLs with choline, ethanolamine or serine as headgroups by phospholipase D which generates phosphatidic acids [15]. Chemically, GPLs are excellently suited to serve as mAC effectors because termination of SDPA signaling is easily accomplished by phospholipase C. The relationship between SDPA and forskolin is debatable. The agents do not cooperatively interact at mAC proteins. Certainly, the structural changes caused by either agent promote the interactions between AC and G $\alpha$ . Yet this is no proof that such changes are identical or even similar.

A critical observation was the potentiation by SDPA of G $\alpha$ -activated mAC activity in mouse brain cortical membranes. mAC3 has been reported to be abundantly expressed in brain [20,31]. The efficacy of SDPA was comparable to that determined in mAC3-HEK293 membranes. This demonstrated that the effect of GPLs observed in HEK293 expressed AC isoforms is of physiological significance. Our approach has then discovered intracellular processes, which in conjunction with the established canonical GPCR/G $\alpha$ -regulation of mACs add a new dimension of mAC regulation. Currently, we cannot exclude the possibility that other GPLs exist which have an inhibitory input. Actually,

thermodynamic considerations would argue in favor of such a possibility. Whether this is realized as a biological mechanism remains an open possibility. Presently, many important questions remain unanswered, such as how are intracellular GPL levels regulated, which of the intracellular GPLs have access to the membrane delimited ACs, are GPL concentrations persistently or acutely adjusted in a cell, e.g., by stress, diet, diurnal, or seasonal effects or by peculiar disease states? In other words, are we dealing with a long-term regulation of the G $\alpha$ -sensitivity of the cAMP generating system or with coordinated short term signaling events? Answering these medically relevant questions remains a formidable challenge in the future.

#### Credit author statement

Anubha Seth, Marius Landau, Anita Schultz, Sheif Elsabagh: Investigation. Andrej Shevchenko and Sofia Traikov: Methodology; Joachim E. Schultz: Conceptualization, Formal analysis, Funding acquisition, supervision, Writing - original draft.

#### Declaration of Competing Interest

None.

#### Acknowledgements

We thank U. Kurz for a continuous supply of G $\alpha$  (Q227L), Dr. V. Watts, for supplying us with HEK293 $\Delta$ mAC3 $\Delta$ mAC6 cells, and Prof. Dr. A. Lupas for continuous encouragement. We gratefully acknowledge constructive suggestions from Dr. J. Linder. Supported by the Deutsche Forschungsgemeinschaft and institutional funds from the Max-Planck-Society.

#### Appendix A. Supplementary data

Supplementary data to this article can be found online at <https://doi.org/10.1016/j.cellsig.2022.110396>.

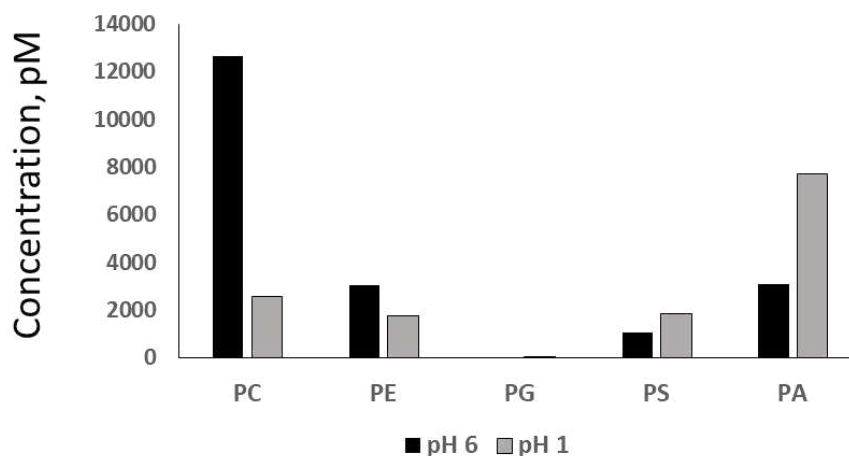
#### References

- [1] T.A. Baldwin, Y. Li, C.S. Brand, V.J. Watts, C.W. Dessauer, Insights into the regulatory properties of human adenylyl cyclase type 9, *Mol. Pharmacol.* 95 (2019) 349–360.
- [2] J. Bassler, J.E. Schultz, A.N. Lupas, Adenylate cyclases: receivers, transducers, and generators of signals, *Cell. Signal.* 46 (2018) 135–144.
- [3] S. Beltz, J. Bassler, J.E. Schultz, Regulation by the quorum sensor from *Vibrio* indicates a receptor function for the membrane anchors of adenylate cyclases, *Elife* (2016) 5.
- [4] E.G. Bligh, W.J. Dyer, A rapid method of total lipid extraction and purification, *Can. J. Biochem. Physiol.* 37 (1959) 911–917.
- [5] R.J. Cater, G.L. Chua, S.K. Erramilli, J.E. Keener, B.C. Choy, P. Tokarz, C.F. Chin, D. Q.Y. Quek, B. Kloss, J.G. Pepe, et al., Structural basis of omega-3 fatty acid transport across the blood-brain barrier, *Nature* 595 (2021) 315–319.
- [6] M.G. Cumbay, V.J. Watts, Novel regulatory properties of human type 9 adenylate cyclase, *J. Pharmacol. Exp. Ther.* 310 (2004) 108–115.
- [7] C.W. Dessauer, V.J. Watts, R.S. Ostrom, M. Conti, S. Dove, R. Seifert, International union of basic and clinical pharmacology. CI. Structures and small molecule modulators of mammalian adenylyl cyclases, *Pharmacol. Rev.* 69 (2017) 93–139.
- [8] S. Diel, K. Klass, B. Wittig, C. Kleuss, Gbetagamma activation site in adenylyl cyclase type II. Adenylyl cyclase type III is inhibited by Gbetagamma, *J. Biol. Chem.* 281 (2006) 288–294.
- [9] J. Duan, Y. Song, X. Zhang, C. Wang, Effect of omega-3 polyunsaturated fatty acids-derived bioactive lipids on metabolic disorders, *Front. Physiol.* 12 (2021), 646491.
- [10] M.P. Graziano, M. Freissmuth, A.G. Gilman, Expression of Gs alpha in *Escherichia coli*. Purification and properties of two forms of the protein, *J. Biol. Chem.* 264 (1989) 409–418.
- [11] M.P. Graziano, M. Freissmuth, A.G. Gilman, Purification of recombinant Gs alpha, *Methods Enzymol.* 195 (1991) 192–202.
- [12] Y.L. Guo, T. Seebacher, U. Kurz, J.U. Linder, J.E. Schultz, Adenylyl cyclase Rv1625c of *Mycobacterium tuberculosis*: a progenitor of mammalian adenylyl cyclases, *EMBO J.* 20 (2001) 3667–3675.
- [13] D. Heras-Sandoval, J. Pedraza-Chaverri, J.M. Perez-Rojas, Role of docosahexaenoic acid in the modulation of glial cells in Alzheimer's disease, *J. Neuroinflammation* 13 (2016) 61.

- [14] D. Hishikawa, W.J. Valentine, Y. Iizuka-Hishikawa, H. Shindou, T. Shimizu, Metabolism and functions of docosahexaenoic acid-containing membrane glycerophospholipids, *FEBS Lett.* 591 (2017) 2730–2744.
- [15] J.H. Jang, C.S. Lee, D. Hwang, S.H. Ryu, Understanding of the roles of phospholipase D and phosphatidic acid through their binding partners, *Prog. Lipid Res.* 51 (2012) 71–81.
- [16] T. Kanacher, A. Schultz, J.U. Linder, J.E. Schultz, A GAF-domain-regulated adenylyl cyclase from *Anabaena* is a self-activating cAMP switch, *EMBO J.* 21 (2002) 3672–3680.
- [17] E.E. Kooijman, K.N. Burger, Biophysics and function of phosphatidic acid: a molecular perspective, *Biochim. Biophys. Acta* 1791 (2009) 881–888.
- [18] J.U. Linder, J.E. Schultz, The class III adenylyl cyclases: multi-purpose signalling modules, *Cell. Signal.* 15 (2003) 1081–1089.
- [19] Q. Lu, C. Murakami, Y. Murakami, F. Hoshino, M. Asami, T. Usuki, H. Sakai, F. Sakane, 1-Stearyl-2-docosahexaenoyl-phosphatidic acid interacts with and activates Praja-1, the E3 ubiquitin ligase acting on the serotonin transporter in the brain, *FEBS Lett.* 594 (2020) 1787–1796.
- [20] M.G. Ludwig, K. Seuwen, Characterization of the human adenylyl cyclase gene family: cDNA, gene structure, and tissue distribution of the nine isoforms, *J. Recept. Signal Transduct. Res.* 22 (2002) 79–110.
- [21] V. Matyashi, G. Liebisch, T.V. Kurzchalia, A. Shevchenko, D. Schwudke, Lipid extraction by methyl-tert-butyl ether for high-throughput lipidomics, *J. Lipid Res.* 49 (2008) 1137–1146.
- [22] W.L. Ng, Y. Wei, L.J. Perez, J. Cong, T. Long, M. Koch, M.F. Semmelhack, N. S. Wingreen, B.L. Bassler, Probing bacterial transmembrane histidine kinase receptor-ligand interactions with natural and synthetic molecules, *Proc. Natl. Acad. Sci. U. S. A.* 107 (2010) 5575–5580.
- [23] L.N. Nguyen, D. Ma, G. Shui, P. Wong, A. Cazenave-Gassiot, X. Zhang, M.R. Wenk, E.L. Goh, D.L. Silver, Mfsd2a is a transporter for the essential omega-3 fatty acid docosahexaenoic acid, *Nature* 509 (2014) 503–506.
- [24] K.F. Ostrom, J.E. LaVigne, T.F. Brust, R. Seifert, C.W. Dessauer, V.J. Watts, R. S. Ostrom, Physiological roles of mammalian transmembrane adenylyl cyclase isoforms, *Physiol. Rev.* 102 (2022) 815–857.
- [25] C. Pinto, D. Papa, M. Hubner, T.C. Mou, G.H. Lushington, R. Seifert, Activation and inhibition of adenylyl cyclase isoforms by forskolin analogs, *J. Pharmacol. Exp. Ther.* 325 (2008) 27–36.
- [26] R.T. Premont, I. Matsuoka, M.G. Mattei, Y. Pouille, N. Defer, J. Hanoune, Identification and characterization of a widely expressed form of adenylyl cyclase, *J. Biol. Chem.* 271 (1996) 13900–13907.
- [27] C. Qi, S. Sorrentino, O. Medalia, V.M. Korkhov, The structure of a membrane adenylyl cyclase bound to an activated stimulatory G protein, *Science* 364 (2019) 389–394.
- [28] X. Qiu, Biosynthesis of docosahexaenoic acid (DHA, 22:6-4, 7,10,13,16,19): two distinct pathways, *Prostaglandins Leukot. Essent. Fat. Acids* 68 (2003) 181–186.
- [29] C.V. Robinson, T. Rohacs, S.B. Hansen, Tools for understanding nanoscale lipid regulation of ion channels, *Trends Biochem. Sci.* 44 (2019) 795–806.
- [30] R. Sadana, C.W. Dessauer, Physiological roles for G protein-regulated adenylyl cyclase isoforms: insights from knockout and overexpression studies, *Neurosignals* 17 (2009) 5–22.
- [31] C. Sanabra, G. Mengod, Neuroanatomical distribution and neurochemical characterization of cells expressing adenylyl cyclase isoforms in mouse and rat brain, *J. Chem. Neuroanat.* 41 (2011) 43–54.
- [32] J.E. Schultz, J. Natarajan, Regulated unfolding: a basic principle of intraprotein signaling in modular proteins, *Trends Biochem. Sci.* 38 (2013) 538–545.
- [33] J.E. Schultz, B.H. Schmidt, Treatment of rats with thyrotropin (TSH) reduces the adrenoceptor sensitivity of adenylyl cyclase from cerebral cortex, *Neurochem. Int.* 10 (1987) 173–178.
- [34] A. Seth, M. Finkbeiner, J. Grischin, Schultz JE (2020) Gsalpha stimulation of mammalian adenylyl cyclases regulated by their hexahelical membrane anchors, *Cell. Signal.* 68 (2020), 109538.
- [35] J.J. Shin, C.J. Loewen, Putting the pH into phosphatidic acid signaling, *BMC Biol.* 9 (2011) 85.
- [36] S.C. Sinha, S.R. Sprang, Structures, mechanism, regulation and evolution of class III nucleotidyl cyclases, *Rev. Physiol. Biochem. Pharmacol.* 157 (2006) 105–140.
- [37] M. Soto-Velasquez, M.P. Hayes, A. Alpsy, E.C. Dykhuizen, V.J. Watts, A novel CRISPR/Cas9-based cellular model to explore adenylyl cyclase and cAMP signaling, *Mol. Pharmacol.* 94 (2018) 963–972.
- [38] R.K. Sunahara, R. Taussig, Isoforms of mammalian adenylyl cyclase: multiplicities of signaling, *Mol. Interv.* 2 (2002) 168–184.
- [39] W.J. Tang, A.G. Gilman, Construction of a soluble adenylyl cyclase activated by Gs alpha and forskolin, *Science* 268 (1995) 1769–1772.
- [40] J.J. Tesmer, S.R. Sprang, The structure, catalytic mechanism and regulation of adenylyl cyclase, *Curr. Opin. Struct. Biol.* 8 (1998) 713–719.
- [41] J.J. Tesmer, R.K. Sunahara, A.G. Gilman, S.R. Sprang, Crystal structure of the catalytic domains of adenylyl cyclase in a complex with Gsalpha.GTPgammaS, *Science* 278 (1997) 1907–1916.
- [42] O. Vvedenskaya, T.D. Rose, O. Knittelfelder, A. Palladini, J.A.H. Wodke, K. Schuhmann, J.M. Ackerman, Y. Wang, C. Has, M. Brosch, et al., Nonalcoholic fatty liver disease stratification by liver lipidomics, *J. Lipid Res.* 62 (2021), 100104.
- [43] C.A.P. Wood, J. Zhang, D. Aydin, Y. Xu, B.J. Andreone, U.H. Langen, R.O. Dror, C. Gu, L. Feng, Structure and mechanism of blood-brain-barrier lipid transporter MFS2A, *Nature* 596 (2021) 444–448.
- [44] G. Zhang, Y. Liu, A.E. Ruoho, J.H. Hurley, Structure of the adenylyl cyclase catalytic core, *Nature* 386 (1997) 247–253.
- [45] Z. Zhu, Z. Tan, Y. Li, H. Luo, X. Hu, M. Tang, J. Hescheler, Y. Mu, L. Zhang, Docosahexaenoic acid alters Gsalpha localization in lipid raft and potentiates adenylyl cyclase, *Nutrition* 31 (2015) 1025–1030.
- [46] M. Ziegler, J. Bassler, S. Beltz, A. Schultz, A.N. Lupas, J.E. Schultz, A novel signal transducer element intrinsic to class IIIa and IIIb adenylyl cyclases, *FEBS J.* 284 (2017) 1204–1217.

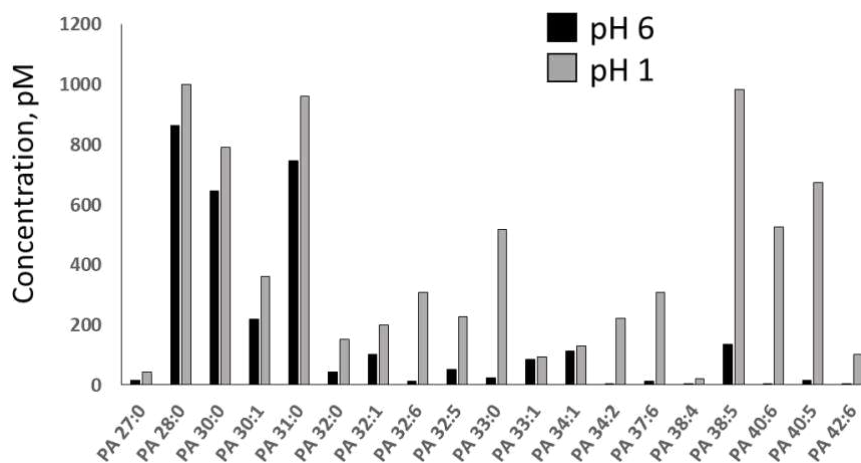
## Supplemental Material

### Appendix Figure 1



Lipid class composition of MTBE / methanol extracts. MonoQ-purified fractions were extracted at pH 1.0 and pH 6.0. Expectantly, the extract recovered under acidic conditions was enriched with PA. Y-axis: total abundance of lipid classes, pmol/L (n=2).

### Appendix Figure 2



Molecular composition of PA species extracted by MTBE / methanol from the fractions with pH 6.0 and pH 1.0. Acidic extraction increased the recovery of PA by more than 2-fold and also enriched the extract with the molecular species comprising long polyunsaturated fatty acid moieties. Y-axes: molar abundance of lipid species, in pmol/L (n=2).

## Appendix Table 1:

List of lipids tested:

from Avanti lipids:

- 131303P Cerebrosides
- 131305P Sulfatides
- 800818C-1-stearoyl-2-arachidonoyl-sn-glycerol
- 800819 --stearoyl-2-docosahexaenoyl-sn-glycerol
- 830855C 1,2-dipalmitoyl-sn-glycero-3-phosphate
- 840051P L- $\alpha$ -phosphatidylcholine (Egg, Chicken)
- 840055C L- $\alpha$ -phosphatidylcholine (Liver, Bovine)
- 840065C 1-stearoyl-2-docosahexaenoyl-sn-glycero-3-phospho-L-serine
- 840101C L- $\alpha$ -phosphatidic acid (Egg, Chicken) (sodium salt)
- 840859C 1-palmitoyl-2-arachidonoyl-sn-glycero-3-phosphate (sodium salt)
- 840860C 1-palmitoyl-2-docosahexaenoyl-sn-glycero-3-phosphate (sodium salt)
- 840862C 1-stearoyl-2-linoleoyl-sn-glycero-3-phosphate (sodium salt)
- 840863C 1-stearoyl-2-arachidonoyl-sn-glycero-3-phosphate (sodium salt)
- 840864C 1-stearoyl-2-docosahexaenoyl-sn-glycero-3-phosphate (sodium salt)
- 840875C 1,2-dioleoyl-sn-glycero-3-phosphate (sodium salt)
- 840885C 1,2-dilinoleoyl-sn-glycero-3-phosphate (sodium salt)
- 840886C 1,2-diarachidonoyl-sn-glycero-3-phosphate (sodium salt)
- 840887C 1,2-didocosahexaenoyl-sn-glycero-3-phosphate (sodium salt)
- 850469C 1-stearoyl-2-arachidonoyl-sn-glycero-3-phosphocholine
- 850472C 1-stearoyl-2-docosahexaenoyl-sn-glycero-3-phosphocholine
- 850804C 1-stearoyl-2-arachidonoyl-sn-glycero-3-phosphoethanolamine
- 850806C 1-stearoyl-2-docosahexaenoyl-sn-glycero-3-phosphoethanolamine
- 850852C 1,2-dioleoyl-sn-glycero-3-phosphoethanolamine-N,N-dimethyl
- 857130P 1-oleoyl-2-hydroxy-sn-glycero-3-phosphate (sodium salt)
- 857328P 1-oleoyl-sn-glycero-2,3-cyclic-phosphate (ammonium salt)
- 860053P total ganglioside extract (Brain, Porcine-Ammonium Salt)
- 860492 Sphingosine-1-phosphate; D-erythro-sphingosine-1-phosphate

- LIPOID (Heidelberg) donated the following lipids:
- 30. 556200 Lipoid PC 14:0/14:0; 1,2-Dimyristoyl-sn-glycero-3-phosphatidylcholine (DMPC)
- 31. 556300 Lipoid PC 16:0/16:0; 1,2-Dipalmitoyl-sn-glycero-3-phosphatidylcholine (DPPC)
- 32. 556500 Lipoid PC 18:0/18:0; 1,2-Distearoyl-sn-glycero-3-phosphocholine (DSPC)
- 33. 556600 Lipoid PC 18:1/18:1; 1,2-Dioleoyl-sn-glycero-3-phosphocholine (DOPC)
- 34. 556400 Lipoid PC 16:0/18:1; 1-Palmitoyl-2-oleoyl-sn-glycero-3-phosphocholine (POPC)
- 35. 557100 Lipoid PC 22:1/22:1; 1,2-Dierucoyl-sn-glycero-3-phosphocholine (DEPC)
- 36. 566300 Lipoid PA 16:0/16:0; 1,2-Dipalmitoyl-sn-glycero-3-phosphate, monosodium salt (DPPA-Na)
- 37. 567600 Lipoid PS 18:1/18:1; 1,2-Dioleoyl-sn-glycero-3-phosphoserine, sodium salt (DOPS-Na)
- 38. 560200 Lipoid PG 14:0/14:0; 1,2-Dimyristoyl-sn-glycero-3-phospho-rac-glycerol-Na (DMPG)
- 39. 560300 Lipoid PG 16:0/16:0; 1,2-Dipalmitoyl-sn-glycero-3-phospho-rac-glycerol-Na (DPPG)
- 40. 560400 Lipoid PG 18:0/18:0; 1,2-Distearoyl-sn-glycero-3-phospho-rac-glycerol-Na (DSPG)
- 41. 565600 Lipoid PE 14:0/14:0; 1,2-Dimyristoyl-sn-glycero-3-phosphoethanolamine (DMPE)
- 42. 565300 Lipoid PE 16:0/16:0; 1,2-Dipalmitoyl-sn-glycero-3-phosphoethanolamine (DPPE)
- 43. 565400 Lipoid PE 18:0/18:0; 1,2-Distearoyl-sn-glycero-3-phosphoethanolamine (DSPE)
- 44. 565600 Lipoid PE 18:1/18:1; 1,2-Dioleoyl-sn-glycero-3-phosphoethanolamine (DOPE)

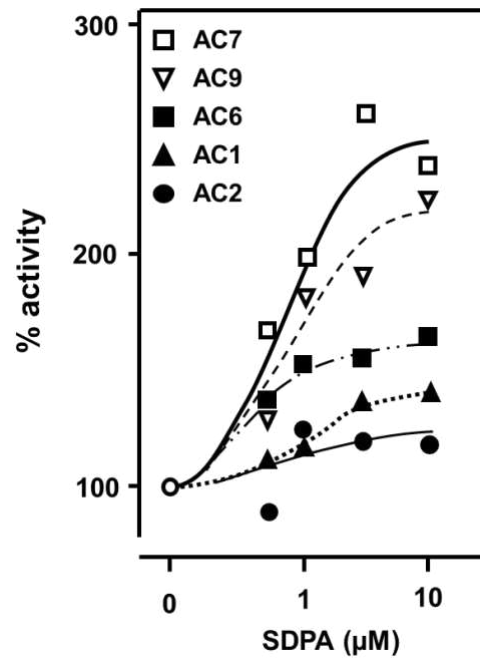
Appendix Table 2

**mAC activities in HEK293 cell membranes**  
**transfected with human mAC isoforms**

	<u>nmol cAMP•mg<sup>-1</sup>•min<sup>-1</sup></u>	
	<b><u>basal activity</u></b>	<b><u>+ 0.6 μM Gsα</u></b>
HEK293	0.02	0.19 (10-fold)
HEK293 AC1	0.16	0.71 (4-fold)
HEK293 AC2	0.34	5.17 (15-fold)
HEK293 AC3	0.03	0.55 (16-fold)
HEK293 AC4	0.02	0.2 (9-fold)
HEK293 AC5	0.07	2.46 (37-fold)
HEK293 AC6	0.08	1.41 (18-fold)
HEK293 AC7	0.03	0.19 (7-fold)
HEK293 AC8	0.15	1.08 (7-fold)
HEK293 AC9	0.03	1.87 (71-fold)
HEK293ΔAC3,6	0.006	0.06 (10-fold)

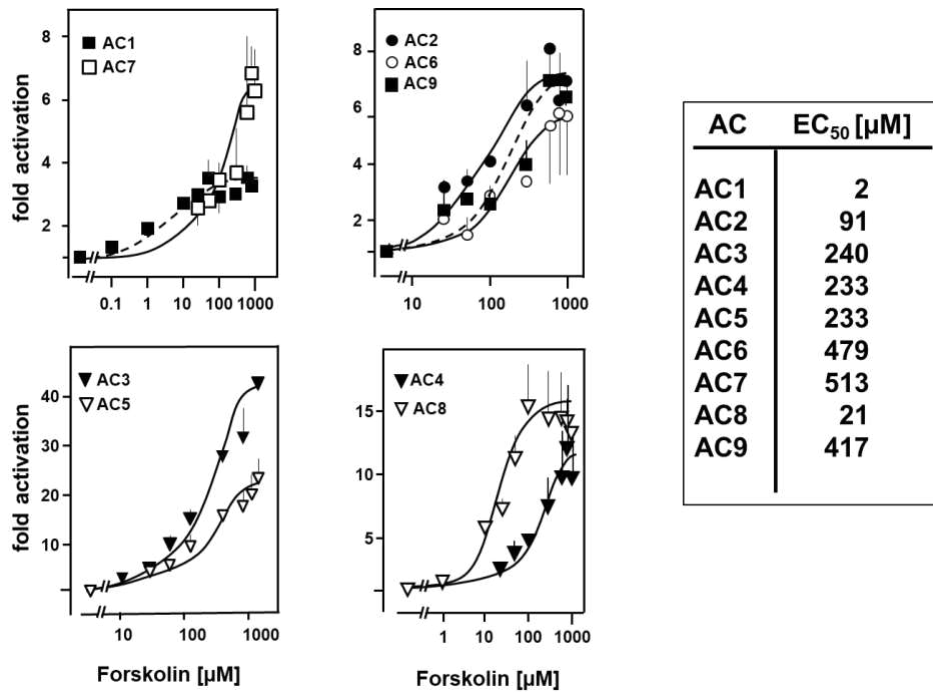
(n= 5-12)

### Appendix Figure 3



Concentration-response curves for SDPA potentiation of mAC isoforms 7, 9, 6, 1, and 2. Basal and  $G\alpha$ -activated activities are listed in Appendix table 2. n=2-5.

**Appendix Figure 4:**



Forskolin concentration-response curves for the nine human mAC isoforms expressed in HEK293 cells. Error bars denote S.E.M. The calculated  $\text{EC}_{50}$  concentrations are listed at right.  $n = 2-4$ .

### Appendix Table 3

With hAC3 transfected HEK293 cells in a 396 well plate were incubated and stimulated at 37°C for 45 min by adenosine, isoproterenol and prostaglandin E<sub>2</sub> ± 10 µM SDPA.

n = 3 to 4, mean ± S.E.M. Incubations were stopped by addition of detection and lysis buffer of the cAMP assay kit (10 µl/well; Cisbio).

	pMoles cAMP/ 10 <sup>4</sup> cells
<u>basal</u>	0.06 ± 0.02
<u>SDPA, 10 µM</u>	0.02 ± 0.01
<u>2.5 µM isoproterenol</u>	0.24 ± 0.03
<u>2.5 µM isoproterenol + 10 µM SDPA</u>	0.25 ± 0.03
<u>1 µM prostaglandin E<sub>2</sub></u>	0.10 ± 0.01
<u>1 µM prostaglandin E<sub>2</sub> + 10 µM SDPA</u>	0.11 ± 0.02
<u>10 µM adenosine</u>	0.17 ± 0.07
<u>10 µM adenosine + 10 µM SDPA</u>	0.07 ± 0.01

[Please note that isolated HEK293 membrane preparations did not respond to adenosine, isoproterenol or PGE<sub>2</sub>]

## Additional Experiments (not shown in the publication)

### A- Effect of SDPA on cAMP accumulation in HEK293-mAC3

In chapter I, SDPA was shown to enhance  $G_s\alpha$ -stimulated activity of mAC3. To examine its effect *in vivo*, I tested the effect of SDPA on HEK293 cells permanently transfected with mAC3. 14000 cells/well were seeded into 384 well plates, and cAMP generation was triggered by 10  $\mu$ M isoproterenol. As shown in Figure 1, SDPA up to 50  $\mu$ M had no effect on cAMP accumulation on mAC3 intact cells.

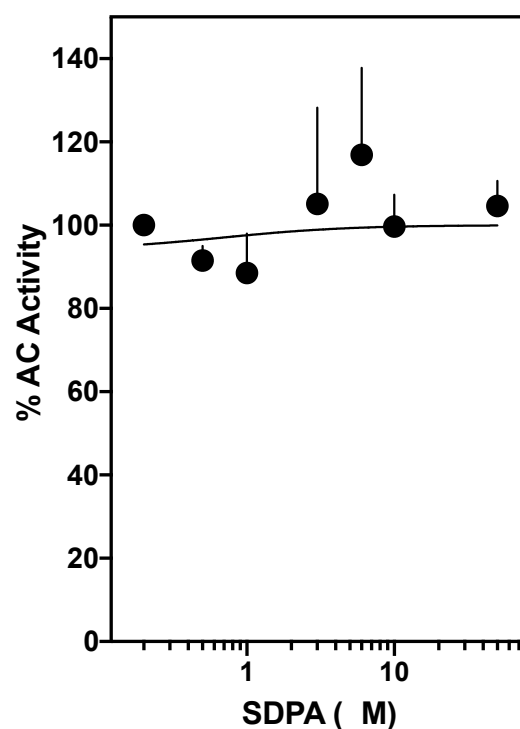


**Figure 1. Effect of SDPA on HEK293-mAC3 stimulated by 10  $\mu$ M isoproterenol.** Basal and isoproterenol stimulated (set as 100%) activities were  $0.11 \pm 0.03$  and  $2.75 \pm 0.36$  pmol cAMP/14000 cells. Error bars denote SEM of  $n = 2$  done in triplicates.

### 3.2 Publication II

**Elsabbagh, S.**, Landau, M., Gross, H., Schultz, A., & Schultz, J. E. (2023). Heme b inhibits class III adenylyl cyclases. *Cellular signalling*, *103*, 110568. <https://doi.org/10.1016/j.cellsig.2022.110568>

#### **Position in list of authors: 1**

Author contributions: I carried out experiments and analyzed data (except Fig. 6 and 7 right). All data for appendix figures are based on my experiments (except for Appendix Fig. 6). I contributed to manuscript revising and editing. I estimate my own contribution by 70%.



ELSEVIER

Contents lists available at ScienceDirect

## Cellular Signalling

journal homepage: [www.elsevier.com/locate/cellsig](http://www.elsevier.com/locate/cellsig)

## Heme b inhibits class III adenylyl cyclases

Sherif Elsabbagh, Marius Landau, Harald Gross, Anita Schultz, Joachim E. Schultz\*

Pharmazeutisches Institut der Universität Tübingen, Tübingen, Germany

## ARTICLE INFO

## Keywords:

Adenylyl cyclase  
 Membrane anchor  
 Heme b  
 Hematin  
 Hematin  
 Protoporphyrin IX  
 Biliverdin  
 Chlorophyll

## ABSTRACT

Acidic lipid extracts from mouse liver, kidney, heart, brain, and lung inhibited human pseudoheterodimeric adenylyl cyclases (hACs) expressed in HEK293 cells. Using an acidic lipid extract from bovine lung, a combined MS- and bioassay-guided fractionation identified heme b as inhibitor of membrane-bound ACs. IC<sub>50</sub> concentrations were 8–12 μM for the hAC isoforms. Hemopexin and bacterial hemophore attenuated heme b inhibition of hAC5. Structurally related compounds, such as hematin, protoporphyrin IX, and biliverdin, were significantly less effective. Monomeric bacterial class III ACs (mycobacterial ACs Rv1625c; Rv3645; Rv1264; cyanobacterial AC CyaG) were inhibited by heme b with similar efficiency. Surprisingly, structurally related chlorophyll a similarly inhibited hAC5. Heme b inhibited isoproterenol-stimulated cAMP accumulation in HEK293 cells. Using cortical membranes from mouse brain hemin efficiently and reversibly inhibited basal and G $\alpha$ -stimulated AC activity. The physiological relevance of heme b inhibition of the cAMP generating system in certain pathologies is discussed.

## 1. Introduction

The regulation of vertebrate adenylyl cyclases is a field attracting researchers from many diverse areas and across most subspecialties in medicine [1–5]. The reasons are obvious: the enzymatic product is the universal second messenger 3', 5'-cyclic AMP (cAMP). After nine distinct membrane-bound ACs were sequenced [2,5–7], biochemical studies on regulation were considerably expanded. The initial speculation of a function of the two hexahelical membrane anchors as ion channels or transporters was never confirmed [6]. Subsequently, the regulation of the vertebrate ACs via the GPCR/G $\alpha$  axis was nearly 'codified'. Additional regulatory inputs are phosphorylation of amino acid residues at the cytosolic side, Ca<sup>2+</sup>, calmodulin, and G $\beta\gamma$  [2]. Surprisingly, it was tacitly accepted that the AC membrane anchors which comprise up to 40% of the proteins were just that and otherwise functionally inert.

Since 1990, our laboratory is attempting to find a physiological function beyond anchoring using a variety of approaches [8–13]. In 2016 we demonstrated that an isosteric hexahelical membrane receptor, the quorum-sensing receptor CqsS from *Vibrio*, regulated the canonical mycobacterial class III AC Rv1625c [12]. We further characterized a conserved cyclase-transducing element, CTE, also termed helical domain, which is located between the membrane and catalytic domains [12,14–16]. In 2020, we reported that the quorum-sensing receptor

CqsS from *Vibrio* regulated the extent of G $\alpha$  activation of the mammalian AC2 [17]. We further demonstrated that fetal bovine serum (FBS) contains components which concentration-dependently attenuated the G $\alpha$  activated AC2 [17]. Based on these findings, we proposed a model for AC regulation in which all AC domains were assigned specific functionalities. The AC membrane anchors were proposed to be orphan receptors for yet unknown ligands. Since then, our efforts have been focused on identification of potential AC ligands. Here, we report the surprising finding that heme b, isolated from a bovine lung homogenate, inhibited all human membrane bound ACs at low micromolar concentrations and with high structural specificity in vitro and in HEK293 cells.

## 2. Materials and methods

## 2.1. Reagents and materials

ATP, creatine kinase, creatine phosphate, bovine hemin (Cat.# H9039;  $\geq 90\%$  pure), protoporphyrin IX (Cat. # 258385), biliverdin (Cat.# 30,891), hematin (Cat.# H3281) and chlorophyll a (Cat. # C6144) were purchased from Merck-Sigma as was hemopexin from human plasma (Cat. # SRP6514). Porcine hemin  $>98\%$  pure was supplied by Roth chemicals (Cat. # 7629.1). Porcine hemin was used to exclude interference by potential impurities in bovine hemin (see

Abbreviations: AC, adenylyl cyclase..

\* Corresponding author at: Pharmazeutisches Institut der Universität Tübingen, Auf der Morgenstelle 8, 72076 Tübingen, Germany.

E-mail address: [joachim.schultz@uni-tuebingen.de](mailto:joachim.schultz@uni-tuebingen.de) (J.E. Schultz).

<https://doi.org/10.1016/j.cellsig.2022.110568>

Received 9 November 2022; Received in revised form 12 December 2022; Accepted 19 December 2022

Available online 21 December 2022

0898-6568/© 2022 Elsevier Inc. All rights reserved.

Appendix Table 1). The constitutively active G $\alpha$ Q227L mutant was expressed and purified as described earlier [18–20]. Forskolin was a gift from Hoechst, Frankfurt, Germany. Fetal bovine serum (FBS) was from Gibco, Life Technologies, Darmstadt, Germany (Cat. # 10270; lot number: 42Q8269K). Sera for sheep, rabbit, goat, and chicken were from Sigma (Cat. Numbers S2263; R4505; G6767; C5405), and fish serum was from my BioSource, San Diego, CA, USA (Cat. # MBS318429). NADH, D-Lactic dehydrogenase from *Lactobacillus leichmannii*, sodium pyruvate, trypsin from porcine pancreas, N- $\alpha$ -benzoyl-L-arginine ethyl ester (BAEE) were purchased from Merck-Sigma.

## 2.2. General experimental procedures

HPLC was performed using a Waters system, with a Waters 996 controller and pump and photodiode array detector, a Rheodyne 7725i injector and a 200 series PerkinElmer vacuum degasser. For LC-MS analysis, a 1100 Series HPLC system (Agilent Technologies) was fitted with a G1322A degasser, a G1312A binary pump, a G1329A autosampler and a G1315A diode array detector. The Agilent HPLC components were connected to an ABSCIEX 3200 QTRAP LC/MS/MS mass spectrometer (Sciex, Darmstadt, Germany). The high resolution mass spectrum was recorded on an HR-ESI-TOF-MS Bruker maXis 4G mass spectrometer. All solvents were purchased as HPLC or LC-MS grade.

## 2.3. Extraction of lung tissue

1.24 kg bovine lung was minced using a meat grinder and 1.2 l 50 mM MOPS pH 7.5 were added into in a waring blender (4 °C) resulting in 2.3 l homogenate. It was centrifuged (30 min at 4 °C, 7200  $\times$ g) resulting in 1.2 l supernatant. The pH of the supernatant was adjusted to 1 using 7% HCl. Equal volumes of CH<sub>2</sub>Cl<sub>2</sub>: MeOH (2:1) were mixed with the supernatant in a separatory funnel and shaken vigorously. Centrifugation was at 5300  $\times$ g for 30 min. The lower organic (CH<sub>2</sub>Cl<sub>2</sub>) layer was recovered, and the solvent evaporated using a rotary evaporator at 35 °C. 2 g of dried crude extract was obtained.

## 2.4. Fractionation

The material was dissolved in petrol ether (40–60 °C boiling point) and chromatographed on silica gel 60H (Supelco; vacuum liquid chromatography; VLC). The column was developed stepwise with solvents of increasing polarity, i.e., from 10:90 EtOAc/petrol ether to 100% EtOAc, followed by 100% MeOH. 17 fractions (A to Q) of 300 ml each were collected. Fraction O (eluted with 100% MeOH) was further subjected to RP-HPLC using a linear gradient from 70:30 to 100% MeOH/H<sub>2</sub>O (0.1% TFA) over a period of 20 mins (Knauer Eurospher II C18P 250  $\times$  8 mm, 1 ml/min, UV monitoring at 215 and 380 nm). Three subfractions, designated O-1, O-2 and O-3, were obtained.

For LC/MS, fractions were dissolved in methanol and injected into the LC/MS using an acetonitrile/H<sub>2</sub>O (0.1%TFA) gradient 10/90 to 50/50 over 24 min. Commercial hemin was dissolved in DMSO (10 mM), diluted in methanol, and analyzed.

## 2.5. Lactate dehydrogenase assay

LDH, pyruvate and NADH were dissolved in 67.2 mM Tris/HCl pH 7.5 The reaction was monitored for 3 min at 340 nm. Hemin, final concentration (40  $\mu$ M) was added from a 10 mM DMSO stock.

## 2.6. Trypsin assay

Trypsin and the substrate N- $\alpha$ -benzoyl-L-arginine ethyl ester were dissolved in 67 mM Tris-HCl, pH 9, buffer. The reaction was monitored at 253 nm for 3 min.

## 2.7. Plasmid construction and protein expression

HEK293 cells were maintained in Dulbecco's modified Eagle's medium (DMEM) containing 10% FBS at 37 °C with 5% CO<sub>2</sub>. Transfection of HEK293 cells with single mAC plasmids was with PolyJet (SigmaGen, Frederick, MD, USA). Permanent cell lines were generated by selection for 7 days with G418 (600  $\mu$ g/ml) and maintained with 300  $\mu$ g/ml G418 [21–23]. For membrane preparation, cells were trypsinized and collected by centrifugation (3000  $\times$ g, 5 min). Cells were lysed and homogenized in 20 mM HEPES, pH 7.5, 1 mM EDTA, 2 mM MgCl<sub>2</sub>, 1 mM DTT, and one tablet of complete, EDTA-free (for 50 ml), 250 mM sucrose by 20 strokes in a potter homogenizer. Debris was removed by centrifugation (5 min at 1000  $\times$ g), membranes were then collected by centrifugation at 100000  $\times$ g for 60 min at 0 °C, resuspended and stored at –80 °C in 20 mM MOPS, pH 7.5, 0.5 mM EDTA, 2 mM MgCl<sub>2</sub>. Membrane preparation from mouse brain cortex was according to [17,24]. For each preparation three cerebral cortex were dissected and homogenized in 4.5 ml cold 48 mM Tris-HCl, pH 7.4, 12 mM MgCl<sub>2</sub>, and 0.1 mM EGTA with a Polytron hand disperser (Kinematica AG, Switzerland). The homogenate was centrifuged for 15 min at 12000  $\times$ g at 4 °C and the pellet was washed once with 5 ml 1 mM potassium bicarbonate. The final suspension in 2 ml 1 mM KHCO<sub>3</sub> was stored in aliquots at –80 °C.

## 2.8. Adenylyl cyclase assay

mAC activities were determined in a volume of 10  $\mu$ l using 1 mM ATP, 2 mM MgCl<sub>2</sub> (3 mM MnCl<sub>2</sub> with bacterial ACs), 3 mM creatine phosphate, 60  $\mu$ g/ml creatine kinase, 50 mM MOPS, pH 7.5. The cAMP assay kit from Cisbio (Codolet, France) was used according to the supplier's instructions. For each assay a cAMP standard curve was established.

## 2.9. HasA preparation

pQE32-pHisHasA-ApR plasmid was transformed into *E. coli* BL21DE3<sub>[pRep4]</sub>. The cells were cultured in LB medium containing 100  $\mu$ g/ml ampicillin and 25  $\mu$ g/ml kanamycin to an OD<sub>600</sub> of 0.62 at 30 °C. After induction (1 mM IPTG) incubation was continued for 4 h at 30 °C. Cells were harvested by centrifugation and resuspended in 20 mM MOPS, pH 7.5 containing complete EDTA free protease inhibitor (buffer A). Cells were disrupted by French press and the lysate was centrifuged (4300  $\times$ g; 30 min) followed by ultracentrifugation (100,000 g, 60 min). The supernatant was loaded onto a Ni-NTA column equilibrated with buffer A + 20 mM imidazole. After washing with buffer A (+ 5 mM and 15 mM imidazole) HasA was eluted with buffer A + 250 mM imidazole and dialyzed against 20 mM MOPS, pH 7.5, to remove imidazole.

## 2.10. cAMP accumulation assay

HEK293 cells stably expressing AC3, AC5, AC7, and AC9 were plated at 2500–10000 cells/well into 384 well plates. Cells were then treated with varying concentrations of hemin and incubation was continued for 15–45 min. 10  $\mu$ M isoproterenol was added to stimulate cAMP production and the incubation was continued for 10–30 min. Cisbio HTRF detection reagents were then added and incubated for 1 h at room temperature.

## 2.11. Data and statistical analysis of assay results

All incubations were in duplicates or triplicates. For easier presentation data were mostly normalized to respective controls and n and S.E. M values are indicated in all figures. Data analysis was with GraphPad prism 8.1.2 using a two-tailed *t*-test.

**Table 1**

The effect of different animal sera on  $G\alpha$  stimulated activity of hAC5 expressed in Sf9 cells. The % activities listed are at 20% serum. Basal hAC5 activity was  $0.29 \pm 0.09$  and 600 nM  $G\alpha$  stimulated activity (100%) was  $5.2 \pm 1.15$  nmol cAMP•mg<sup>-1</sup>•min<sup>-1</sup>. Means  $\pm$  S.E.M of 3–4 experiments, each with two technical replicates are depicted.

Serum	% hAC5 activity
FBS	11 $\pm$ 1
Rabbit	9 $\pm$ 1
Sheep	40 $\pm$ 14
Goat	13 $\pm$ 5
Chicken	16 $\pm$ 4
Fish	10 $\pm$ 1

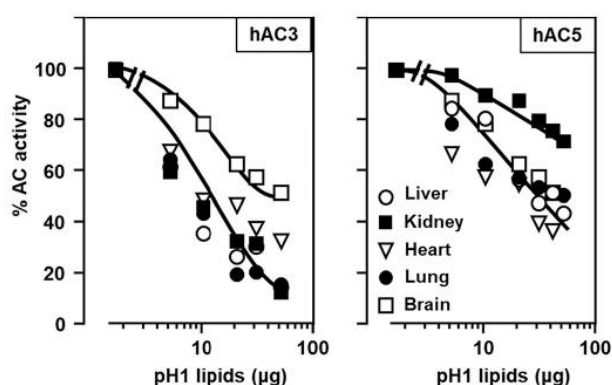


**Fig. 1.** Effect of acidic lipid extracts from mouse tissues on  $G\alpha$ -stimulated hAC3 and 5. The dried residues from each tissue were dissolved at 10 mg/ml DMSO, hAC3 and hAC5 were stimulated by 300 nM  $G\alpha$ . hAC3, 100% activity was 0.6 nmol cAMP•mg<sup>-1</sup>•min<sup>-1</sup> (basal activity was 0.01). hAC5, 100% activity was 2.74 nmol cAMP•mg<sup>-1</sup>•min<sup>-1</sup> (basal activity was 0.03). Data are from one experiment with two technical replicates.

### 3. Results

#### 3.1. Identification of heme b

We have reported that components present in FBS attenuated  $G\alpha$ -activated hAC2 expressed in Sf9 cells [17]. Here, we examined sera from sheep, goat, rabbit, chicken, and fish using  $G\alpha$ -activated hAC5 expressed in Sf9 cells (Table 1). We observed that these sera attenuated hAC5 with comparable efficacies reported earlier [17]. We concluded

that yet unidentified components are present in sera from different species possibly indicating a common evolutionary history with eukaryotic ACs because birds (chicken) and fish (salmon) diverged from mammals several hundred million years ago. The conservation of vertebrate ACs goes back about 0.5 billion years to the coelacanth and elephant shark [7,15]. For chemical identification of potential ligands, the use of serum as a source material is deemed unsuitable, not least because of the projected cost.

Expecting the presence of AC ligands in other tissues, we prepared pH 1 lipid extracts from mouse liver, kidney, heart, lung and brain [25]. Inhibition of  $G\alpha$ -activated AC3 and AC5 expressed in HEK293 cells were observed with all acidic lipid extracts. AC5 was somewhat less attenuated indicating graded responses (Fig. 1).

Because the extract from lung had a high ‘inhibitory’ efficiency we continued with bovine lung as a source material. A lung homogenate was acidified to pH 1 and lipids were extracted with dichloromethane/methanol [25]. After solvent removal the solids were dissolved in petrol ether and separated by VLC on silica gel 60H (see scheme). Stepwise elution with petrol ether, ethyl acetate and methanol resulted in 17 fractions (A-Q; 300 ml each) which were brought to dryness. The residues were dissolved at 5 mg/ml DMSO and tested with  $G\alpha$ -activated hAC5. Fractions with inhibitory potency (F, J-Q) were analyzed by low resolution LC/MS. In the slightly brownish fractions K to Q, a peak at  $m/z$  616.3 was prominent. Since fraction O represented contained the compound already in a semi-pure form, we continued working with it. 24 mg of fraction O were dissolved in 0.5 ml methanol and were subjected to RP-HPLC (Fig. 2, left).

Three major peaks were resolved (O-1, O-2, and O-3). The absorption profile at 380 nm indicated the presence of compounds with highly conjugated  $\pi$ -electron systems. The three fractions were taken to dryness, dissolved at 5 mg/ml DMSO, and tested against  $G\alpha$ -stimulated hAC5 activity (Fig. 2 right).

Fraction O-3 with the best inhibitory efficiency was analyzed by low resolution LC/MS (Appendix Fig. 2). Its mass spectrum displayed a prominent peak at  $m/z$  616.3, beside some minor peaks at  $m/z$  614, 617 and 618. High resolution ESI-MS analysis of fraction O-3 revealed an  $[M-2H^++Fe^{3+}]^+$  ion ( $m/z$  616.1772) consistent with a molecular formula of  $C_{34}H_{32}FeN_4O_4$  (Appendix Fig. 3). A literature and database search identified the compound as heme b (*syn.* Fe<sup>III</sup>-protoporphyrin IX). This was supported by the analysis of the MS isotope pattern. The ratio of the peak areas for 614:616:617:618 were determined to be 7:100:43.8:12.6 (Appendix Fig. 2) which was in agreement with the predicted Fe isotope distribution of 6.3:100:40.9:9.3 attributable to <sup>54</sup>Fe, <sup>56</sup>Fe, <sup>57</sup>Fe and <sup>58</sup>Fe [26]. Furthermore, the fragment at 557.1640 and a minor at 498.1508, observed in the HR-MS spectrum, indicated the sequential loss of two ethanoic acid groups ( $C_2H_3O_2$ ) (Appendix Fig. 3), which is also characteristic for this compound class [27]. We further corroborated the identity of heme b by comparing the retention time and mass-spectra of

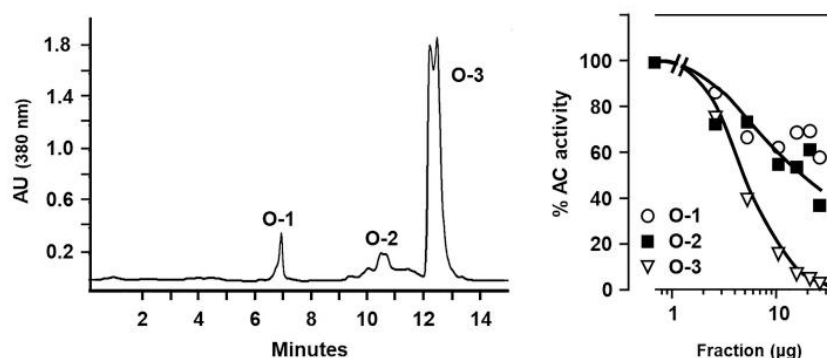


**Fig. 2.** Left: Fraction O is resolved into three subfractions by RP-HPLC. Right: Effect of subfractions O-1, O-2, and O-3 on 300 nM  $G\alpha$  stimulated hAC5. 100% activity corresponded to 1.43 nmol cAMP•mg<sup>-1</sup>•min<sup>-1</sup> (basal activity was 0.035). The data represent the mean of two experiments with two technical replicates.

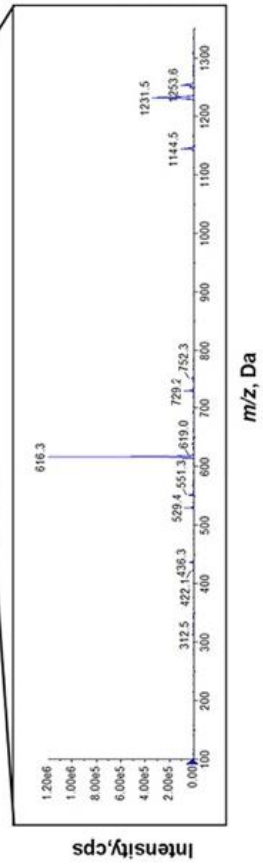
**Acidic lipid extract from bovine lung**

Si-VLC																	
Fraction	A	B	C	D	E	F	G	H	I	J	K	L	M	N	O	P	Q
Solvent	100% PE	90:10 PE:EA	80:20 PE:EA	60:40 PE:EA	40:60 PE:EA	20:80 PE:EA	100% EA	25:75 MeOH:EA	100% MeOH								
weight [mg]	3.1	4.5	459.1	404	285.8	70.1	29.5	21.6	344.6	753.3	95.7	85.3	175.5	136.3	54.7	27.4	17.9
AC5 % activity	116.5	125	100.5	80	85	48.5	84	87.5	102.5	44.5	11	1	30	50	44.5	38	25
m/z 616.3	-	-	-	-	-	-	-	-	-	-	+	+	+	+	+	+	+

**RP18-HPLC**

Fraction	O-1	O-2	O-3
weight [mg]	20	0.94	0.52
m/z 616.3	-	-	+

**Fractionation Scheme.** Si-VLC: Silica-Vacuum Liquid Chromatography, RP-HPLC: Reversed phase-High performance liquid chromatography, EA: Ethyl acetate, PE: Petrol ether, MeOH: Methanol, % remaining AC5 activity; values represent mean of 2 experiments in triplicates. 1 µg of fractions (5 mg/mL in DMSO) were added to the assay. Basal AC5 activity was 0.05 nmol cAMP·mg<sup>-1</sup>·min<sup>-1</sup>; 300 nM Gsα-stimulated AC5 activity was 2.1 nmol cAMP·mg<sup>-1</sup>·min<sup>-1</sup>.



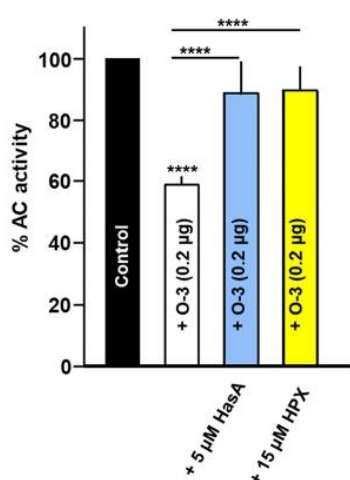


Fig. 3. Hemophore (HasA) and hemopexin (HPX) attenuate inhibition of hAC5 by fraction O-3. Basal activity was  $0.04 \pm 0.017$  nmol cAMP $\cdot$ mg $^{-1}$  $\cdot$ min $^{-1}$ . 300 nM Gs $\alpha$  activity (100%) was  $0.63 \pm 0.17$  nmol cAMP $\cdot$ mg $^{-1}$  $\cdot$ min $^{-1}$ . HPX and Has A did not affect basal or Gs $\alpha$ -stimulated hCA5 activity. \*\*\*\*;  $p < 0.0001$ . Error bars denote SEM ( $n = 4$  with two technical repetitions).

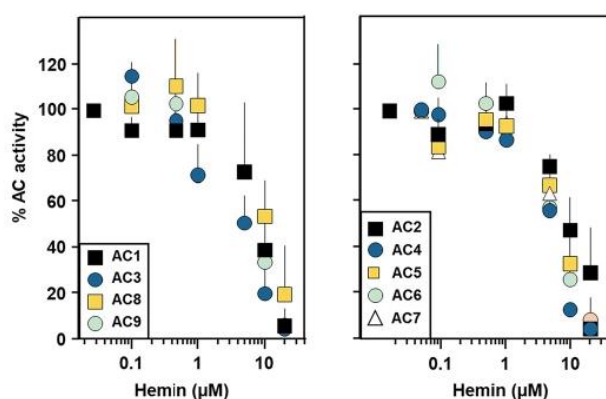


Fig. 4. Concentration-response curves for hemin inhibition of 300 nM Gs $\alpha$ -stimulated hAC isoforms. Basal and 100% Gs $\alpha$  stimulated activities together with the IC $_{50}$  concentrations are listed in appendix Table 1. Error bars denote SEM of 3–4 experiments with two technical replicates.

a commercial heme b standard (hemin) with fraction O-3 (Appendix Fig. 4). Hemin is heme b chloride. Below, we denote the isolated material from lung as heme b and the commercial sample used for most assays as hemin.

To biologically confirm the identity of heme b, we used the heme-binding proteins human hemopexin and bacterial hemophore HasA. In mammals, hemopexin, produced by the liver serves as heme b scavenger with high affinity ( $K_D$  values 320 to 0.1 pM [28,29]). Hemopexin is involved in heme b detoxification [30]. We produced the heme b-binding protein hemophore (HasA) from *Serratia marcescens*. HasA is an extracellular heme-binding protein for iron acquisition, binding heme with a  $K_d$  of  $5 \times 10^{10}$  ( $M^{-1}$ ) [31]. Hemopexin as well as hemophore significantly inhibited the action of fraction O-3 (Fig. 3).

### 3.2. Action of hemin on mammalian and bacterial class III adenylyl cyclases

Hemin attenuated Gs $\alpha$ -activated AC activity of all nine membranous AC isoforms expressed in HEK293 cells with IC $_{50}$  concentrations of 7.5 to

12  $\mu$ M (Fig. 4; Appendix Table 1). The IC $_{50}$  was independent from the concentration of Gs $\alpha$  used for hAC stimulation, e.g., at 700 nM Gs $\alpha$  the IC $_{50}$  for hAC5 was 10.4  $\mu$ M (data not shown). This indicated that Gs $\alpha$  and hemin were not competing for identical binding sites. Similarly, we investigated the effect of hemin on basal activities of hAC1, 2, 5 and 9 (one from each subclass). Basal activities were similarly inhibited in a concentration dependent manner (see Appendix Fig. 5).

To examine the structure-activity relationship for hemin we used hematin, protoporphyrin IX, biliverdin and chlorophyll *a* (the structural formula are depicted in Appendix Fig. 1). Hematin is the ferric protoporphyrin hydroxide [32]. Protoporphyrin IX is the last common precursor in heme and chlorophyll biosynthesis and lacks a central metal ion. Biliverdin, a product of heme catabolism, has an opened porphyrin ring system and lacks the ferric ion [33]. At 10  $\mu$ M, protoporphyrin IX, hematin and biliverdin had no significant effect on Gs $\alpha$ -stimulated hAC5 activity (Fig. 5). At 40  $\mu$ M, only up to 30% inhibition was observed for protoporphyrin IX or hematin, much less than with hemin (Fig. 5; Appendix Table 2).

The catalytic domains of eukaryotic ACs share extensive sequence similarity with their bacterial class III progenitors [15]. The possibly regulatory N-termini in bacterial AC isoforms vary considerably [9,15]. The bacterial membrane anchoring domains have two, four and six  $\alpha$ -helices and many bacterial ACs have none and are soluble [15]. Bacterial ACs are not regulated by Gs $\alpha$ . We investigated the effect of hemin and structurally related compounds using the mycobacterial AC Rv1625c, a likely precursor of human ACs with a hexahelical membrane anchor [10], the mycobacterial AC Rv3645 which has a hexahelical membrane anchor and a HAMP domain between membrane exit and catalytic domain [11], the membrane-bound cyanobacterial AC CyaG from *Arthrospira maxima* with two membrane spans, an S-helix and a HAMP domain in front of the catalytic domain [34] and the soluble mycobacterial AC Rv1264 which is regulated by pH [35]. Further, we analyzed the soluble construct of Rv1625c, D204-G443 [10]. Without exception, hemin inhibited these bacterial ACs with comparable efficacy to the human AC isoforms (Fig. 5; Appendix Table 2). Significant differences in sensitivity were apparent for hematin, protoporphyrin IX, and biliverdin (Fig. 5, Appendix Table 2). The soluble AC Rv1264 and the soluble construct Rv1625c-D204-G443 construct were inhibited by hematin, protoporphyrin IX and biliverdin (Appendix Fig. 6 and table 2). The data suggest a direct inhibitory attack at the catalytic dimer. The presence of a HAMP domain (Rv3645) or a HAMP domain in line with an S-helix in front of the catalytic domain as in CyaG did not affect inhibition by hemin (Fig. 5, Appendix Fig. 6 and table 2).

Structurally, chlorophyll is closely related to hemin. It shares the tetrapyrrole ring system and several side chains. It carries a central magnesium atom ( $Mg^{2+}$ ) and a tetra-isoprenoid C20 phytol esterified to a propionic acid sidechain. To determine whether redox reactions, possibly mediated by the central  $Fe^{3+}$  of hemin, might be involved in inhibition we examined the effect of chlorophyll *a* on hAC5. Surprisingly, chlorophyll *a* inhibited hAC5 and the membranous mycobacterial Rv1625c AC (Fig. 6). The inhibition was only somewhat less pronounced compared with hemin. Calculated IC $_{50}$  concentrations were 30 and 10  $\mu$ M for hAC5 and Rv1625c, respectively. The data excluded redox processes as a cause for class III AC inhibition by hemin.

### 3.3. Hemin inhibits cAMP accumulation in HEK293 cells

The effect of hemin on cAMP accumulation in intact HEK293 cells transfected with hAC3, 5, 7 and 9, i.e., one of each subclass was examined. Hemin at concentrations above 50  $\mu$ M has been reported to be cytotoxic during extended incubations of astrocytes (12 to 24 h; [36]). We checked hemin toxicity for HEK293 cells under our incubation conditions (50  $\mu$ M hemin, 45 min). Cells remained viable. Isoproterenol was used for stimulating intracellular cAMP production in HEK293 cells. Hemin inhibited cAMP accumulation with IC $_{50}$  concentrations comparable to HEK293 membrane preparations (Fig. 7). This left the

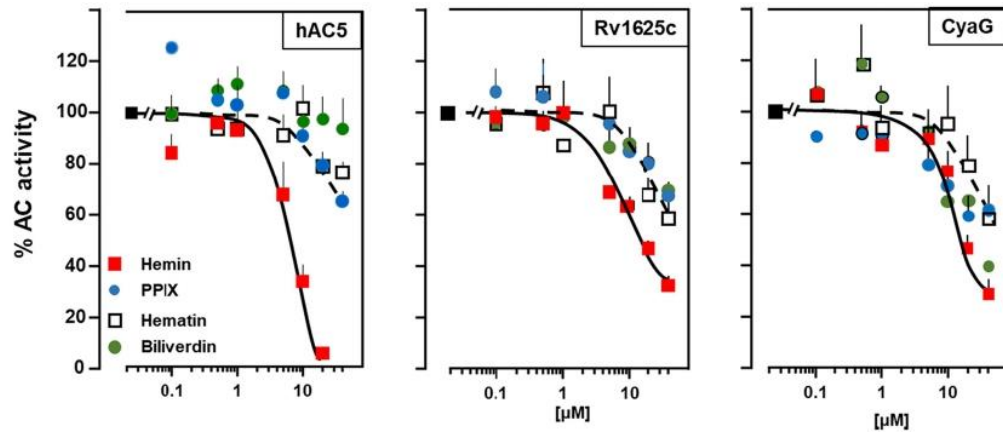


Fig. 5. Structural activity relationship of hemin inhibition of hAC5, mycobacterial AC Rv1625c and cyanobacterial AC CyaG from *Arthrosira maxima*. hAC5 Gs $\alpha$  (300 nM) activity (100%) corresponded to  $1.56 \pm 0.05$  nmol cAMP $\cdot$ mg $^{-1}\cdot$ min $^{-1}$  (basal was  $0.02 \pm 0.002$ ). Rv1625c activity (100%) was  $2.5 \pm 0.9$   $\mu$ mol cAMP $\cdot$ mg $^{-1}\cdot$ min $^{-1}$ . CyaG activity (100%) was  $0.6 \pm 0.07$   $\mu$ mol cAMP $\cdot$ mg $^{-1}\cdot$ min $^{-1}$ . Error bars denote SEM of 3–5 experiments with two technical repetitions.

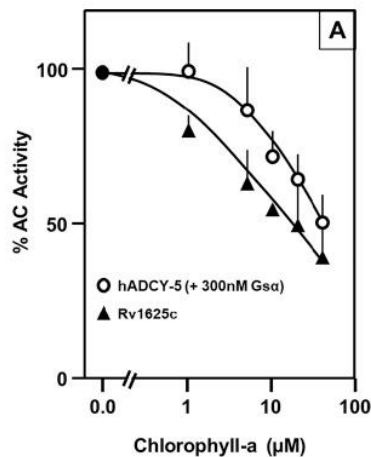


Fig. 6. Chlorophyll *a* inhibits hAC5 expressed in HEK293 membranes and mycobacterial AC Rv1625c. hAC5 Gs $\alpha$  activity (100%) corresponded to  $1.4 \pm 0.2$  nmol cAMP $\cdot$ mg $^{-1}\cdot$ min $^{-1}$  (basal activity was 0.03). Rv1625c activity (100%) was  $2.3 \pm 0.3$   $\mu$ mol cAMP $\cdot$ mg $^{-1}\cdot$ min $^{-1}$ . Error bars denote SEM of 4–6 experiments with two technical repetitions.

possibility open that hemin acted via an extracellular binding site. However, because the hydrophobic hemin can pass the cell membrane such a conclusion is premature [37,38]. Chlorophyll *a* did not inhibit isoproterenol-stimulated cAMP formation in HEK293 cells (Fig. 7, right). Probably chlorophyll with its C20 phytyl ester cannot cross into the cytosol. This data supports the notion that the membrane anchors of hACs are not involved in the inhibitory action of hemin, in line with the inhibition of ACs without membrane anchors such as Rv1264 or Rv1625c-D204-G443.

#### 3.4. Hemin inhibits adenylyl cyclases in brain cortical membranes

Next, we prepared membranes from mouse brain cortex in which most mAC isoforms are expressed (except mAC4) [39]. Basal, as well as Gs $\alpha$  stimulated activities of mACs were significantly inhibited by hemin (Fig. 8A and Appendix Fig. 7). Hemin concentration response curves showed an IC $_{50}$  of 9 and 8.5  $\mu$ M for basal and Gs $\alpha$  stimulated activities, respectively. These concentrations are almost identical to those observed in hAC isoforms expressed in HEK293 cells. The data suggest that (a) ACs in brain cortex are similarly sensitive to hemin inhibition,

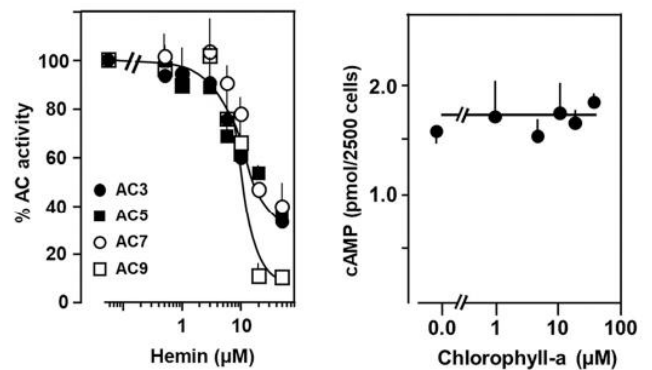
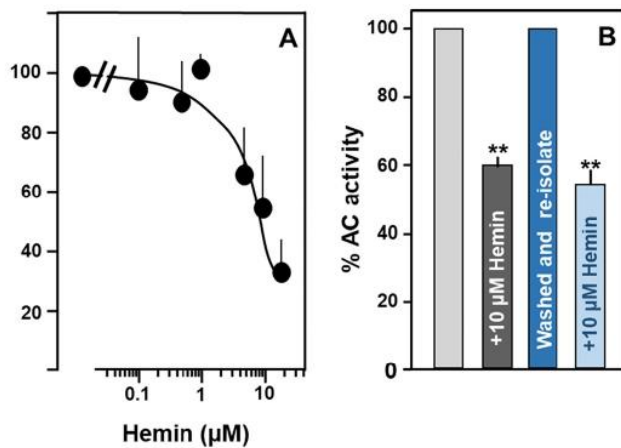


Fig. 7. Hemin inhibits cAMP accumulation in HEK293 cells, chlorophyll *a* does not. HEK293 cells transfected with respective hAC isoforms were stimulated with 10  $\mu$ M isoproterenol. Basal and isoproterenol stimulated activities are listed in appendix Table 3. IC $_{50}$  of hemin against AC3, 5, 7 and 9 were 8.8, 8.9, 11.8 and 11.6  $\mu$ M, respectively. Error bars denote SEM of 3–4 experiments each with three technical replicates.

and, (b) the effect of hemin may have physiological relevance. Hemin inhibition was also observed when Gs $\alpha$ -stimulation was synergistically enhanced by 10  $\mu$ M forskolin (Appendix Fig. 8). This indicated that forskolin activation and hemin inhibition possibly were acting at separate sites of the protein.

Due to its lipophilicity, hemin may irreversibly enter the hydrophobic phospholipid layer causing membrane disorder and inhibition of membrane bound ACs. Alternatively, hemin may reversibly affect the catalytic activity. We used cortical membranes to test these possibilities. Membranes were incubated for 15 min with 10  $\mu$ M hemin. After collection and washing, the isolated membranes were again subjected to Gs $\alpha$ -stimulation  $\pm$  hemin (Fig. 8B). The data indicated that hemin inhibition is reversible, i.e., it is not tightly lodged in the membrane and inhibition probably is not caused by permanently disturbing membrane integrity or covalently binding to the hAC protein.

Hemin is a reactive compound, and at higher concentrations a rather toxic blood component. Therefore, it may also affect the activity of other proteins and enzymes. As a control we used the tetrameric enzyme lactate dehydrogenase and the monomeric protease trypsin. The activity of both enzymes was not affected by 40  $\mu$ M hemin (Appendix Fig. 9).



**Fig. 8.** A) Hemin inhibits  $G_{s\alpha}$ -stimulated cAMP accumulation in mouse brain cortical membranes. 300 nM  $G_{s\alpha}$  stimulated activity (100%) was  $6.8 \pm 0.64$  nmol cAMP $\cdot$ mg $^{-1}\cdot$ min $^{-1}$ . The  $IC_{50}$  for hemin was 8.5  $\mu$ M. Error bars denote SEM.  $N = 3$ , each with two technical replications. B) Inhibition of  $G_{s\alpha}$  stimulated brain cortical membranes by hemin is reversible. After stimulation by 600 nM  $G_{s\alpha} \pm 10 \mu$ M hemin, membranes were collected by centrifugation at 100,000 g and re-assayed.  $N = 4$ , error bars denote SEM. 100% stimulation was  $6.6 \pm 0.3$  nmol cAMP/mg/min.  $p < 0.01$ .

#### 4. Discussion

This work started with the intention to identify a ligand or ligands for the tandem of membrane anchors of nine mammalian AC isoforms. We screened bovine lung extracts for inhibitory activity because lung is a rather complex tissue composed of various cell types and is easily available. The identification of non-protein bound heme b, a well-known blood component, as an efficient and general inhibitor of class III ACs, particularly mammalian ACs, was surprising. The chemical identity of heme b was unequivocally proven by LC/MS and by direct comparison with commercial hemin (see Appendix Figs 2–4). The biochemical identity and functionality were demonstrated using the human cytoprotective agent hemopexin which is secreted into the blood from the liver, binds heme b with high affinity and delivers it to the liver for degradation. Further, we used the bacterial hemophore HasA from *Serratia marcescens* which similarly binds heme b with very high affinity. HasA is used to fill the bacterial need for iron. Hemopexin and HasA attenuated heme b inhibition of hAC5 by fraction O-3, unequivocally demonstrating the biological activity (Fig. 3).

So far, the connections between cAMP and heme b were induction of heme oxygenase-1 by the membrane-permeable cAMP derivative dibutyl cAMP in smooth muscle cells [40–42], an inhibitory effect on isoproterenol-stimulated lipolysis in fat cells [43], and stimulation of cAMP production in blood mononuclear cells [44]. Our data indicate that free hemin efficiently inhibited all membrane-delimited mammalian ACs. Therefore, free heme b does not qualify as a specific ligand for any individual isoform. Further, for a specific AC ligand we would not expect a compound such as heme b, which is abundant. Our data do not allow to propose a mechanism of action for heme b. Hemin inhibited basal as well as  $G_{s\alpha}$ -stimulated ( $\pm$  forskolin) hAC activities. This indicated that heme b possibly bound at the AC proteins at sites differing from  $G_{s\alpha}$  or forskolin. We assume that heme b binds directly at the catalytic dimer. This assumption is in line with the inhibition of the soluble AC Rv1264 and the soluble AC construct from Rv1625c (Appendix Fig. 6 and Appendix Table 2). The inhibition of isoproterenol-stimulated cAMP in HEK293 cells presumably involves entry of heme b into the cells as it readily crosses cell membranes ([45] and ref.'s therein). Chlorophyll *a* inhibited *in vitro* but not in intact cells (Fig. 6

and 7). Chlorophyll *a* with its tetra-isoprenoid C20 phytol ester probably is retained in the membrane and cannot cross into the cytosol. This differs from hemin.

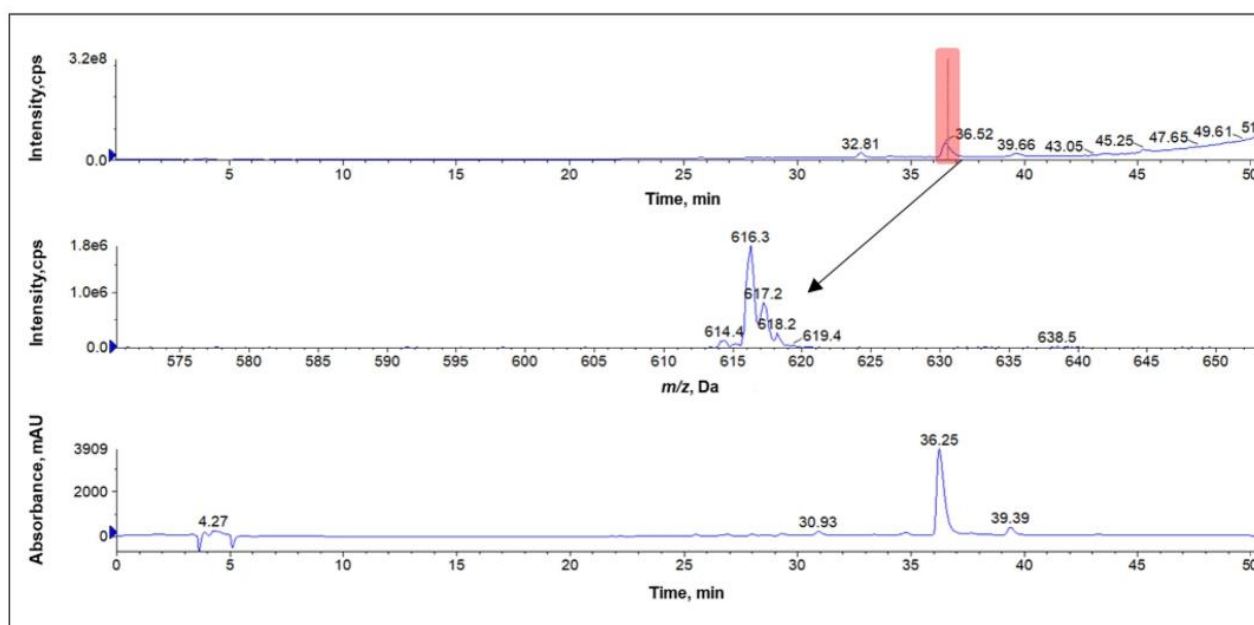
The structural specificity of heme action as compared to protoporphyrin IX, an immediate biosynthetic precursor, to biliverdin, the first metabolic degradation product by heme-oxygenase-1, and to hematin was remarkable. Several reasons might explain this observation. The large loss of efficiency of the more lipophilic protoporphyrin IX strongly indicates that subtle structural differences caused by the centrally coordinated metal ion may contribute to specific binding and inhibition. Biliverdin is an open chain of four pyrrolic rings and its geometry differs profoundly from hemin or protoporphyrin, thus more easily explaining the loss of inhibitory activity. The scant inhibitory efficiency of hematin was a further surprise because it differs from hemin only by replacement of the coordinated chloride at the  $Fe^{3+}$  ion by a hydroxy group. The covalent radii of the chloride anion (102 pm) and a hydroxy group (110 pm) are similar. A major difference is that the hydroxy group is a hydrogen bond acceptor and donor whereas the chloride in heme b cannot form hydrogen bridges; it may form weak van der Waals contacts. The formation of hydrogen bridges may attenuate hematin binding and be responsible for loss of inhibitory efficiency. Heme can bind in either of two flipped orientations defined by the asymmetry of the vinyl and propionyl substituents of the porphyrin skeleton [46]. It is possible that hemin binds in an inhibitory orientation which is disfavored in hematin. Such disparate properties obviously could contribute to differences in biochemical properties.

An unexpected result was that chlorophyll *a* inhibited hAC5 as well as the mycobacterial Rv1625 AC (Fig. 6). In chlorophyll the tetrapyrrole ring system has  $Mg^{2+}$  at the center. These data virtually exclude that the inhibitory action of hemin is caused by redox reactions. Chlorophyll *a* had no effect on cAMP formation in intact HEK293 cells (Fig. 7).

Another aspect merits discussion, the  $\beta$ -subunit of the soluble guanylyl cyclase contains a ferrous b-type haem prosthetic group (heme b) facilitating NO binding and regulation [47,48]. The heme binds via its carboxylic groups to tyrosine (Y135) and arginine (R139). Histidine (H105) is a reversible axial ligand at the  $Fe^{2+}$  in heme b [48]. This heme-binding triad is N-terminal to the catalytic site. An alignment with mammalian ACs shows that such a binding triad is absent in ACs. The coincidence that heme b inhibits soluble guanylyl cyclases and inhibits class III ACs provokes the question concerning the evolution of these proteins and their disparate properties.

Taken together, the data add a novel aspect of heme b activity within the existing broad spectrum of physiological and toxic actions which applies to all cells and tissues. Heme is a known pro-oxidant and has pro-inflammatory and cytotoxic effects [49]. Heme b is further reported to be a signalling molecule regulating transcription factors and MAP kinases [45]. An important question is whether the concentrations of extracellular heme b under pathophysiological conditions are sufficient to attenuate AC activities [50]. Normally, concentrations of extracellular heme b are low (about 1  $\mu$ M) and tightly controlled by binding to hemopexin, and, less specifically, to serum albumin. In addition, heme-oxygenase's effectively keep cytosolic heme b concentrations low under normal conditions [49,51]. However, in several haemolytic pathologies, such as sickle cell disease, extravascular haemolysis, malaria attacks, sepsis and septic shock, atherosclerosis, and after transfusion of packed red blood cells, heme b concentrations are reported to increase considerably [49,52]. Serum levels from 20 up to 350  $\mu$ M have been observed [50,53]. Considering the low concentrations of heme b required for inhibition of hAC activities it may well contribute to pathologic symptoms which are common to these disease states. Therefore, this report may and should call medical attention to a central second messenger system in pathophysiological conditions of elevated heme b concentrations.





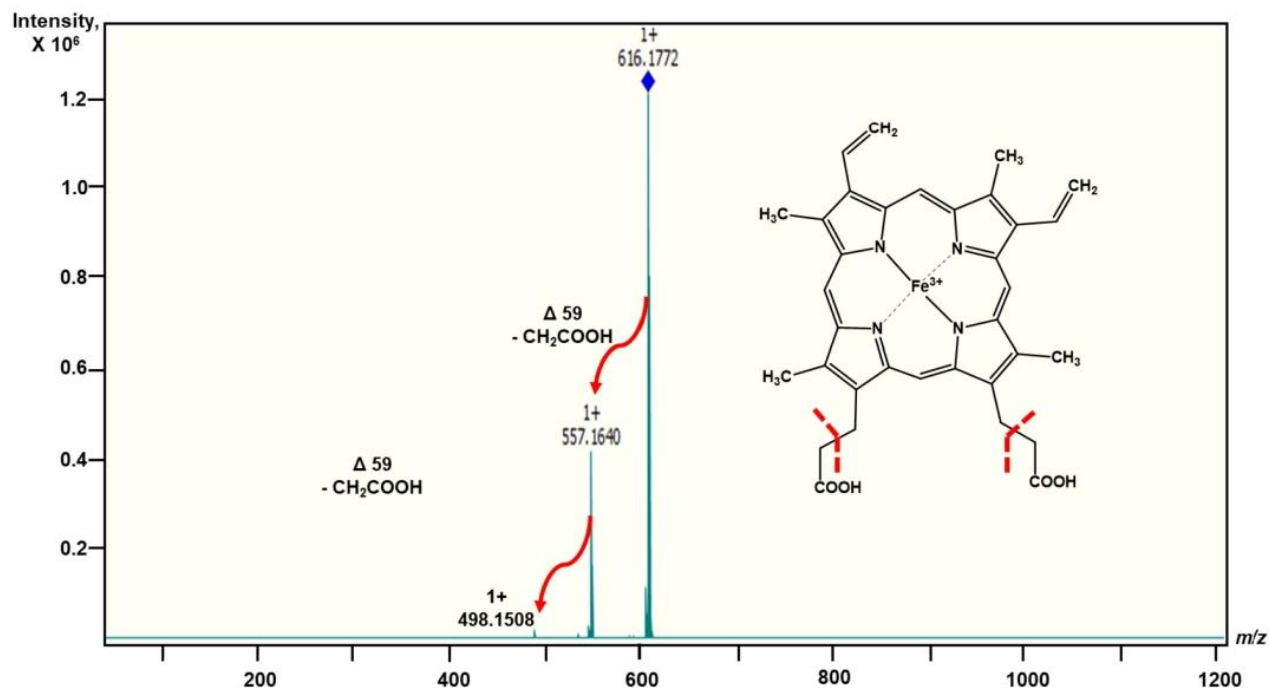
**Appendix Fig. 2.** Low-resolution-LC-MS of fraction O-3.

Top panel: LC-MS Total ion chromatogram (TIC) of fraction O-3.

Middle panel: MS spectrum of the peak at 36.52 min (shaded in red). It shows the dominant ion of  $m/z$  616.3  $[\text{Fe(III)PTP}]^+$  and further ions at  $m/z$  614, 617 and 618, corresponding to the predicted isotopic composition of  $\text{Fe}^{3+}$  ( $^{54}\text{Fe}$ ,  $^{57}\text{Fe}$  and  $^{56}\text{Fe}$ ).

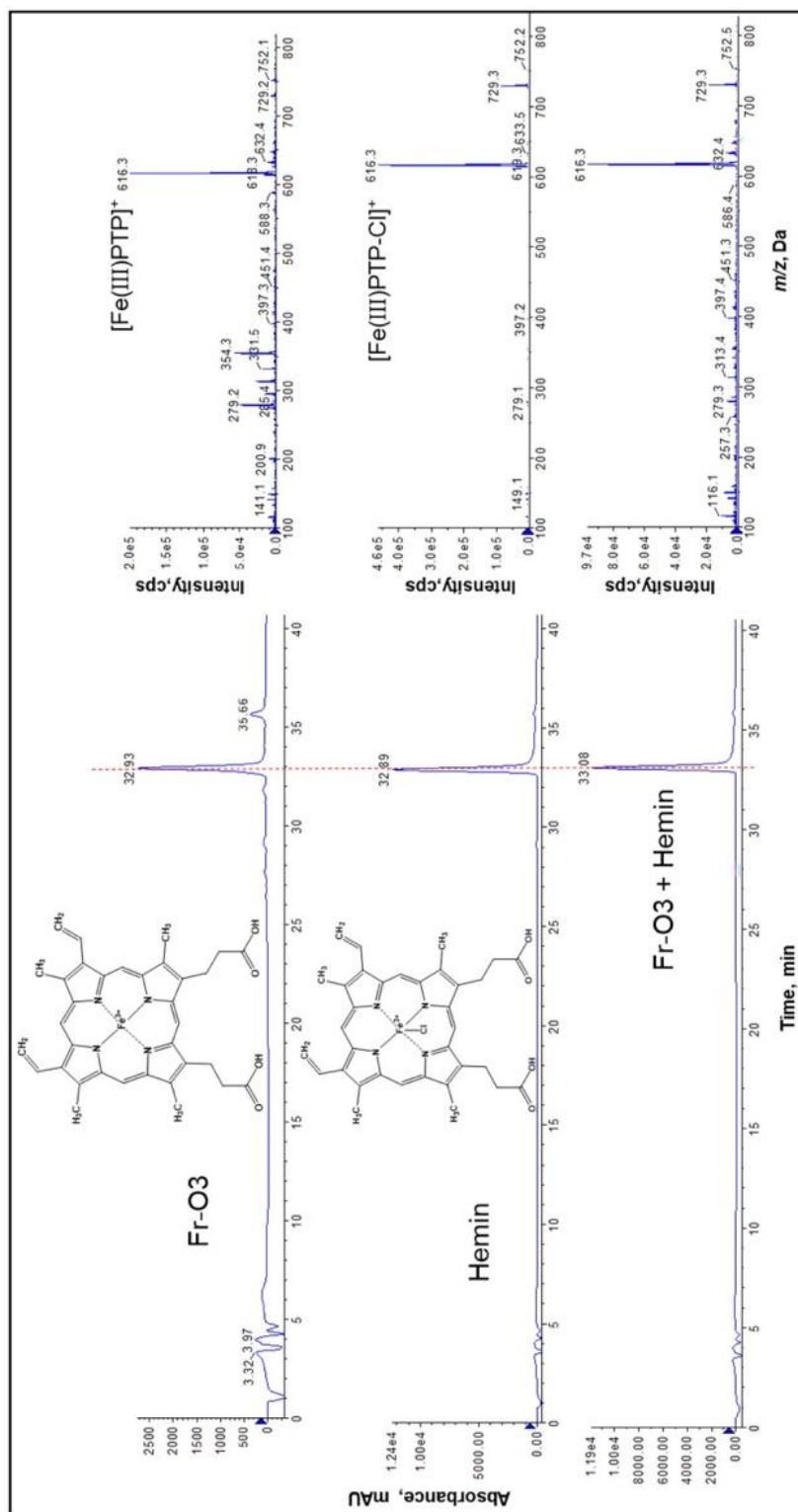
Bottom panel: Extracted wavelength chromatogram (XWC) from 380 to 400 nm is shown.

Abbreviations: cps: counts per second, mAU: milli absorbance units



**Appendix Fig. 3.** HR-ESI-MS/MS spectrum of fraction O-3 and fragmentation pattern

$m/z$  616.1772  $[\text{Fe(III)PTP}]^+$  calculated for  $\text{C}_{34}\text{H}_{32}\text{FeN}_4\text{O}_4$   $m/z$  616.1773,  $\Delta$  (mass error) =  $-0.2$  ppm. The x-axis is stretched such that the Fe-isotope pattern is not clearly visible (compare to appendix Fig. 2).



**Appendix Fig. 4.** Comparison of standard hemein and fraction O-3 harbouring heme b

Top panel:

Left: Extracted wavelength chromatogram (XWC) at 380 nm of an LC-MS run of fraction O-3 harbouring heme b.

Right: LR-MS spectrum, extracted at 32.93 min, showing the ion peak  $[M-2H^+ + Fe^{3+}]^+$  at  $m/z$  616.3.

Middle panel:

Left: XWC at 380 nm of the reference compound hemein (ferric chloride heme).

Right: LR-MS spectrum, extracted at 32.89 min, showing a pseudo-molecular ion peak  $[M-2H^+ - Cl + Fe^{3+}]^+$  at  $m/z$  651.3 under ESI-MS conditions.

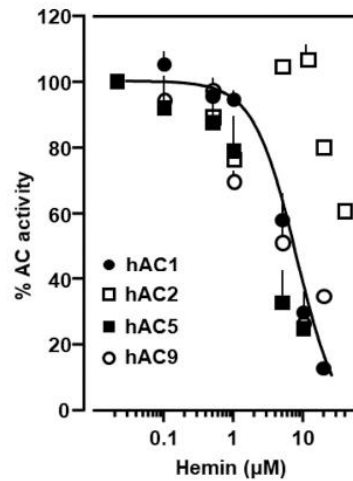
$Fe^{3+}$  was not detectable at  $m/z$  651.3 under ESI-MS conditions.

Bottom panel:

Left: XWC at 380 nm of an LC-MS run of fraction O-3 and co-injected hemein standard. In agreement with literature reports [27], both compounds coelute forming a broader peak at a slightly higher retention time.

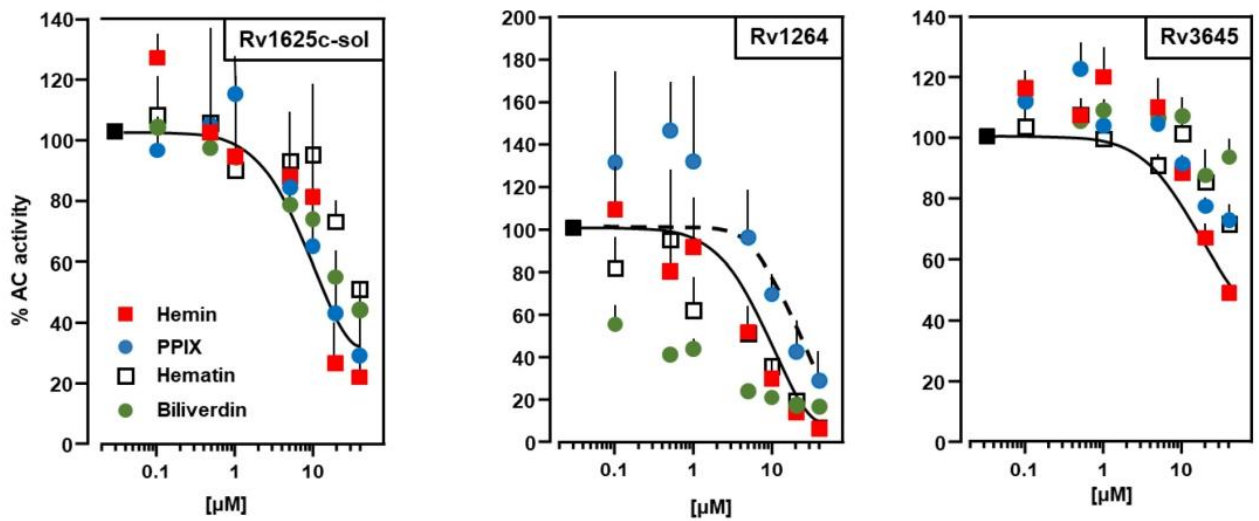
Right: LR-MS spectrum, extracted at 33.08 min, showing congruently the pseudo-molecular ion peak  $[M-2H^+ - Cl + Fe^{3+}]^+$  of hemein and the molecular ion  $[M-2H^+ + Fe^{3+}]^+$  of heme-b, both at  $m/z$  616.3.

Abbreviations: cps: counts per second, mAU: milli absorbance units



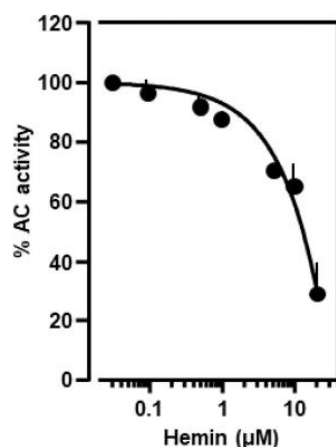
**Appendix Fig. 5.** Hemin inhibition of hAC basal activities

Basal activities of hAC1, 2, 5 and 9 were  $0.016 \pm 0.05$ ,  $0.03 \pm 0.004$ ,  $0.013 \pm 0.002$  and  $0.01 \pm 0.003$   $\text{nmol cAMP}\cdot\text{mg}^{-1}\cdot\text{min}^{-1}$ , respectively. Hemin  $\text{IC}_{50}$  values against AC1, 2, 5 and 9 were 6.3,  $\approx 40$ , 2 and 3  $\mu\text{M}$  respectively. Error bars denote SEM of 3–4 experiments with two technical replicates.

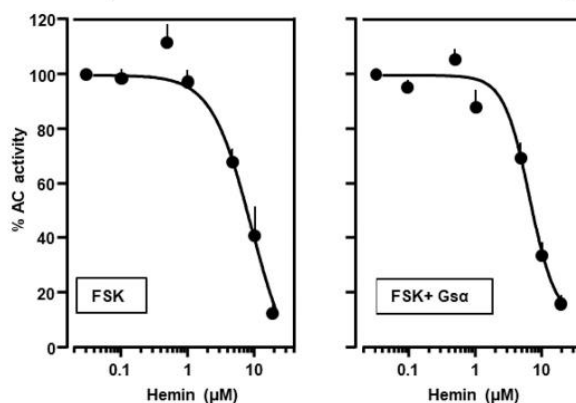


**Appendix Fig. 6.** Effect of hemin and its analogues on bacterial ACs.

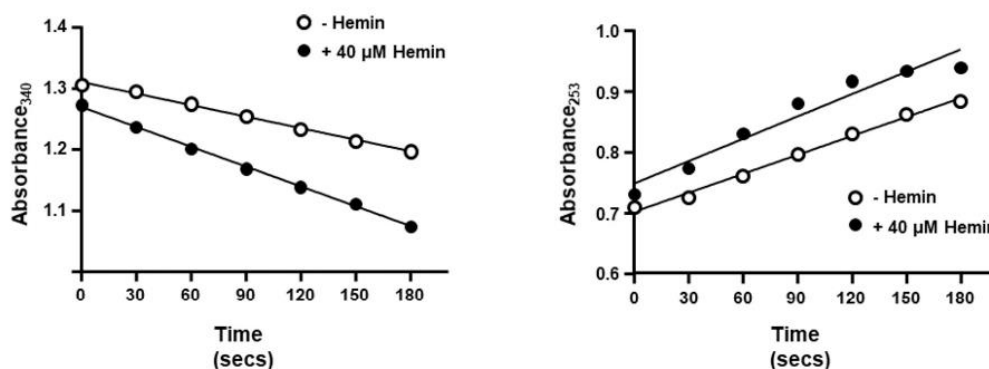
Rv1625c soluble monomer (sol) basal activity (100%) was  $52.7 \pm 10.9$   $\mu\text{mol cAMP}\cdot\text{mg}^{-1}\cdot\text{min}^{-1}$ . Rv1264 basal activity (100%) was  $10.18 \pm 2.6$   $\mu\text{mol cAMP}\cdot\text{mg}^{-1}\cdot\text{min}^{-1}$ . Rv3645 basal activity (100%) was  $0.93 \pm 0.09$   $\mu\text{mol cAMP}\cdot\text{mg}^{-1}\cdot\text{min}^{-1}$ . Error bars denote SEM of 3–5 experiments.



**Appendix Fig. 7.** Hemin inhibits basal activity of adenylyl cyclase in brain cortical membrane prepared from mouse. Basal activity (100%) was  $0.238 \pm 0.02 \text{ nmol cAMP} \cdot \text{mg}^{-1} \cdot \text{min}^{-1}$ . Error bars denote SEM.  $N = 3$ . The calculated  $\text{IC}_{50}$  of hemin was  $9 \mu\text{M}$ .



**Appendix Fig. 8.** Hemin inhibition of hAC5 activity stimulated by forskolin and forskolin +  $\text{G}\alpha$ . Left: Inhibition of  $250 \mu\text{M}$  forskolin stimulated hAC5. 100% activity was  $1.3 \pm 0.5 \text{ nmol cAMP} \cdot \text{mg}^{-1} \cdot \text{min}^{-1}$ . Basal activity was  $0.008 \pm 0.001 \text{ nmol cAMP} \cdot \text{mg}^{-1} \cdot \text{min}^{-1}$ . Hemin  $\text{IC}_{50}$  concentration was  $8.8 \mu\text{M}$ . Right: Inhibition of hAC5 activity stimulated by  $10 \mu\text{M}$  forskolin and  $300 \text{ nM}$   $\text{G}\alpha$ . 100% stimulation was  $3.44 \pm 0.4 \text{ nmol cAMP} \cdot \text{mg}^{-1} \cdot \text{min}^{-1}$ . The  $\text{IC}_{50}$  concentration of hemin was  $6.9 \mu\text{M}$ . Error bars denote SEM of 3 experiments.



**Appendix Fig. 9.** Hemin effect on lactate dehydrogenase and trypsin. Left:  $40 \mu\text{M}$  hemin did not inhibit lactate dehydrogenase activity. Absorbance at  $340 \text{ nm}$  was recorded for 3 mins. Right: Trypsin activity was not affected by hemin. Absorbance at  $253 \text{ nm}$  was monitored for 3 min.

**Appendix Table 1**  
Basal and G $\alpha$  stimulated activities of hACs cultured in HEK293 cells.

hAC isoform	Basal Activity nmol cAMP•mg <sup>-1</sup> •min <sup>-1</sup>	300 nM G $\alpha$ stimulated Activity nmol cAMP•mg <sup>-1</sup> •min <sup>-1</sup>	IC <sub>50</sub> of hemin ( $\mu$ M)
AC1	0.07 $\pm$ 0.02	0.3 $\pm$ 0.06	10
AC2	0.19 $\pm$ 0.08	2.82 $\pm$ 0.79	7.4
AC3	0.02 $\pm$ 0.01	0.2 $\pm$ 0.03	8.5
AC4	0.01 $\pm$ 0.01	0.11 $\pm$ 0.05	5.5
AC5	0.05 $\pm$ 0.01	1.76 $\pm$ 0.37	8.4
AC5 (Porcine hemin)	0.01 $\pm$ 0.004	1.21 $\pm$ 0.05	8.6
AC6	0.01 $\pm$ 0.01	0.11 $\pm$ 0.01	7.5
AC7	0.01 $\pm$ 0.002	0.14 $\pm$ 0.05	7.9
AC8	0.21 $\pm$ 0.03	2.27 $\pm$ 0.78	13.7
AC9	0.04 $\pm$ 0.01	1.38 $\pm$ 0.09	12

Activities are mean  $\pm$  SEM. N = 3–4 with 2–3 technical repetitions each.  
Porcine hemin was  $\geq$ 98% pure.

**Appendix Table 2**  
IC<sub>50</sub> values ( $\mu$ M) of hemin and its analogues against ACs.

	Hemin	Protoporphyrin IX	Hematin	Biliverdin
hAC5	8.5	$\approx$ 100	> 100	$\approx$ 1000
Rv1625c	11	$\approx$ 100	$\approx$ 100	> 100
Rv3645	14	$\approx$ 100	> 100	> 100
Rv1625c soluble monomer	12	10 <sup>(1)</sup>	$\approx$ 30	$\approx$ 40
Rv1264	6	$\approx$ 20 <sup>(2)</sup>	$\approx$ 10	$\approx$ 1
CyaG	15	> 100	$\approx$ 80	$\approx$ 20

Significances:

(1) Rv1625c soluble monomer; PPIX IC<sub>50</sub> differs significantly from hematin and biliverdin,  $p < 0.05$ .

(2) Rv1264; PPIX IC<sub>50</sub> differs significantly from hemin,  $p < 0.05$ , and hematin and biliverdin,  $p < 0.01$ .

**Appendix Table 3**  
Basal and isoproterenol stimulated activities of hACs transfected in HEK293 cells.

hAC isoform	Basal activity cAMP pmol/20 $\mu$ L	Isoproterenol stimulated activity cAMP pmol/20 $\mu$ L
AC3	0.05 $\pm$ 0.03	1.92 $\pm$ 0.69
AC5	0.89 $\pm$ 0.25	1.95 $\pm$ 0.54
AC7	0.32 $\pm$ 0.01	0.43 $\pm$ 0.07
AC9	0.21 $\pm$ 0.04	0.72 $\pm$ 0.01

Activities are mean  $\pm$  SEM. N = 3–4 with two technical repetitions each.

## References

- [1] K.F. Ostrom, et al., Physiological roles of mammalian transmembrane adenylyl cyclase isoforms, *Physiol. Rev.* 102 (2022) 815–857.
- [2] C.W. Dessauer, et al., International Union of Basic and Clinical Pharmacology. CI. Structures and small molecule modulators of mammalian adenylyl Cyclases, *Pharmacol. Rev.* 69 (2017) 93–139.
- [3] W.J. Tang, A.G. Gilman, Type-specific regulation of adenylyl cyclase by G protein beta gamma subunits, *Science* 254 (1991) 1500–1503.
- [4] W.J. Tang, A.G. Gilman, Adenylyl cyclases, *Cell* 70 (1992) 869–872.
- [5] R.K. Sunahara, R. Taussig, Isoforms of mammalian adenylyl cyclase: multiplicities of signaling, *Mol. Interv.* 2 (2002) 168–184.
- [6] J. Krupinski, et al., Adenylyl cyclase amino acid sequence: possible channel- or transporter-like structure, *Science* 244 (1989) 1558–1564.
- [7] J.E. Schultz, The evolutionary conservation of eukaryotic membrane-bound adenylyl cyclase isoforms, *Front. Pharmacol.* 13 (2022) 1009797.
- [8] J.E. Schultz, S. Klumpp, R. Benz, W.J. Schurhoff-Goeters, A. Schmid, Regulation of adenylyl cyclase from Paramecium by an intrinsic potassium conductance, *Science* 255 (1992) 600–603.
- [9] J.E. Schultz, J. Natarajan, Regulated unfolding: a basic principle of intraprotein signaling in modular proteins, *Trends Biochem. Sci.* 38 (2013) 538–545.
- [10] Y.L. Guo, T. Seebacher, U. Kurz, J.U. Linder, J.E. Schultz, Adenylyl cyclase Rv1625c of mycobacterium tuberculosis: a progenitor of mammalian adenylyl cyclases, *EMBO J.* 20 (2001) 3667–3675.
- [11] K. Kanchan, et al., Transmembrane signaling in chimeras of the Escherichia coli aspartate and serine chemotaxis receptors and bacterial class III adenylyl cyclases, *J. Biol. Chem.* 285 (2010) 2090–2099.
- [12] S. Beltz, J. Bassler, J.E. Schultz, Regulation by the quorum sensor from Vibrio indicates a receptor function for the membrane anchors of adenylyl cyclases, *Elife* 5 (2016).
- [13] T. Seebacher, J.U. Linder, J.E. Schultz, An isoform-specific interaction of the membrane anchors affects mammalian adenylyl cyclase type V activity, *Eur. J. Biochem.* 268 (2001) 105–110.

- [14] M. Ziegler, et al., A novel signal transducer element intrinsic to class IIIa and IIIb adenylyl cyclases, *FEBS J.* 284 (2017) 1204–1217.
- [15] J. Bassler, J.E. Schultz, A.N. Lupas, Adenylyl cyclases: receivers, transducers, and generators of signals, *Cell. Signal.* 46 (2018) 135–144.
- [16] C. Qi, S. Sorrentino, O. Medalia, V.M. Korkhov, The structure of a membrane adenylyl cyclase bound to an activated stimulatory G protein, *Science* 364 (2019) 389–394.
- [17] A. Seth, M. Finkbeiner, J. Grischin, J.E. Schultz, G $\alpha$  stimulation of mammalian adenylyl cyclases regulated by their hexahelical membrane anchors, *Cell. Signal.* 68 (2020), 109538.
- [18] S. Diel, K. Klass, B. Wittig, C. Kleuss, Gbetagamma activation site in adenylyl cyclase type II. Adenylyl cyclase type III is inhibited by Gbetagamma, *J. Biol. Chem.* 281 (2006) 288–294.
- [19] M.P. Graziano, M. Freissmuth, A.G. Gilman, Expression of Gs alpha in *Escherichia coli*. Purification and properties of two forms of the protein, *J. Biol. Chem.* 264 (1989) 409–418.
- [20] M.P. Graziano, M. Freissmuth, A.G. Gilman, Purification of recombinant Gs alpha, *Methods Enzymol.* 195 (1991) 192–202.
- [21] T.A. Baldwin, Y. Li, C.S. Brand, V.J. Watts, C.W. Dessauer, Insights into the regulatory properties of human adenylyl cyclase type 9, *Mol. Pharmacol.* 95 (2019) 349–360.
- [22] M.G. Cumbay, V.J. Watts, Novel regulatory properties of human type 9 adenylyl cyclase, *J. Pharmacol. Exp. Ther.* 310 (2004) 108–115.
- [23] M. Soto-Velasquez, M.P. Hayes, A. Alpsy, E.C. Dykhuizen, V.J. Watts, A novel CRISPR/Cas9-based cellular model to explore adenylyl cyclase and cAMP signaling, *Mol. Pharmacol.* 94 (2018) 963–972.
- [24] J.E. Schultz, B.H. Schmidt, Treatment of rats with thyrotropin (TSH) reduces the adrenoceptor sensitivity of adenylyl cyclase from cerebral cortex, *Neurochem. Int.* 10 (1987) 173–178.
- [25] E.G. Bligh, W.J. Dyer, A rapid method of total lipid extraction and purification, *Can. J. Biochem. Physiol.* 37 (1959) 911–917.
- [26] M. Gledhill, The detection of iron protoporphyrin (heme b) in phytoplankton and marine particulate material by electrospray ionisation mass spectrometry - comparison with diode array detection, *Anal. Chim. Acta* 841 (2014) 33–43.
- [27] Y. Isaji, N.O. Ogawa, Y. Takano, N. Ohkouchi, Quantification and carbon and nitrogen isotopic measurements of Heme B in environmental samples, *Anal. Chem.* 92 (2020) 11213–11222.
- [28] M.S. Detzel, et al., Revisiting the interaction of heme with hemopexin, *Biol. Chem.* 402 (2021) 675–691.
- [29] E. Tolosano, F. Altruda, Hemopexin: structure, function, and regulation, *DNA Cell Biol.* 21 (2002) 297–306.
- [30] E. Tolosano, S. Fagoonee, N. Morello, F. Vinchi, V. Fiorito, Heme scavenging and the other facets of hemopexin, *Antioxid. Redox Signal.* 12 (2010) 305–320.
- [31] N. Izadi, et al., Purification and characterization of an extracellular heme-binding protein, HasA, involved in heme iron acquisition, *Biochemistry* 36 (1997) 7050–7057.
- [32] R. Glueck, D. Green, I. Cohen, C.H. Ts'ao, Hematin: unique effects of hemostasis, *Blood* 61 (1983) 243–249.
- [33] B. Andria, et al., Biliverdin protects against liver ischemia reperfusion injury in swine, *PLoS One* 8 (2013), e69972.
- [34] K. Winkler, A. Schultz, J.E. Schultz, The S-helix determines the signal in a *Tar* receptor/adenylyl cyclase reporter, *J. Biol. Chem.* 287 (2012) 15479–15488.
- [35] Tews, et al., The structure of a pH-sensing mycobacterial adenylyl cyclase holoenzyme, *Science* 308 (2005) 1020–1023.
- [36] J.E. Owen, G.M. Bishop, S.R. Robinson, Uptake and toxicity of heme and iron in cultured mouse astrocytes, *Neurochem. Res.* 41 (2016) 298–306.
- [37] V.C. Tsolaki, et al., Hemin accumulation and identification of a heme-binding protein clan in K562 cells by proteomic and computational analysis, *J. Cell. Physiol.* 237 (2022) 1315–1340.
- [38] V. Jeney, et al., Pro-oxidant and cytotoxic effects of circulating heme, *Blood* 100 (2002) 879–887.
- [39] C. Sanabra, G. Mengod, Neuroanatomical distribution and neurochemical characterization of cells expressing adenylyl cyclase isoforms in mouse and rat brain, *J. Chem. Neuroanat.* 41 (2011) 43–54.
- [40] W. Durante, et al., cAMP induces heme oxygenase-1 gene expression and carbon monoxide production in vascular smooth muscle, *Am. J. Phys.* 273 (1997) H317–H323.
- [41] S. Immenschuh, et al., Transcriptional activation of the haem oxygenase-1 gene by cGMP via a cAMP response element/activator protein-1 element in primary cultures of rat hepatocytes, *Biochem. J.* 334 (Pt 1) (1998) 141–146.
- [42] S. Immenschuh, et al., The rat heme oxygenase-1 gene is transcriptionally induced via the protein kinase a signaling pathway in rat hepatocyte cultures, *Mol. Pharmacol.* 53 (1998) 483–491.
- [43] T. Szkudelski, K. Frackowiak, K. Szkudelska, Hemin attenuates response of primary rat adipocytes to adrenergic stimulation, *PeerJ* 9 (2021), e12092.
- [44] H.M. Lander, D.M. Levine, A. Novogrodsky, Hemin stimulation of cAMP production in human lymphocytes, *FEBS Lett.* 303 (1992) 242–246.
- [45] S.M. Mense, L. Zhang, Heme: a versatile signaling molecule controlling the activities of diverse regulators ranging from transcription factors to MAP kinases, *Cell Res.* 16 (2006) 681–692.
- [46] S. Schneider, J. Marles-Wright, K.H. Sharp, M. Paoli, Diversity and conservation of interactions for binding heme in b-type heme proteins, *Nat. Prod. Rep.* 24 (2007) 621–630.
- [47] Y. Kang, R. Liu, J.X. Wu, L. Chen, Structural insights into the mechanism of human soluble guanylate cyclase, *Nature* 574 (2019) 206–210.
- [48] P.M. Schmidt, M. Schramm, H. Schroder, F. Wunder, J.P. Stasch, Identification of residues crucially involved in the binding of the heme moiety of soluble guanylate cyclase, *J. Biol. Chem.* 279 (2004) 3025–3032.
- [49] S. Immenschuh, V. Vijayan, S. Janciauskiene, F. Gueler, Heme as a target for therapeutic interventions, *Front. Pharmacol.* 8 (2017) 146.
- [50] M.T. Hopp, et al., Heme determination and quantification methods and their suitability for practical applications and everyday use, *Anal. Chem.* 92 (2020) 9429–9440.
- [51] S. Kumar, U. Bandyopadhyay, Free heme toxicity and its detoxification systems in human, *Toxicol. Lett.* 157 (2005) 175–188.
- [52] A.P. Pietropaoli, et al., Total plasma heme concentration increases after red blood cell transfusion and predicts mortality in critically ill medical patients, *Transfusion* 59 (2019) 2007–2015.
- [53] U. Muller-Eberhard, J. Javid, H.H. Liem, A. Hanstein, M. Hanna, Plasma concentrations of hemopexin, haptoglobin and heme in patients with various hemolytic diseases, *Blood* 32 (1968) 811–815.

## Additional Experiments (not included in the publication)

### A- Hormones as ligands?

In the beginning of this work, we had no clue about the possible chemical nature of the ligands. Serum, which demonstrated inhibitory effect on mAC activity is a complex mixture of many constituents such as proteins, lipids, hormones, nutrients, antibodies, carbohydrates, etc. In a preliminary investigation, a group of hormones listed in Table 1 were screened against 600 nM Gs $\alpha$  stimulated mAC3 and 5 transfected expressed in Sf9 cells in the presence and absence of 2.5% exosome depleted FBS (FBSexo).

**Table 1.** List of screened hormones and their concentrations used in assays. All concentrations are within normal physiological concentrations.

DHEA: Dehydroepiandrosterone

Hormone	Assay concentration
Cortisol	700 nM
Corticosterone	45 nM
Deoxycorticosterone	0.3 nM
Estradiol	1300 pM
Progesterone	10 nM
Aldosterone	600 pM
Testosterone	42 nM
DHEA	3.95 $\mu$ M
T <sub>3</sub> (total)	3 nM
T <sub>4</sub> (total)	215 nM

Deoxycorticosterone significantly inhibited mAC3 activity by 50% in the absence of FBSexo (Figure 1A). Cortisol enhanced mAC3 activity about three and 2.5-fold (not significant) in the absence and presence of FBSexo, respectively (Figure 1A and 1B). In the presence of FBSexo, corticosterone, testosterone and T3 enhanced mACs activity two-fold (Figure 1B).

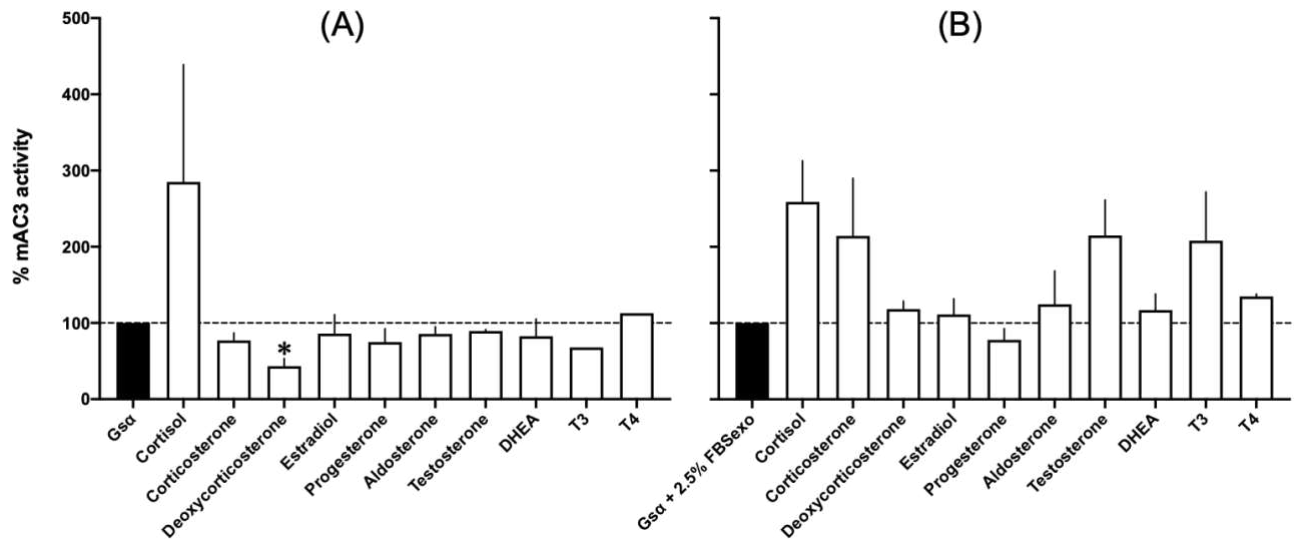


**Figure 1.** Effect of hormones on mAC3 stimulated by 600 nM Gsa in the absence (**A**) and presence (**B**) of 2.5% FBSexo. (**A**) Basal and Gsa-stimulated (100%) activities of mAC3 were  $0.02 \pm 0.004$  and  $0.91 \pm 0.09$  nmol cAMP/mg/min. (**B**) Basal and Gsa-stimulated activities of mAC3 in presence of FBSexo (set as 100%) were  $0.06 \pm 0.04$  and  $0.57 \pm 0.25$  nmol cAMP/mg/min. One sample *t* test: \**P* < 0.05 compared to 100%. Error bars denote SEM. *n* = 1-3 each done in triplicates.

With mAC5, no significant effect was observed with the tested hormones (Figure 2).

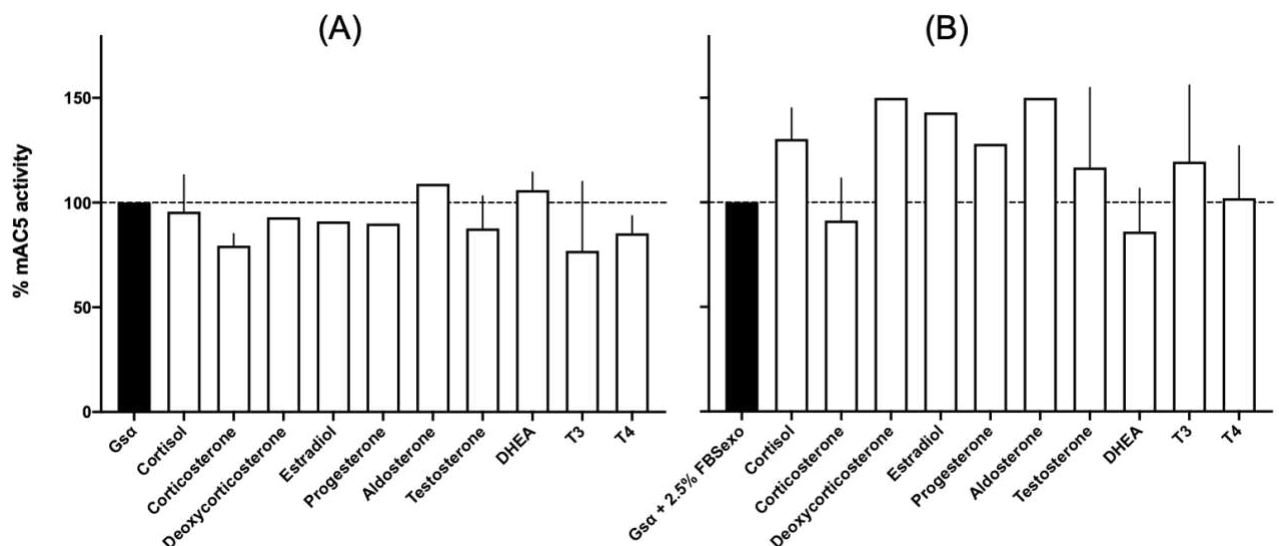


**Figure 2.** Effect of hormones on mAC5 stimulated by 600 nM Gsa in the absence (**A**) and presence (**B**) of 2.5% FBSexo. (**A**) Basal and Gsa-stimulated (100%) activities of mAC5  $0.06$  were  $0.02 \pm 0.03$  and  $7.72 \pm 2.46$  nmol cAMP/mg/min. (**B**) Basal and Gsa-stimulated activities of mAC3 in presence of FBSexo (set as 100%) were  $0.12 \pm 0.04$  and  $3.24 \pm 0.77$  nmol cAMP/mg/min. Error bars denote SEM. *n* = 1-3 each done in triplicates.

### B- Serum effect on mACs transfected in HEK293 cells

We previously showed that human serum and FBS could attenuate mACs activity expressed in Sf9 cells (Seth, Finkbeiner et al. 2020). I wanted to examine the effect of serum on mACs expressed in HEK293 cells. Indeed, FBSexo concentration-dependently attenuated 300 nM Gs $\alpha$  stimulated mAC2 activity with an IC<sub>50</sub> of 1.2%. At 20%, mAC2 activity was inhibited by 80 % (Figure 3).

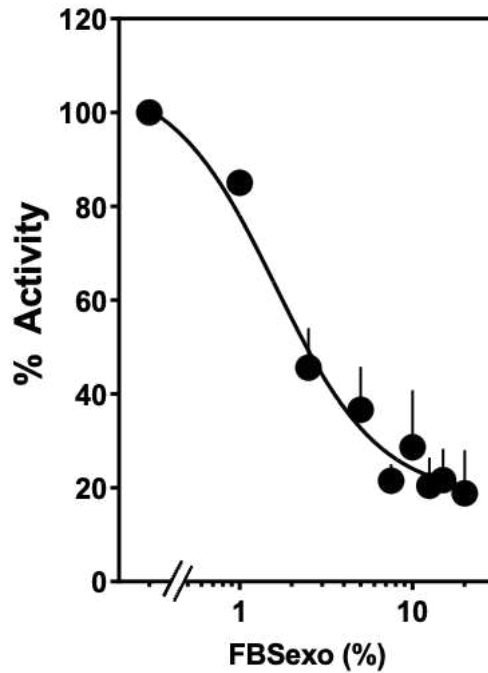


**Figure 3. FBSexo attenuates 300 nM Gs $\alpha$ -stimulated mAC2 activity.** Basal and Gs $\alpha$ -stimulated (100%) activities were  $0.24 \pm 0.07$  and  $2.57 \pm 0.55$  nmol cAMP/mg/min. Error bars denote SD of n= 2-4.

Using mAC3 permanently expressed in HEK293 cells (HEK-mAC3), the effect of FBSexo was examined *in vivo* (Figure 4). 10000 HEK-mAC3 cells/well were seeded into 384 well plates, and cAMP generation was stimulated by addition of 100  $\mu$ M isoproterenol. Addition of FBSexo attenuated HEK-mAC3 activity in a concentration dependent manner. 20% FBSexo inhibited mAC3 activity by 20% (not significant). Higher concentrations of FBSexo might be needed to achieve higher inhibition.

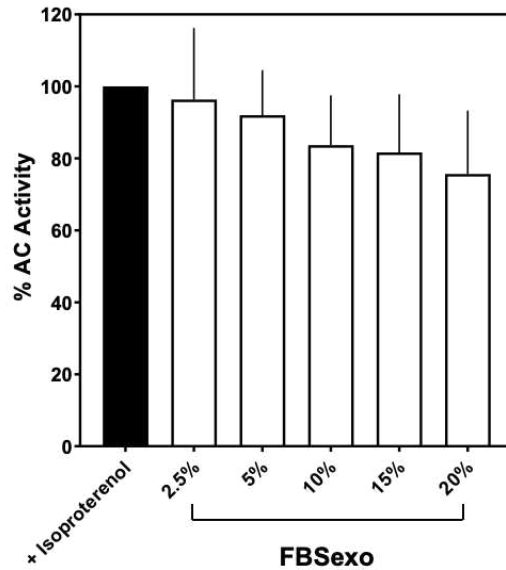


**Figure 4. Effect of FBSexo on HEK293-mAC3 stimulated by 100  $\mu$ M isoproterenol.** Basal and isoproterenol stimulated (set as 100%) activities were  $0.11 \pm 0.02$  and  $1.15 \pm 0.17$  pmol cAMP/10000 cells. Error bars denote SEM of  $n = 3$ .

### C- Hemin effect on soluble catalytic dimer

In publication II, we proposed that heme b might bind to the catalytic dimers of mAC affecting its activity, evidenced by the attenuation of bacterial ACs devoid of TM domain (Appendix Fig. 6). To further support this notion, I tested the effect of hemin on the basal and  $Gs\alpha$ -stimulated activities of a soluble catalytic dimer (mAC1-C1:mAC2-C2). 10  $\mu$ M hemin attenuated both activities implying that its effect is not dependent on the presence of membrane anchors (Figure 5).

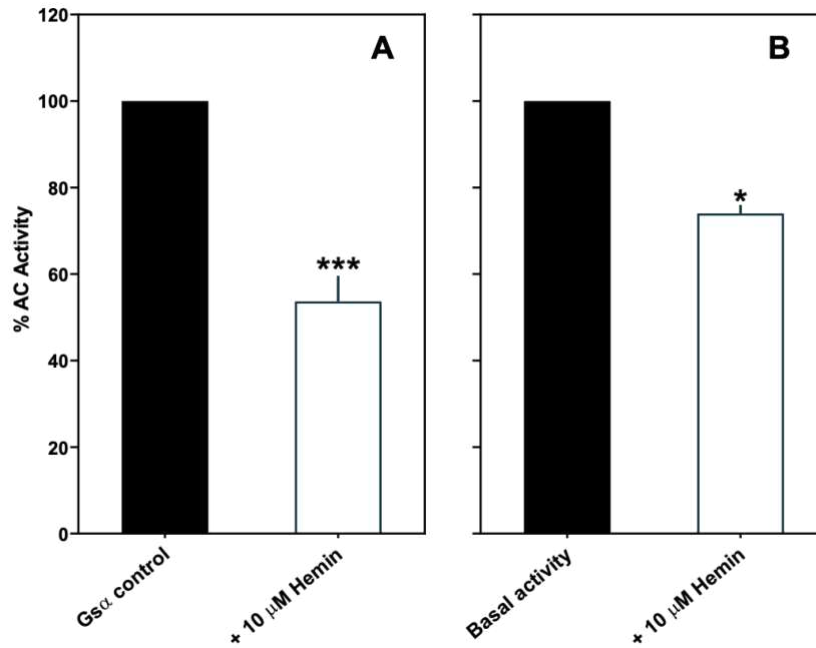


**Figure 5. Hemin effect on the 300 nM Gsα-stimulated (A) and basal (B) activities of the soluble catalytic dimer.** (A, B) Basal and Gsα-stimulated activities were  $0.01 \pm 0.002$  and  $0.05 \pm 0.009$  nmol cAMP·mg<sup>-1</sup>·min<sup>-1</sup>, respectively. Error bars denote SEM of n=2-3. One sample *t* test: \**P* < 0.05; \*\*\**P* < 0.001 compared to 100%.

#### D- mAC5 kinetics ± hemin

In this experiment, the effect of 10 μM hemin on the kinetics of mAC5 was investigated (Figure 6). Michaelis-Menten curve was hyperbolic indicating absence of cooperativity. According to a Hanes-Woolf plot, in the absence and presence of hemin, *K<sub>m</sub>* of ATP was 86 and 171 μM, respectively. Additionally, hemin decreased *V<sub>max</sub>* from 0.98 to 0.57 nmol cAMP/mg/min.

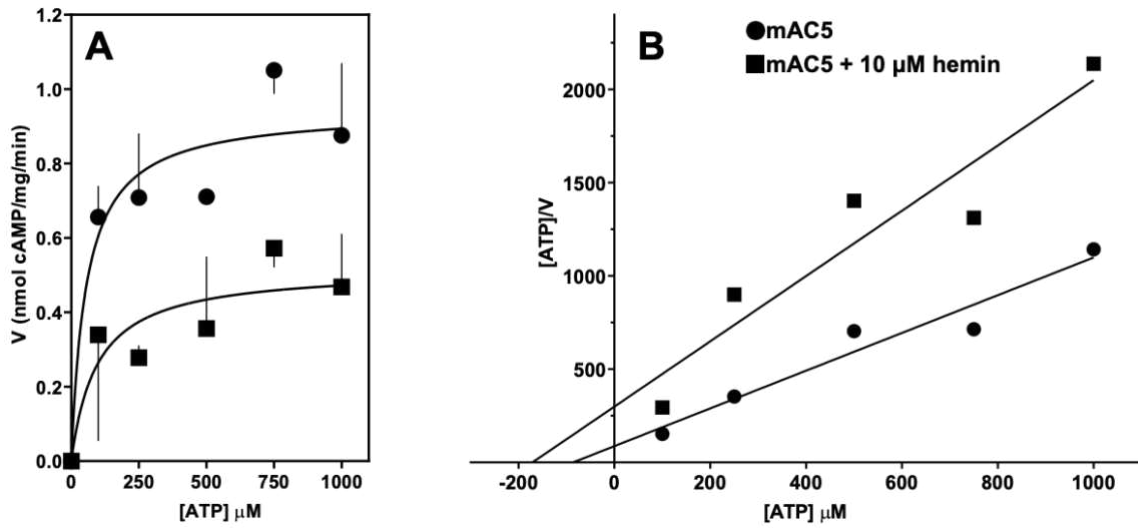


**Figure 6. Enzyme kinetics of mAC5 ± 10 μM hemin.** (A) Michaelis-Menten curve. (B) Hanes-Woolf plot. The assay was performed at 37°C, 15 min.

**3.3** Landau, M., **Elsabbagh, S.**, Gross, H., Fischer, A., Schultz, A., Schultz, J. E (2024). A new class of receptors: the membrane anchors of mammalian adenylyl cyclases.

**Submitted**

**Position in list of authors: 2**

**Author contributions:** Carried out experiments and evaluated data for the following manuscript figures: Fig. 1 (except 1F), Fig.2, Fig. 3A, Fig. 4A. Supplementary figures were generated by me except Fig. S6, S17, S18, S20 and S21. I contributed to manuscript revising and editing. I estimate my own contribution by 45%.

# A new class of receptors: the membrane anchors of mammalian adenylyl cyclases

Marius Landau<sup>1</sup>, **Sherif Elsabbagh**<sup>1</sup>, Harald Gross<sup>1</sup>, Adrian Fischer<sup>2</sup>, Anita C.F. Schultz<sup>1</sup>, Joachim E. Schultz<sup>1\*</sup>

<sup>1</sup>Pharmazeutisches Institut der Universität Tübingen, Auf der Morgenstelle 8

<sup>2</sup>Max-Planck-Institut für Biologie, Max-Planck-Ring 5, 72076 Tübingen, Germany

\*Corresponding author:

Dr. Joachim E Schultz

Pharmazeutisches Institut der Universität Tübingen,  
Auf der Morgenstelle 8, 72076 Tübingen, Germany

## Abstract

The biosynthesis of cAMP by mammalian membrane-bound adenylyl cyclases (mACs) is predominantly regulated by the cytosolic G $\alpha$  subunit of trimeric G-proteins. We proposed a model in which the two mAC membrane anchors operate as a dodecahedral receptor controlling G $\alpha$  activation. Here, we validate this model. We identify aliphatic fatty acids and anandamide as receptor ligands of mAC isoforms 1 to 7 and 9. The ligands enhance or attenuate G $\alpha$ -activated mACs *in vitro* and *in vivo*. Substitution of the stimulatory receptor of mAC3 by the inhibitory receptor of mAC5 results in a ligand attenuated mAC5-mAC3 chimera. Thus, we discovered a new class of membrane receptors which set the stage for tonic lipid and transient GPCR-G $\alpha$  signaling in cAMP biosynthesis.

## Introduction

The second messenger cAMP is present in virtually all mammalian cells and mediates diverse cellular processes (Dessauer, Watts et al. 2017, Ostrom, LaVigne et al. 2022). Hence, the regulation of cAMP biosynthesis is critical. Nine membrane-embedded, pseudoheterodimeric adenylyl cyclase isoforms (mACs) with an identical domain composition are encoded in mammals (Dessauer, Watts et al. 2017). The two hexahelical membrane domains, TM1 and TM2, form a tight dodecahelical membrane complex (Gu, Sorkin and Cooper 2001, Qi, Sorrentino et al. 2019, Qi, Lavriha et al. 2022). The catalytically active center is assembled at the interface of two complementary cytosolic domains (C1 and C2), both contributing catalytic residues (Tesmer and Sprang 1998). The currently prevailing consensus is that mACs are regulated via cytosolic effectors. The major input is activation by the G $\alpha$  subunit of the trimeric G-proteins released upon stimulation of GPCRs (Dessauer, Watts et al. 2017). Additional reported regulatory inputs are phosphorylation (Beazely and Watts 2006), calmodulin-binding (Diel, Beyermann et al. 2008), G $\alpha$  (Dessauer, Tesmer et al. 1998) and G $\beta\gamma$  (Dessauer, Watts et al. 2017). Considering the isoform-specific conservation of the membrane anchors in mACs for about 0.5 billion years we expected and searched for a contribution to function and regulation which goes beyond mere membrane anchoring (Bassler, Schultz and Lupas 2018, Schultz 2022).

In 2016, we replaced the hexahelical membrane anchor of the mycobacterial AC Rv1625c, a progenitor of mACs (Guo, Seebacher et al. 2001, Bassler, Schultz and Lupas 2018), by the hexahelical quorum-sensing receptor from *V. cholerae*, CqsS, a histidine kinase (Beltz, Bassler and Schultz 2016, Ziegler, Bassler et al. 2017). The CqsS-Rv1625c chimera was activated by the cholera-autoinducer-1, (S)-3-hydroxytridecan-4-one (Beltz, Bassler and Schultz 2016). This suggested that the quorum-sensing receptor functioned as a receptor for AC Rv1625c (Beltz, Bassler and Schultz 2016). Next, we replaced both hexahelical domains of the human mAC2 with the CqsS quorum-sensing receptor. The cholera-autoinducer-1 attenuated G $\alpha$ -activated mAC2 activity indicating that signal transduction through the CqsS membrane receptor to mAC2 was operational (Seth, Finkbeiner et al. 2020). Based on these data we proposed a model of mAC regulation in which the membrane anchor serves as a receptor (Seth, Finkbeiner et al. 2020). The mAC receptor domain is envisaged to transduce extracellular signals to the cytosolic catalytic dimer and

determine the extent of Gs $\alpha$  activation (Seth, Finkbeiner et al. 2020). Based on this concept, we searched for mAC ligands. In this paper we identify aliphatic lipids as ligands for mAC isoforms 1 to 7 and 9. Isoform-dependently, these ligands either attenuate or enhance Gs $\alpha$ -activation *in vitro* and *in vivo*. Receptor-properties are transferable by interchanging the membrane anchor between mAC3 and 5. The results define a new class of membrane receptors and establish a new level of regulation of cAMP biosynthesis in which tonic and phasic signaling processes are combined.

### **Oleic acid enhances Gs $\alpha$ -stimulated mAC3, but not mAC5 activity**

Based on the results cited above we expected lipids as ligands (Tews, Findeisen et al. 2005, Abdel Motaal, Tews et al. 2006, Beltz, Bassler and Schultz 2016, Seth, Finkbeiner et al. 2020). We used bovine lung as a starting material because lipids are important for lung development and function (Anggard and Samuelsson 1965, Dautel, Kyle et al. 2017). Lipids were extracted from a cleared lung homogenate, acidified to pH 1, with dichloromethane/methanol (2:1). The dried organic phase was chromatographed on silica gel (employing vacuum-liquid-chromatography) and fractions were assayed (fractionation scheme in suppl. mat.). Fraction E enhanced Gs $\alpha$ -stimulated mAC3 activity four-fold, while mAC5 activity was unaffected (Fig.1A). Fraction E was separated by RP-HPLC into five subfractions (E1 – E5; Fig. S1). The mAC3 activating constituents appeared in fraction E2. It enhanced Gs $\alpha$ -stimulated mAC3 four-fold but had no effect on mAC5 (Fig. 1B). <sup>1</sup>H and <sup>13</sup>C-NMR spectra of E2 indicated the presence of aliphatic lipids (Fig. S2). Subsequent GC/MS analysis identified palmitic, stearic, oleic and myristic acid in E2 (Fig. 1C). Concentration-response curves were established for these compounds with mACs 3 and 5 activated by 300 nM Gs $\alpha$  (Fig. 1D). 20  $\mu$ M oleic acid enhanced Gs $\alpha$ -activated mAC3 activity three-fold ( $EC_{50}$  = 10.4  $\mu$ M) and 20  $\mu$ M palmitic acid two-fold ( $EC_{50}$  = 6.4  $\mu$ M), while stearic or myristic acid had no significant effect. None of these fatty acids affected mAC5 activity.

The action of oleic acid on mAC3 was instantaneous and linear for >25 min (Fig. S3). The  $K_m$  of mAC3 for ATP (335  $\mu$ M) was unaffected.  $V_{max}$  was increased from 0.62 to 1.23 nmol cAMP/mg/min (Fig. S4). Oleic acid did not affect the activity of a soluble, Gs $\alpha$  activated construct formerly used for generating a C1 and C2 catalytic dimer from mAC1 and 2, ruling out spurious detergent effects (Tang and Gilman 1995)

(Fig. S5). The isoform specificity for oleic acid was further evaluated by G $\alpha$  concentration-response curves of mAC3 and 5  $\pm$  20  $\mu$ M oleic acid (Fig. 1E, left and center). For mAC3 EC<sub>50</sub> for G $\alpha$  in presence and absence of oleic acid were 549 and 471 nM, respectively. Over the G $\alpha$  concentration range, the enhancement by 20  $\mu$ M oleic was uniformly about 3.4-fold (Fig. 1E, Right). In the case of mAC5, G $\alpha$  stimulation was not enhanced by oleic acid.

Using HEK293 cells permanently transfected with mAC3 (HEK-mAC3) or mAC5 (HEK-mAC5) the effect of oleic acid was probed *in vivo*. Intracellular cAMP formation via G $\alpha$  was triggered via stimulation of the endogenous  $\beta$ -receptor with 2.5  $\mu$ M of the  $\beta$ -agonist isoproterenol, a submaximal concentration (Pillay, Nagiah et al. 2020). Addition of oleic acid enhanced cAMP formation in HEK-mAC3 1.5-fold (Fig. 1F). Stearic acid was inactive. Under identical conditions, cAMP formation in HEK-mAC5 cells was unaffected. The EC<sub>50</sub> for oleic acid in HEK293-mAC3 cells was 0.5  $\mu$ M, i.e., the potency appeared to be increased compared to respective membrane preparations whereas the efficiency was reduced, possibly reflecting the regulatory interplay within the cell. To exclude experimental artifacts, transfection efficiencies were tested by PCR. mAC3 and mAC5 transfections were similar (Fig. S6). Taken together, the results suggest that the enhancement of G $\alpha$ -activated mAC3 activity by oleic acid might be due to binding of oleic acid to or into an mAC3 membrane receptor (Beltz, Bassler and Schultz 2016, Schultz 2022).

To explore the ligand space, we tested 18 aliphatic C<sub>12</sub> to C<sub>20</sub> lipids (Table S1). At 20  $\mu$ M, elaidic, *cis*-vaccenic and linoleic acids were efficient enhancers. Palmitic, palmitoleic, linolenic, eicosapentaenoic acids and oleamide were less efficacious; other compounds were inactive (Fig. 1G). Notably, the saturated C<sub>18</sub> stearic acid was inactive here and throughout, albeit otherwise variations in chain length, and the number, location, and conformation of double bonds were tolerated to some extent, e.g., *cis*-vaccenic, linoleic, and linolenic acids. The relaxed ligand specificity was anticipated as aliphatic fatty acids are highly bendable and bind to a flexible dodecahedral protein dimer embedded in a fluid lipid membrane. The ligand space of mAC3 somewhat resembled the fuzzy and overlapping ligand specificities of the free-fatty-acid receptors 1 and 4 (Kimura, Ichimura et al. 2020, Grundmann, Bender et al. 2021, Samovski, Jacome-Sosa and Abumrad 2023).

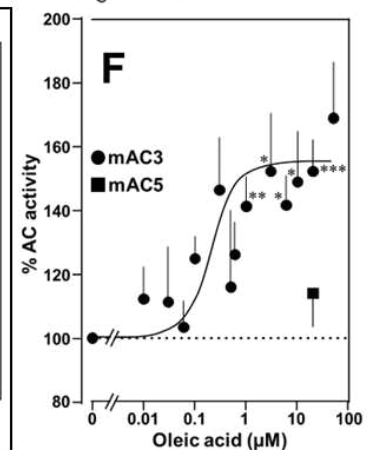
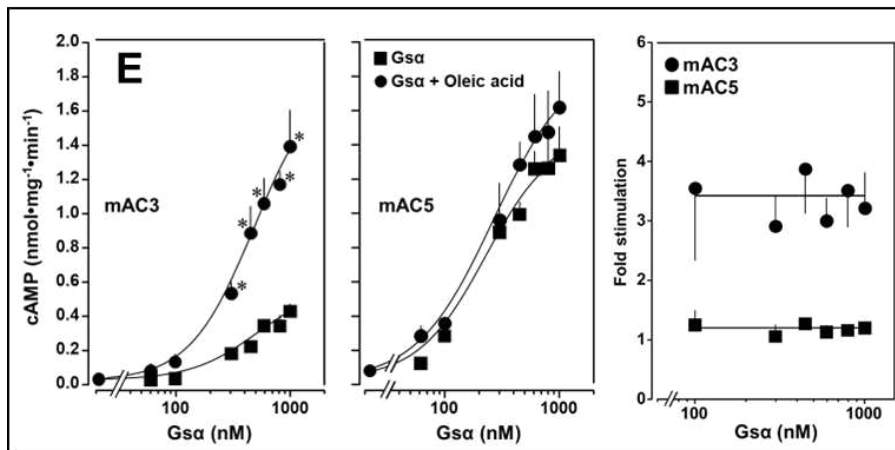
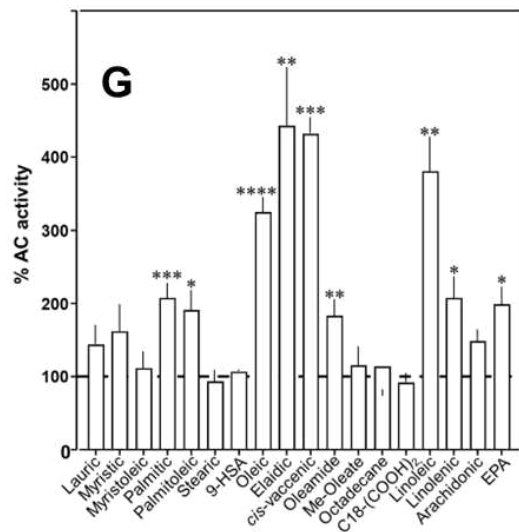
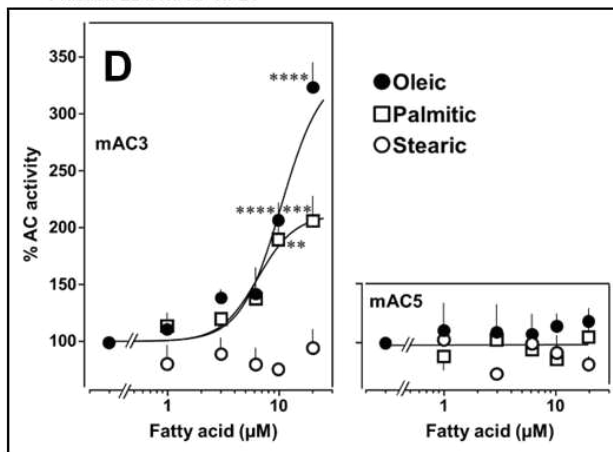
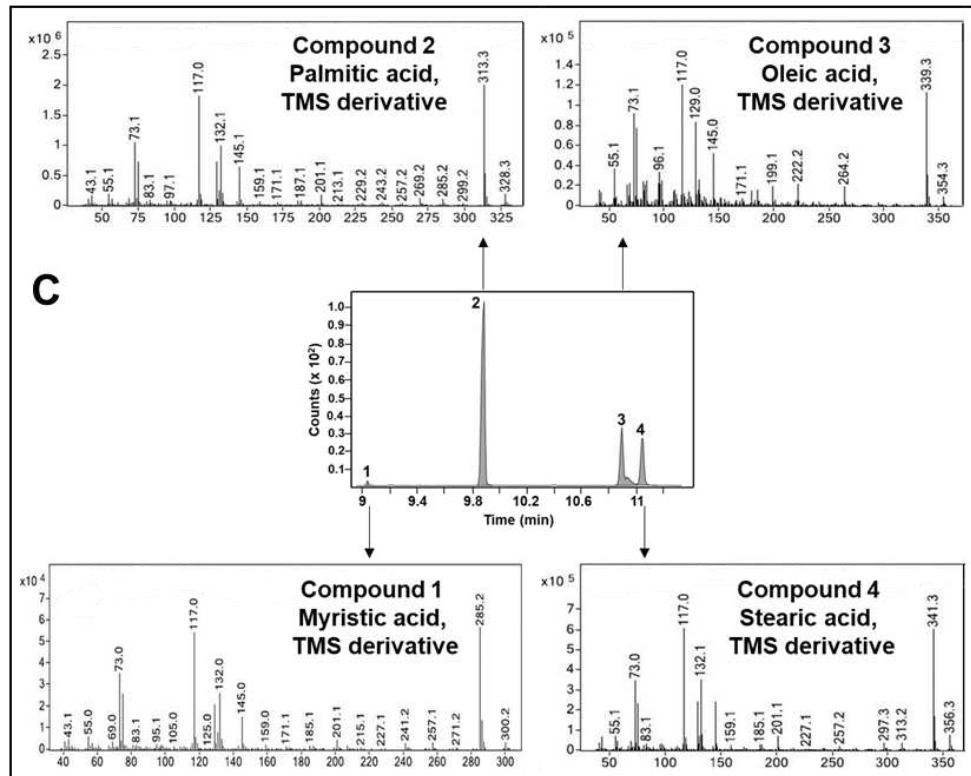
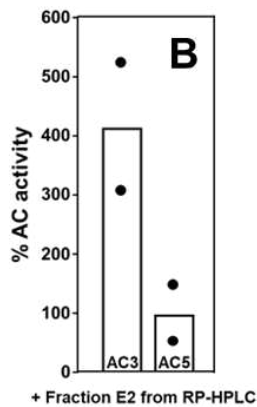
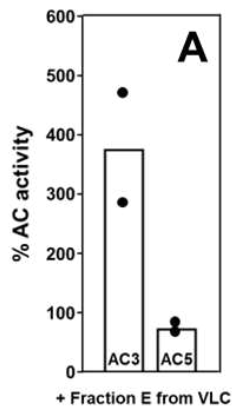


**Fig. 1. Identification of mAC3 activating fatty acids.** (A and B) Effect of 1  $\mu\text{g}$ /assay of fractions E (A) and E2 (B) on 300 nM  $\text{G}\alpha$ -stimulated mACs 3 and 5. Activities are shown as % compared to 300 nM  $\text{G}\alpha$  stimulation (100%;  $n=2$ , each point represents two technical replicates). (A) Basal and  $\text{G}\alpha$ -stimulated activities of mAC3 were 0.01 and 0.07 and of mAC5 0.06 and 1.32  $\text{nmol cAMP}\cdot\text{mg}^{-1}\cdot\text{min}^{-1}$ , respectively. (B) Basal and  $\text{G}\alpha$ -stimulated activities of mAC3 were 0.02 and 0.12 and of mAC5 were 0.09 and 1.1  $\text{nmol cAMP}\cdot\text{mg}^{-1}\cdot\text{min}^{-1}$ , respectively. (C) GC-MS chromatogram of fraction E2 (center) and mass spectra of the eluted peaks are shown. Fatty acids' identity was confirmed by comparing with their corresponding standards. TMS: Trimethylsilyl. (D) Effect of fatty acids identified by GC-MS on 300 nM  $\text{G}\alpha$ -stimulated mAC3 and mAC5. Basal and  $\text{G}\alpha$  stimulated activities of mAC3 were  $0.023 \pm 0.02$  and  $0.17 \pm 0.03$  and of mAC5 were  $0.08 \pm 0.02$  and  $0.44 \pm 0.09$   $\text{nmol cAMP}\cdot\text{mg}^{-1}\cdot\text{min}^{-1}$ , respectively.  $n=3-23$ . (E) 20  $\mu\text{M}$  oleic acid affects  $\text{G}\alpha$  stimulation of mAC 3 not 5 (left). mAC3 basal activity  $\pm$  20  $\mu\text{M}$  oleic acid was  $30 \pm 24$   $\text{pmol cAMP}\cdot\text{mg}^{-1}\cdot\text{min}^{-1}$ . (Middle)  $\text{EC}_{50}$  of  $\text{G}\alpha$  in the absence of oleic acid was 245 nM and in the presence of 20  $\mu\text{M}$  oleic acid, it was 277 nM (not significant). mAC5 basal activity  $\pm$  20  $\mu\text{M}$  oleic acid was  $84 \pm 60$   $\text{pmol cAMP}\cdot\text{mg}^{-1}\cdot\text{min}^{-1}$ .  $n=2-3$ , each with two technical replicates. (Right) Fold stimulation of mAC3 and 5 activities incubated with different concentrations of  $\text{G}\alpha$  + oleic acid.  $n=2-3$ . (F) Effect of oleic acid on HEK293 cells permanently transfected with mACs 3 and 5 stimulated by 2.5  $\mu\text{M}$  isoproterenol (set as 100%). Basal and isoproterenol-stimulated cAMP levels of HEK-mAC3 were  $0.02 \pm 0.006$  and  $1.35 \pm 0.24$  and of HEK-mAC5 were  $2.13 \pm 0.69$  and  $2.60 \pm 0.88$   $\text{pmol cAMP}/10000$  cells, respectively.  $n=3-9$ . (G) Effect of 20  $\mu\text{M}$  lipids on 300 nM  $\text{G}\alpha$ -stimulated mAC3. Basal and  $\text{G}\alpha$ -stimulated activities were  $0.02 \pm 0.001$  and  $0.17 \pm 0.01$   $\text{nmol cAMP}\cdot\text{mg}^{-1}\cdot\text{min}^{-1}$ , respectively. EPA: Eicosapentaenoic acid; 9-HSA: 9-hydroxystearic acid. Data are mean  $\pm$  SEM (except A and B). One-sample  $t$  tests (D, F and G), Paired  $t$  test for E (left and middle) and one-way ANOVA for E (right). Significances: \* $P < 0.05$ , \*\* $P < 0.01$ , \*\*\* $P < 0.001$ ; \*\*\*\* $P < 0.0001$ .

## Oleic acid enhances $\text{G}\alpha$ -stimulated mAC 2, 7, and 9 activities

Next, we examined other AC isoforms with oleic acid as a ligand. 20  $\mu\text{M}$  oleic acid significantly enhanced  $\text{G}\alpha$ -stimulated activities of isoforms 2, 7, and 9, mAC1 was slightly attenuated, and isoforms 4, 5, 6, and 8 were unaffected (Fig. 2A).

Concentration-response curves were carried out for mACs 2, 7, and 9 (Fig. 2B). The  $\text{EC}_{50}$  concentrations for oleic acid were 8.6, 6.7, and 7.8  $\mu\text{M}$ , respectively comparable to that determined for mAC3. Exploration of the ligand space for mACs 2, 7, and 9 with the panel of 18 aliphatic lipids uncovered more active lipids (Fig. 2C). In the case of mAC2, 20  $\mu\text{M}$  *cis*-vaccenic acid doubled cAMP formation ( $\text{EC}_{50} = 10.6$   $\mu\text{M}$ ) while other compounds were inactive (Fig. 2C and Fig. S7). For mAC7 the  $\text{EC}_{50}$  for elaidic was 9.7  $\mu\text{M}$  (Fig. S8). The range of potential ligands for mAC9 was more comprehensive: 3-4-fold enhancement was observed with 20  $\mu\text{M}$  palmitoleic, oleic, elaidic, *cis*-vaccenic, and linoleic acid. With 20  $\mu\text{M}$  myristic, palmitic, palmitoleic,

linolenic, and arachidonic acid, 1.5-2 fold enhancements were observed (Fig. 2C and Fig. S9-S10). Concentration-response curves were established for all activating compounds. In several instances, EC<sub>50</sub> values could not be calculated (Fig. S9-10).

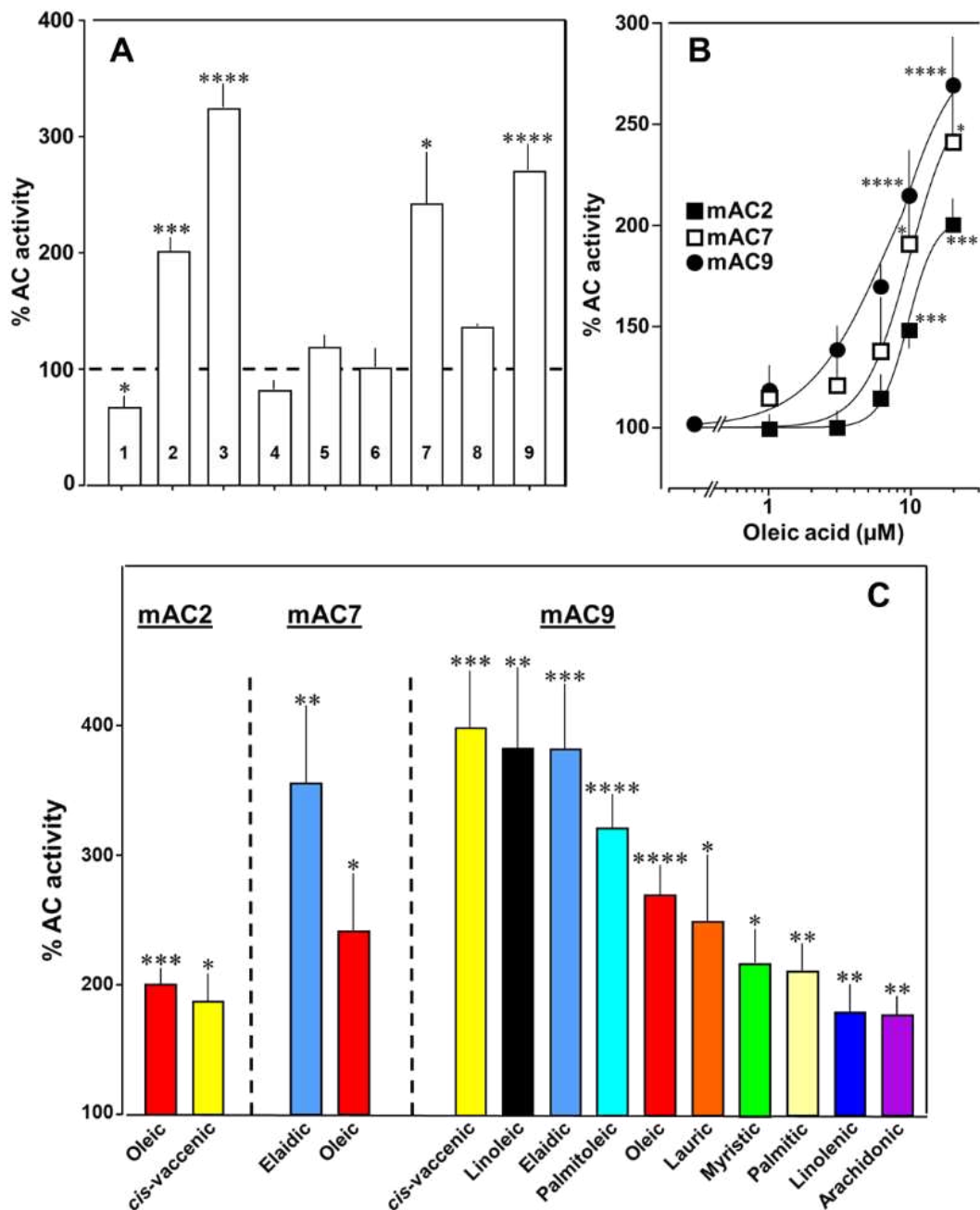


**Fig. 2. Fatty acids enhance mAC isoforms 2, 7, and 9 activities.** (A) Effect of 20 μM oleic acid on 300 nM Gsα-stimulated mACs activities normalized to 100%. Basal and Gsα-stimulated activities for each isoform are in Table S2. n= 2-23. (B) Oleic acid activates mACs 2, 7, and 9 stimulated by 300 nM Gsα. n=7-23. (C) Fatty acids activating mACs 2, 7, and 9 at 20 μM. For basal and Gsα-stimulated activities, see Fig. S7-S10. n= 5-15.

Data are mean ± SEM. One-sample *t* tests were performed. Significances: \**P* < 0.05, \*\**P* < 0.01, \*\*\**P* < 0.001; \*\*\*\**P* < 0.0001.

## Arachidonic acid and anandamide inhibit G $\alpha$ -stimulated activities of mAC1, 4, 5, and 6

Testing the panel of lipids at 20  $\mu$ M with mAC isoforms 1, 4, 5, 6, and 8 we found that isoforms 1 and 4 were significantly attenuated by arachidonic acid, and somewhat less by palmitoleic acid. Other lipids had no effect (Fig. S11-13). Of note is eicosapentaenoic acid which resembles arachidonic acid but for an additional *cis*- $\Delta^{17}$  double bond. Despite its structural similarity to arachidonic acid, it had no effect on mACs activities (Fig. S11-S12). Concentration-response curves for arachidonic acid with G $\alpha$ -stimulated mAC1 and 4 yielded IC<sub>50</sub> values of 23 and 36  $\mu$ M, respectively, i.e., about two-fold higher compared to the EC<sub>50</sub> values of enhancing ligands (Fig. 3A). Next, we examined whether arachidonic acid attenuates mAC1 and 4 in intact HEK 293 cells. Surprisingly, cAMP formation in HEK-mAC1 cells stimulated by 10  $\mu$ M isoproterenol was attenuated with high potency (IC<sub>50</sub> = 250 pM), i.e., with higher potency compared to membranes prepared from the same cell line. In contrast, mAC4 activity examined under identical conditions was not attenuated (Fig. 3B). Currently, we are unable to rationalize these discrepancies. Possibly, mAC4 has another, more specific lipid ligand which is needed in *in vivo*. In general, the enhancing and attenuating effects bolster the hypothesis of specific receptor-ligand interactions and divergent intrinsic activities for different ligands.

At this point we were lacking ligands for mACs 5, 6, and 8 (Fig. S14-16). Possibly, the negative charge of the fatty acid headgroups might impair receptor interactions. A neutral lipid neurotransmitter closely related to arachidonic acid is arachidonylethanolamide (anandamide) (Mock, Gagestein and van der Stelt 2023). Indeed, anandamide attenuated G $\alpha$ -stimulation of mAC5 and 6 with IC<sub>50</sub> values of 42 and 23  $\mu$ M, respectively, i.e. comparable to the effect of arachidonic acid on mACs 1 and 4, and distinctly less potently than the ligands for mAC 2, 3, 7, and 9 (Fig. 3C). mACs 5 and 6 may thus represent new targets for anandamide which is part of a widespread neuromodulatory system (Lu and Mackie 2016). The concentrations of arachidonic acid and anandamide required for attenuation may be achieved *in vivo* by local biosynthesis and degradation. An interfacial membrane-embedded phosphodiesterase cleaves the phosphodiester bond of the membrane lipid *N*-arachidonoyl-ethanolamine-glycerophosphate releasing anandamide into the extracellular space (Liu, Wang et al. 2006, Simon and Cravatt 2008, Mock, Gagestein

and van der Stelt 2023). The lipophilicity and lack of charge should enable it to diffuse readily. Whether the mACs and this biosynthetic phosphodiesterase colocalize or associate with its target mACs is unknown. Degradation of anandamide is by a membrane-bound amidase, generating arachidonic acid and ethanolamine (McKinney and Cravatt 2005). Therefore, we examined whether anandamide at higher concentrations might also affect mAC1 and 4. In fact, anandamide significantly attenuated G $\alpha$ -stimulated mAC1, but distinctly not mAC4. The IC<sub>50</sub> for mAC1 was 29  $\mu$ M (Fig. 3D).

We also tested whether anandamide attenuated cAMP formation *in vivo* using HEK-mAC5 cells primed by 2.5  $\mu$ M isoproterenol (Fig. 3E and 4C). 100  $\mu$ M anandamide attenuated cAMP formation by only 23 % in HEK293-mAC5 cells, the effect was significant ( $P < 0.01$ ).

At this point, we were unable to identify a ligand for mAC8, presumably another lipid (Fig. S16).

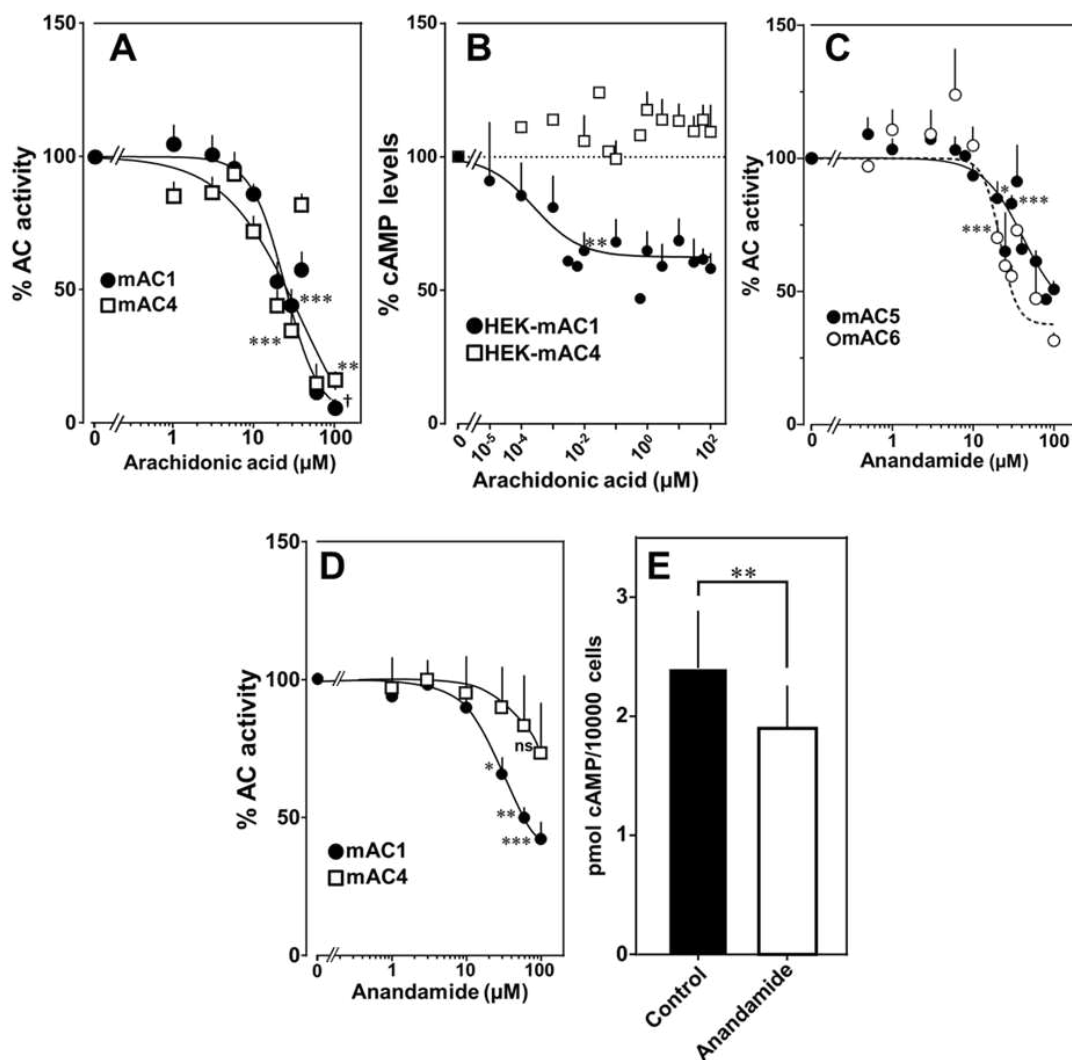


**Fig. 3. Arachidonic acid and anandamide attenuate 300 nM Gs $\alpha$ -stimulated activities of mACs 1, 4, 5 and 6.** (A) Arachidonic acid attenuates Gs $\alpha$ -stimulated mACs 1 and 4. Basal and Gs $\alpha$  stimulated activities of mAC1 were  $0.12 \pm 0.01$  and  $0.42 \pm 0.03$  and of mAC4 were  $0.02 \pm 0.002$  and  $0.14 \pm 0.02$  nmol cAMP $\cdot$ mg $^{-1}\cdot$ min $^{-1}$ , respectively (n= 3-9). (B) Effect of arachidonic acid on HEK-mAC1 and HEK-mAC4 cells. Cells were stimulated by 10  $\mu$ M isoproterenol (set as 100 %) in the presence of 0.5 mM 3-isobutyl-1-methylxanthine. Basal and isoproterenol stimulated cAMP levels in HEK-mAC1 were  $1.03 \pm 0.15$  and  $1.66 \pm 0.28$  and in HEK-mAC4 were  $0.20 \pm 0.04$  and  $0.86 \pm 0.24$  pmol cAMP/10000 cells, respectively (n= 2-11, each with three replicates). (C) Effect of anandamide on Gs $\alpha$ -stimulated mAC5 and 6. Basal and Gs $\alpha$  activities of mAC5 were  $0.05 \pm 0.01$  and  $0.98 \pm 0.12$  and of mAC6  $0.05 \pm 0.01$  and  $0.78 \pm 0.12$  nmol cAMP $\cdot$ mg $^{-1}\cdot$ min $^{-1}$ , respectively (n= 3-32). (D) Anandamide attenuates mAC1 but not mAC4 stimulated by Gs $\alpha$ . Basal and Gs $\alpha$  stimulated activities of mAC1 were  $0.12 \pm 0.01$  and  $0.40 \pm 0.03$  and of mAC4 were  $0.02 \pm 0.002$  and  $0.15 \pm 0.02$  nmol cAMP $\cdot$ mg $^{-1}\cdot$ min $^{-1}$ , respectively (n = 3-4, each with two technical replicates). (E) Effect of anandamide on 2.5  $\mu$ M isoproterenol stimulated HEK-mAC5. Basal and isoproterenol stimulated cAMP levels of HEK-mAC5 were  $1.8 \pm 0.22$  and  $2.4 \pm 0.48$  pmol cAMP/10000 cells, respectively. The control bar represents 2.5  $\mu$ M isoproterenol stimulation alone (n=5-6, each with three technical replicates).

Data are mean  $\pm$  SEM. One-sample *t* tests (A-D) and paired *t* test (E) were performed. Significances: ns: not significant  $P > 0.05$ ; \* $P < 0.05$ , \*\* $P < 0.01$ , \*\*\* $P < 0.001$ ; † $P < 0.0001$ . For clarity, not all significances are indicated.

## Receptor properties are exchangeable between mAC3 and 5 isoforms

To unequivocally validate specific mAC-ligand-receptor interactions and regulation we generated a functional chimera in which the enhancing membrane domains of mAC3, i.e., mAC3-TM1 and 2, were substituted by those of mAC5. The intention was to obtain a chimera, mAC5<sub>(membr)</sub>-AC3<sub>(cat)</sub>, with a loss of receptor function, i.e., no enhancement by oleic acid, and a gain of another receptor function, i.e. attenuation of activity by anandamide. Successful expression and membrane insertion of the chimera in HEK293 cells was demonstrated by specific conjugation to Cy5.5 fluorophore, using the protein ligase connectase (Fig. S17) (Fuchs 2023). cAMP synthesis of isolated membranes from these cells was stimulated up to 10-fold by addition of 300 nM Gs $\alpha$ , comparable to membranes with recombinant mAC3 or mAC5 proteins (Fig. S18 and Fig. 1E). mAC activity in the mAC5<sub>(membr)</sub>-AC3<sub>(cat)</sub> chimera was not enhanced by oleic acid, i.e., loss of receptor function, but was attenuated by anandamide, i.e., gain of receptor function. The attenuation was comparable to results obtained with mAC5 membranes (Fig. 4, A and B, Fig. S19-S20). This means that the

attenuating receptor property of mAC5 was grafted onto the mAC3-catalytic dimer. We take this to support the hypothesis that the mammalian mAC membrane domains operate as receptors using lipid ligands. The data virtually rule out unspecific lipid effects such as disturbance of membrane integrity by intercalation and surfactant or detergent effects. In addition, the data demonstrated that the signal most likely originates from the receptor entity and is transmitted through the subsequent linker regions to the catalytic dimer.

The findings were further substantiated *in vivo* using HEK293-mAC5<sub>(membr)</sub>-mAC3<sub>(cat)</sub> cells. cAMP formation primed by 2.5  $\mu$ M isoproterenol was attenuated by anandamide by 66%, (Fig. 4C), by far exceeding the anandamide attenuation in HEK293-mAC5 cells of 23 %. In HEK293-mAC5<sub>(membr)</sub>-AC3<sub>(cat)</sub> cells oleic acid was ineffective, i.e., loss of function (Fig. 1F and S21). The results support the notion that mAC isoforms are receptors with lipids as ligands.

Lastly, we prepared membranes from mouse brain cortex in which predominantly mAC isoforms 2, 3 and 9 are expressed, isoforms with demonstrated enhancement of G $\alpha$  stimulation by oleic acid (Sanabra and Mengod 2011). In cortical membranes 20  $\mu$ M oleic acid enhanced G $\alpha$  stimulated cAMP formation 1.5-fold with an EC<sub>50</sub> of 5  $\mu$ M, almost identical to the one determined for mAC2, 3, 7 and 9 (Fig. S22). This suggests that mACs in brain cortical membranes are similarly affected by fatty acids.

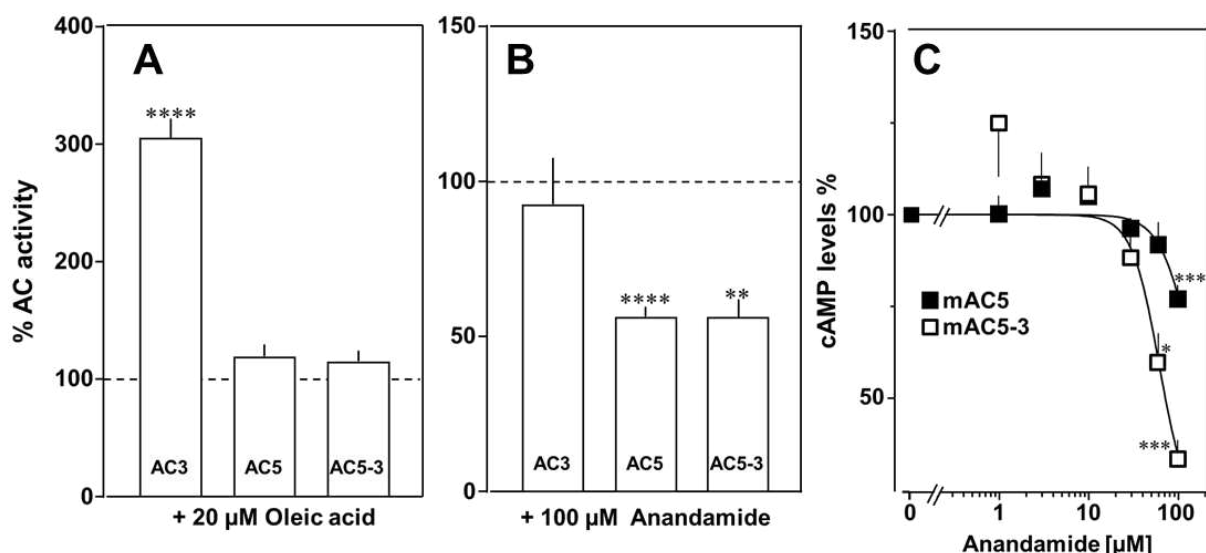


**Fig. 4. Receptor properties are exchangeable between mAC isoforms.** (A) Effect of 20  $\mu$ M oleic acid on 300 nM G $\alpha$ -stimulated mACs 3, 5, and 5-3. Basal and G $\alpha$  stimulated activities of mACs 3, 5, and 5-3 were  $0.02 \pm 0.003$  and  $0.11 \pm 0.02$ ,  $0.05 \pm 0.01$  and  $0.98 \pm 0.12$ , and  $0.01 \pm 0.004$  and  $0.2 \pm 0.02$  nmol cAMP $\cdot$ mg $^{-1}$  $\cdot$ min $^{-1}$ , respectively. n=7-33. (B) Effect

of 100  $\mu\text{M}$  anandamide on 300 nM  $\text{G}\alpha$ -stimulated mACs 3, 5, and 5-3. Basal and  $\text{G}\alpha$  activities of mACs 3, 5, and 5-3 were  $0.02 \pm 0.002$  and  $0.19 \pm 0.02$ ,  $0.05 \pm 0.01$  and  $0.98 \pm 0.12$  and  $0.02 \pm 0.003$  and  $0.23 \pm 0.04$  nmol cAMP $\cdot\text{mg}^{-1}\cdot\text{min}^{-1}$ , respectively.  $n=6-9$ .  $\text{IC}_{50}$  for mAC5 and mAC5-3 were 42 and 29  $\mu\text{M}$ , respectively. (C) Effect of anandamide on HEK-mAC5 and HEK-mAC5-3 cells stimulated by 2.5  $\mu\text{M}$  isoproterenol (set as 100 %). Basal and isoproterenol stimulated cAMP levels in HEK-mAC5 were  $1.80 \pm 0.22$  and  $2.29 \pm 0.39$  and in HEK-mAC5-3 (+ 0.5 mM IBMX) were  $0.17 \pm 0.02$  and  $3.11 \pm 0.55$  pmol cAMP/10000 cells, respectively.  $n= 4-11$ .  $\text{IC}_{50}$  for HEK-mAC5 and HEK-mAC5-3 were 133 and 60  $\mu\text{M}$ , respectively. Anandamide had no effect on the basal activity of HEK-mAC5 and stimulated HEK-mAC3 cells in concentrations up to 100  $\mu\text{M}$  (data not shown).

Data are mean  $\pm$  SEM. One-sample  $t$  tests were performed. Significances: \* $P < 0.05$ , \*\* $P < 0.01$ , \*\*\* $P < 0.001$ ; \*\*\*\* $P < 0.0001$ .

## Discussion and Outlook

In the past, the biology of the membrane anchors of mACs, highly conserved in an isoform-specific manner, remained unresolved. Our data are a transformative step toward resolving this issue and introduce lipids as critical participants in regulating cAMP biosynthesis in mammals. The first salient discovery is the identification of the membrane domains of mACs as a new class of receptors for chemically defined ligands which set the level of stimulation by the GPCR/ $\text{G}\alpha$  system. This conclusion is based on (i) the dodecahedral membrane domains of the nine mAC receptors have distinct, conserved isoform-specific sequences (Schultz 2022); (ii) the receptors have distinct ligand specificities; (iii) isoform dependently ligands either enhance or attenuate  $\text{G}\alpha$ -activated mAC activities; (iv) receptor properties are transferable between isoforms by interchanging membrane domains; (v) isoproterenol-stimulated formation of cAMP *in vivo* is affected by addition of extracellular ligands. (vi)  $\text{G}\alpha$ -stimulated cAMP formation in mouse cortical membranes is enhanced by oleic acid. Therefore, the results establish a new class of receptors, the membrane domains of mACs, with lipids as ligands. The data question the utility of the currently used mAC sub-classification, which groups mAC1, 3, and 8, mAC2, 4, 7, mACs 5, 6, and mAC9 together (Dessauer, Watts et al. 2017). At this point, mAC 1, 4, 5, and 6 which are ligand-attenuated, may be grouped together and a second group may consist of mACs 2, 3, 7, and 9 which are ligand-enhanced. Our data do not contradict earlier findings concerning regulation of mACs, cellular localization of mAC isoforms or regional cAMP signaling (Dessauer, Watts et al. 2017). Instead, the data reveal a completely new

level of direct mAC regulation in conjunction with the indirect regulation via the GPCR/Gs $\alpha$  circuits.

The second, potentially important finding is the observation that the extent of enhancement of mAC3 activity by 20  $\mu$ M oleic acid is uniform up to 1000 nM Gs $\alpha$  (Fig. 1F). We suppose that in mAC3 the equilibrium of two differing ground states favors a Gs $\alpha$  unresponsive state and the effector oleic acid shifts this equilibrium to a Gs $\alpha$  responsive state (Seth, Finkbeiner et al. 2020). In contrast, the equilibrium of ground states of mAC5 probably is opposite, i.e. the one accessible to Gs $\alpha$  stimulation predominates and stimulation by Gs $\alpha$  is high. Addition of oleic acid has little effect because the mAC5 receptor domain does not bind oleic acid (Fig. 1E). Addition of an mAC5 ligand, e.g., anandamide or arachidonic acid, would then stabilize a Gs $\alpha$  inaccessible ground state and inhibit stimulation. The biological balance of ground states appears to be an intrinsic property which are isoform-specifically imprinted. Probably, it defines a major element of mAC regulation and enables distinct inhibitory or stimulatory responses to extracellular ligands. These ground states probably are separated by a low transition energy and are stabilized by receptor occupancy. Hitherto available structures required Gs $\alpha$  and/or forskolin for stabilization and probably did not capture a ground state. Mechanistically, tonic levels of lipid ligands probably affect the balance of ground states and thus set the bounds of cAMP formation elicited by phasic GPCR/Gs $\alpha$ -stimulation. As such lipid signaling through the mAC membrane receptors appears to represent a higher level of a systemic regulatory network reflecting the physiological and nutritional environment of an organism.

Lipid signaling is much less characterized than solute signaling (Eyster 2007). The highly functionalized ligands for GPCRs are storable in vesicles and the release, inactivation and removal are strictly controlled. On the other hand, the very nature of lipids, i.e., high flexibility of aliphatic chains, low water solubility, propensity for nonspecific protein binding, membrane permeability and potential effects on membrane fluidity complicate discrimination between extra- and intracellular lipid actions (Samovski, Jacome-Sosa and Abumrad 2023). Yet, viewed from an evolutionary perspective, lipids possibly are primordial signaling molecules because the emergence of the first cells required lipids to separate an intra- and extracellular space. Possibly, lipids, derived from membrane lipids were used for regulatory purposes early-on. In conjunction with the evolution of bacterial mAC progenitors, lipid

ligands may have persisted in evolution and regulation by GPCR/Gs $\alpha$  in metazoans was acquired and expanded later.

The concentrations of free fatty acids in serum or interstitial fluid usually are rather low (Ulven and Christiansen 2015, Huber and Kleinfeld 2017, Grundmann, Bender et al. 2021). This raises the question of the origin of lipid ligands. One possibility is that the lipid ligands are acutely extracted from membrane lipids by integral membrane hydrolases as known for anandamide and arachidonic acid (Liu, Wang et al. 2006, Muccioli 2010). Additional potential lipid sources usable for ligand generation may be, among other exosomes, serum lipids, chylomicrons, blood triglycerides and even lipids of microbial origin. The lipid ligands for mACs thus broaden the basis of regulation of cAMP generation with potentially wide-ranging consequences in health and disease.

### **Funding and additional information**

Funding was from the Deutsche Forschungsgemeinschaft (Schu275/45-1) and from institutional funds from the Max-Planck-Gesellschaft.

### **Acknowledgments**

We are indebted to Prof. Andrei Lupas, Max-Planck-Institute of Biology, Tübingen, for his continued support, advice, and critique. We thank N. Grzegorzec, Organic Chemistry, for GC/MS measurements.

### **Author contributions**

Experimental realization: ML, SE and AS; HPLC, GC/MS, NMR: SE and HG; Connectase assay, AF; Concept, data evaluation and writing the manuscript: JES.

### **Conflict of interest**

The authors declare no conflict of interest with the contents of this article.

### **Data and Materials availability**

All data are available in the paper or supplementary materials.

## Appendix:

### MATERIALS AND METHODS

#### Reagents and materials

ATP, creatine kinase, and creatine phosphate were from Merck-Sigma. Except for lauric acid (Henkel) and 1,18-Octadecanedicarboxylic acid (ThermoFisher Scientific), lipids were from Merck-Sigma. Lipid stock solutions were prepared in DMSO and kept under nitrogen. The DMSO concentrations in *in vitro* and *in vivo* assays were maximally 1%, a concentration without any effect in the assays. The constitutively active Gs $\alpha$ Q227L mutant was expressed and purified as described earlier (Graziano, Freissmuth and Gilman 1989, Graziano, Freissmuth and Gilman 1991, Sunahara, Dessauer et al. 1997).

#### General Experimental Procedures

For HPLC analysis, a Waters HPLC system (1525 pump, 2996 photodiode array detector, 7725i injector, 200 series PerkinElmer vacuum degasser) was used. Solvents were HPLC or LC-MS grade from Merck-Sigma. One-dimensional  $^1\text{H}$  and  $^{13}\text{C}$ -NMR spectra were recorded on a 400 MHz Bruker AVANCE III NMR spectrometer equipped with a 5 mm broadband SmartProbe and AVANCE III HD Nanobay console. Spectra were recorded in methanol- $d_4$  and calibrated to the residual solvent signal ( $\delta_{\text{H}}$  3.31 and  $\delta_{\text{C}}$  49.15 ppm).

#### Lung tissue extraction and fractionation

1.24 kg bovine lung was minced in a meat grinder, then mixed and homogenized with 1.2 L 50 mM MOPS, pH 7.5, in a Waring blender (4 °C) resulting in 2.3 L homogenate. It was centrifuged (30 min, 4 °C, 7200 $\times$ g) resulting in 1.2 L supernatant. The pH of the supernatant was adjusted to 1 using 7% HCl. Equal volumes of  $\text{CH}_2\text{Cl}_2/\text{MeOH}$  (2:1) were mixed with the supernatant in a separatory funnel and shaken vigorously. Centrifugation was at 5300 $\times$ g for 30 min. The lower organic  $\text{CH}_2\text{Cl}_2$  layer was recovered and the solvent was evaporated affording 2 g of dried crude extract. This was dissolved in 100 ml petroleum ether and subjected to normal-phase silica gel (60 H Supelco) vacuum liquid chromatography. The column was eluted stepwise with solvents of increasing polarity from 90:10 petroleum ether/EtOAc to 100% EtOAc, followed by 100% MeOH. 17 fractions (A-Q) of 300 mL were collected and dried down. Fraction E (eluted with 40:60 petroleum ether/EtOAc) was analyzed

by RP-HPLC using a linear MeOH/H<sub>2</sub>O gradient from 80:20 to 100:0 (0.1% TFA) for 15 min, followed by 100:0 for 30 min (Knauer Eurosphere II C18P 100-5, 250 x 8 mm, 1.2 mL/min flow rate, UV-absorbance monitored at 210 nm) to yield five subfractions; E1-E5.

Fraction E2 was subjected to <sup>1</sup>H- and <sup>13</sup>C-NMR which indicated the presence of aliphatic lipids and fatty acids (Fig. S2).

### **GC-MS analysis**

Fraction E2 was analyzed by GC-MS. Acids were acid trimethylsilylated using *N,O*-bis(trimethylsilyl)trifluoroacetamide + trimethylchlorosilane (BSTFA + TMCS, 99:1 v/v). In brief, 400 µL of was added to the residue of dried fraction E2. The mixture was heated for 2 h at 90 °C. After cooling and clearing the sample was transferred into a GC vial in 200 µL hexane.

An Agilent Technologies GC system (8890 gas chromatograph and 5977B mass spectrometer equipped with a DB-HP5MS UI column, 30 m x 0.25 mm, film thickness of 0.25 µm) was used. Injection volume was 1 µL. The temperature was kept at 100°C for 5 min, and then increased at 53 °C/min to 240°C. The rate was decreased to 3°C/min to reach 305°C. Carrier gas was He<sub>2</sub> (99.9%) with a 1.2 mL/min flow rate. Ionization was with 70 eV and MS spectra were recorded for a mass range *m/z* 35-800 for 35 min. Compounds were identified by comparing the spectra with those in the NIST library. Individual compound content is given as a relative % of the total peak area.

### **Plasmid construction and protein expression**

Full-length human AC sequences were retrieved with NCBI accession numbers; ADCY1: NM\_021116.3, ADCY2: NM\_020546.2, ADCY3: NM\_004036.4, ADCY4: NM\_001198568.2, ADCY5: NM\_183357.2, ADCY6: NM\_015270.4, ADCY7: NM\_001114.4, ADCY8: NM\_001115.2, ADCY9: NM\_001116.3. All mAC genes were obtained from GenScript and fitted with a C-terminal FLAG-tag. The chimera mAC5(TM)\_mAC3(cat) had an N-terminal connectase-tag, MPGAFDADPLVVEIAAAGA followed by AC5(1-402)\_AC3(250-631)\_AC5(761-1009)\_AC3(862-1144). The gene was synthesized by GenScript. HEK293 cells were maintained in Dulbecco's modified Eagle's medium (DMEM) containing 10% fetal bovine serum at 37°C with 5% CO<sub>2</sub>. Transfection with AC plasmids was with PolyJet (SignaGen, Frederick, MD, USA). Permanent cell lines were generated by selection for 7 days with 600 µg/mL G418 and maintained with 300 µg/mL For membrane

preparation, cells were tyrosinized, collected by centrifugation (3000xg, 5 min) and lysed and homogenized in 20 mM HEPES, pH 7.5, 1 mM EDTA, 2 mM MgCl<sub>2</sub>, 1 mM DTT, one tablet of cOmplete, EDTA-free (per 50 mL) and 250 mM sucrose by 20 strokes in a potter homogenizer on ice. Debris was removed by centrifugation for 5 min at 1000xg (0°C), membranes were then collected by centrifugation at 100,000xg, 60 min at 0°C, resuspended, and stored at -80°C in 20 mM MOPS, pH 7.5, 0.5 mM EDTA, 2 mM MgCl<sub>2</sub>. Membrane preparation from mouse brain cortex was according to (Schultz and Schmidt 1987, Seth, Finkbeiner et al. 2020). Three cerebral cortices were dissected and homogenized in 4.5 ml cold 48 mM Tris-HCl, pH 7.4, 12 mM MgCl<sub>2</sub>, and 0.1 mM EGTA with a Polytron hand disperser (Kinematica AG, Switzerland). The homogenate was centrifuged for 15 min at 12000 g at 4°C and the pellet was washed once with 5 mL 1 mM KHCO<sub>3</sub>. The final suspension in 2 mL 1 mM KHCO<sub>3</sub> was stored in aliquots at -80°C.

### **DNA extraction**

DNA from 1x10<sup>6</sup> cells of permanently transfected and non-transfected HEK293 cells was extracted using the High Pure PCR Template Preparation Kit (Roche) according to the manufacturer's instructions. DNA concentrations were determined by photometry at 260 nm using a sub-microliter cell (IMPLEN) in a P330 NanoPhotometer (IMPLEN). Elution buffer (Roche) was used for blanks.

### **Polymerase chain reaction**

100 ng of template DNA was mixed with 0.5 µM Forward primer and 0.5 µM Reverse primer. 12.5 µL 2X KAPA2G Fast (HotStart) Genotyping Mix with dye and water was added to get a total reaction volume of 25 µL according to the KAPA2G Fast HotStart Genotyping Mix kit (Roche) protocol. PCR was performed according to the following cycling protocol in a Biometra T3000 thermocycler:

<b>Step</b>	<b>Temperature</b>	<b>Duration</b>	<b>Cycles</b>
Initial denaturation	95°C	3 min	1
Denaturation	95°C	15 sec	35
Annealing	60°C	15 sec	
Extension	72°C	30-60 sec*	
Final extension	72°C	2-4 min*	1

\*Extension and Final extension times were adjusted to the expected amplicon length.

The PCR products were then directly loaded on a 1.5% agarose gel. As a marker, 1 kb DNA ladder (New England Bio Labs #N3232S) was mixed with Gel Loading Dye Purple 6X (New England Biolabs #B7024S) and water then loaded on the gel. After running the gel for 15-20 minutes at 90 V in 1X TAE buffer, the gel was stained in an Ethidium bromide bath and then left running for another 10-20 minutes. The gels were then evaluated under UV light in a UVP GelStudio PLUS (Analytik Jena) gel imager.

AC isoform	Forward primer (5'-3')	Reverse primer (5'-3')
1	GTCAACAGGTACATCAGCCGCC	AGCCTCCTTCCCAGCTGCTGC
2	AGGAGACTGCTACTACTGTGTATCTGGAC	GGATGCCACGTTGCTCTGGGA
3	TTCATCCTGGTGATGGCAAATGTCGT	GGAGTTGTCCACCACCTGGTG
4	CGGGGATGCCAAGTTCTTCCAGGTCATTG	GCCTAGGGTAGCTGAAGGAGG
5	CCTCATCCTGCGCTGCACCCAGAAGCG	ACTGAGC
6	TCCTGAGCCGTGCCATCGA	ACTGCTGGGGCCCCCATTGAG
7	TCCTCGGCGACTGCTACTACTG	G TTCAGCCCCAGCCCCCTGAAA
8	ACTTGCGGAGTGGCGATAAATTGAGA	TGGCAAATCAGATTTGTCGGTGCC
9	CGCTGTGCTTCTCCTGGTG	CACACTCTTTGAAACGTTGAGC

### Adenylyl cyclase assay

In a volume of 10  $\mu$ l, AC activities were measured using 1 mM ATP, 2 mM  $MgCl_2$ , 3 mM creatine phosphate, 60  $\mu$ g/mL creatine kinase, and 50 mM MOPS pH 7.5. The cAMP assay kit from Cisbio (Codolet, France) was used for detection according to the supplier's instructions. A cAMP standard curve was established for each assay.

### cAMP accumulation assay

HEK293 cells stably expressing mAC isoforms 3, 5, and mAC5(TM)\_mAC3(cat) were plated at 2500-10000 cells/well into 384 well plates. Cells were treated with varying concentrations of lipids and incubated for 10 mins at 37°C and 5%  $CO_2$ . 2.5-10  $\mu$ M isoproterenol was then added to stimulate cAMP production and cells were further incubated for 5 mins. HEK293-AC5-3 was assayed in the presence of the phosphodiesterase inhibitor 0.5 mM isobutyl-methyl-xanthine. Addition of Cisbio HTRF detection reagents stopped the reaction and cAMP levels were determined.

## Statistical analysis

All statistical analysis' and EC<sub>50</sub> and IC<sub>50</sub> values were calculated by GraphPad Prism version 8.4.3 for Windows, GraphPad Software, San Diego, California USA, [www.graphpad.com](http://www.graphpad.com).

## REFERENCES

- Abdel Motaal, A., I. Tews, J. E. Schultz and J. U. Linder (2006). "Fatty acid regulation of adenylyl cyclase Rv2212 from Mycobacterium tuberculosis H37Rv." Febs J **273**(18): 4219-4228.
- Anggard, E. and B. Samuelsson (1965). "Biosynthesis of prostaglandins from arachidonic acid in guinea pig lung. Prostaglandins and related factors. 38." J Biol Chem **240**(9): 3518-3521.
- Bassler, J., J. E. Schultz and A. N. Lupas (2018). "Adenylate cyclases: Receivers, transducers, and generators of signals." Cell Signaling **46**: 135-144.
- Beltz, S., J. Bassler and J. E. Schultz (2016). "Regulation by the quorum sensor from Vibrio indicates a receptor function for the membrane anchors of adenylate cyclases." Elife **5**.
- Dessauer, C. W., J. J. Tesmer, S. R. Sprang and A. G. Gilman (1998). "Identification of a G $\alpha$  binding site on type V adenylyl cyclase." J Biol Chem **273**(40): 25831-25839.
- Dessauer, C. W., V. J. Watts, R. S. Ostrom, M. Conti, S. Dove and R. Seifert (2017). "International Union of Basic and Clinical Pharmacology. Cl. Structures and Small Molecule Modulators of Mammalian Adenylyl Cyclases." Pharmacol Rev **69**(2): 93-139.
- Diel, S., M. Beyermann, J. M. Llorens, B. Wittig and C. Kleuss (2008). "Two interaction sites on mammalian adenylyl cyclase type I and II: modulation by calmodulin and G( $\beta$ gamma)." Biochem J **411**(2): 449-456.
- Eyster, K. M. (2007). "The membrane and lipids as integral participants in signal transduction: lipid signal transduction for the non-lipid biochemist." Adv Physiol Educ **31**(1): 5-16.
- Fuchs, A. C. D. (2023). "Specific, sensitive and quantitative protein detection by in-gel fluorescence." Nat Commun **14**(1): 2505.
- Graziano, M. P., M. Freissmuth and A. G. Gilman (1989). "Expression of Gs alpha in Escherichia coli. Purification and properties of two forms of the protein." J Biol Chem **264**(1): 409-418.
- Graziano, M. P., M. Freissmuth and A. G. Gilman (1991). "Purification of recombinant Gs alpha." Methods Enzymol **195**: 192-202.
- Grundmann, M., E. Bender, J. Schamberger and F. Eitner (2021). "Pharmacology of Free Fatty Acid Receptors and Their Allosteric Modulators." Int J Mol Sci **22**(4).
- Gu, C., A. Sorkin and D. M. F. Cooper (2001). "Persistent interactions between the two transmembrane clusters dictate the targeting and functional assembly of adenylyl cyclase." Curr Biol **11**(3): 185-190.

- Guo, Y. L., T. Seebacher, U. Kurz, J. U. Linder and J. E. Schultz (2001). "Adenylyl cyclase Rv1625c of *Mycobacterium tuberculosis*: a progenitor of mammalian adenylyl cyclases." EMBO J **20**(14): 3667-3675.
- Huber, A. H. and A. M. Kleinfeld (2017). "Unbound free fatty acid profiles in human plasma and the unexpected absence of unbound palmitoleate." J Lipid Res **58**(3): 578-585.
- Kimura, I., A. Ichimura, R. Ohue-Kitano and M. Igarashi (2020). "Free Fatty Acid Receptors in Health and Disease." Physiol Rev **100**(1): 171-210.
- Liu, J., L. Wang, J. Harvey-White, D. Osei-Hyiaman, R. Razdan, Q. Gong, A. C. Chan, Z. Zhou, B. X. Huang, H. Y. Kim and G. Kunos (2006). "A biosynthetic pathway for anandamide." Proc Natl Acad Sci U S A **103**(36): 13345-13350.
- Lu, H. C. and K. Mackie (2016). "An Introduction to the Endogenous Cannabinoid System." Biol Psychiatry **79**(7): 516-525.
- McKinney, M. K. and B. F. Cravatt (2005). "Structure and function of fatty acid amide hydrolase." Annu Rev Biochem **74**: 411-432.
- Mock, E. D., B. Gagestein and M. van der Stelt (2023). "Anandamide and other N-acylethanolamines: A class of signaling lipids with therapeutic opportunities." Prog Lipid Res **89**: 101194.
- Muccioli, G. G. (2010). "Endocannabinoid biosynthesis and inactivation, from simple to complex." Drug Discov Today **15**(11-12): 474-483.
- Ostrom, K. F., J. E. LaVigne, T. F. Brust, R. Seifert, C. W. Dessauer, V. J. Watts and R. S. Ostrom (2022). "Physiological roles of mammalian transmembrane adenylyl cyclase isoforms." Physiol Rev **102**(2): 815-857.
- Pillay, Y., S. Nagiah, A. Phulukdaree, A. Krishnan and A. A. Chuturgoon (2020). "Patulin suppresses alpha(1)-adrenergic receptor expression in HEK293 cells." Sci Rep **10**(1): 20115.
- Qi, C., P. Lavriha, V. Mehta, B. Khanppnavar, I. Mohammed, Y. Li, M. Lazaratos, J. V. Schaefer, B. Dreier, A. Pluckthun, A. N. Bondar, C. W. Dessauer and V. M. Korkhov (2022). "Structural basis of adenylyl cyclase 9 activation." Nat Commun **13**(1): 1045.
- Qi, C., S. Sorrentino, O. Medalia and V. M. Korkhov (2019). "The structure of a membrane adenylyl cyclase bound to an activated stimulatory G protein." Science **364**: 389-394.
- Samovski, D., M. Jacome-Sosa and N. A. Abumrad (2023). "Fatty Acid Transport and Signaling: Mechanisms and Physiological Implications." Annu Rev Physiol **85**: 317-337.
- Sanabra, C. and G. Mengod (2011). "Neuroanatomical distribution and neurochemical characterization of cells expressing adenylyl cyclase isoforms in mouse and rat brain." J Chem Neuroanat **41**(1): 43-54.
- Schultz, J. E. (2022). "The evolutionary conservation of eukaryotic membrane-bound adenylyl cyclase isoforms." Front Pharmacol **13**: 1009797.
- Schultz, J. E. and B. H. Schmidt (1987). "Treatment of rats with thyrotropin (TSH) reduces the adrenoceptor sensitivity of adenylate cyclase from cerebral cortex." Neurochem Int **10**(2): 173-178.
- Seth, A., M. Finkbeiner, J. Grischin and J. E. Schultz (2020). "G $\alpha$  stimulation of mammalian adenylate cyclases regulated by their hexahelical membrane anchors." Cell Signal **68**: 109538.
- Simon, G. M. and B. F. Cravatt (2008). "Anandamide biosynthesis catalyzed by the phosphodiesterase GDE1 and detection of glycerophospho-N-acyl ethanolamine precursors in mouse brain." J Biol Chem **283**(14): 9341-9349.

- Sunahara, R. K., C. W. Dessauer, R. E. Whisnant, C. Kleuss and A. G. Gilman (1997). "Interaction of G $\alpha$  with the cytosolic domains of mammalian adenylyl cyclase." J Biol Chem **272**(35): 22265-22271.
- Tang, W. J. and A. G. Gilman (1995). "Construction of a soluble adenylyl cyclase activated by G $\alpha$  and forskolin." Science **268**(5218): 1769-1772.
- Tesmer, J. J. and S. R. Sprang (1998). "The structure, catalytic mechanism and regulation of adenylyl cyclase." Curr Opin Struct Biol **8**: 713-719.
- Tews, F. Findeisen, I. Sinning, A. Schultz, J. E. Schultz and J. U. Linder (2005). "The structure of a pH-sensing mycobacterial adenylyl cyclase holoenzyme." Science **308**: 1020–1023.
- Ulven, T. and E. Christiansen (2015). "Dietary Fatty Acids and Their Potential for Controlling Metabolic Diseases Through Activation of FFA4/GPR120." Annu Rev Nutr **35**: 239-263.
- Ziegler, M., J. Bassler, S. Beltz, A. Schultz, A. N. Lupas and J. E. Schultz (2017). "A novel signal transducer element intrinsic to class IIIa and IIIb adenylate cyclases." FEBS J. **284**: 1204-1217.

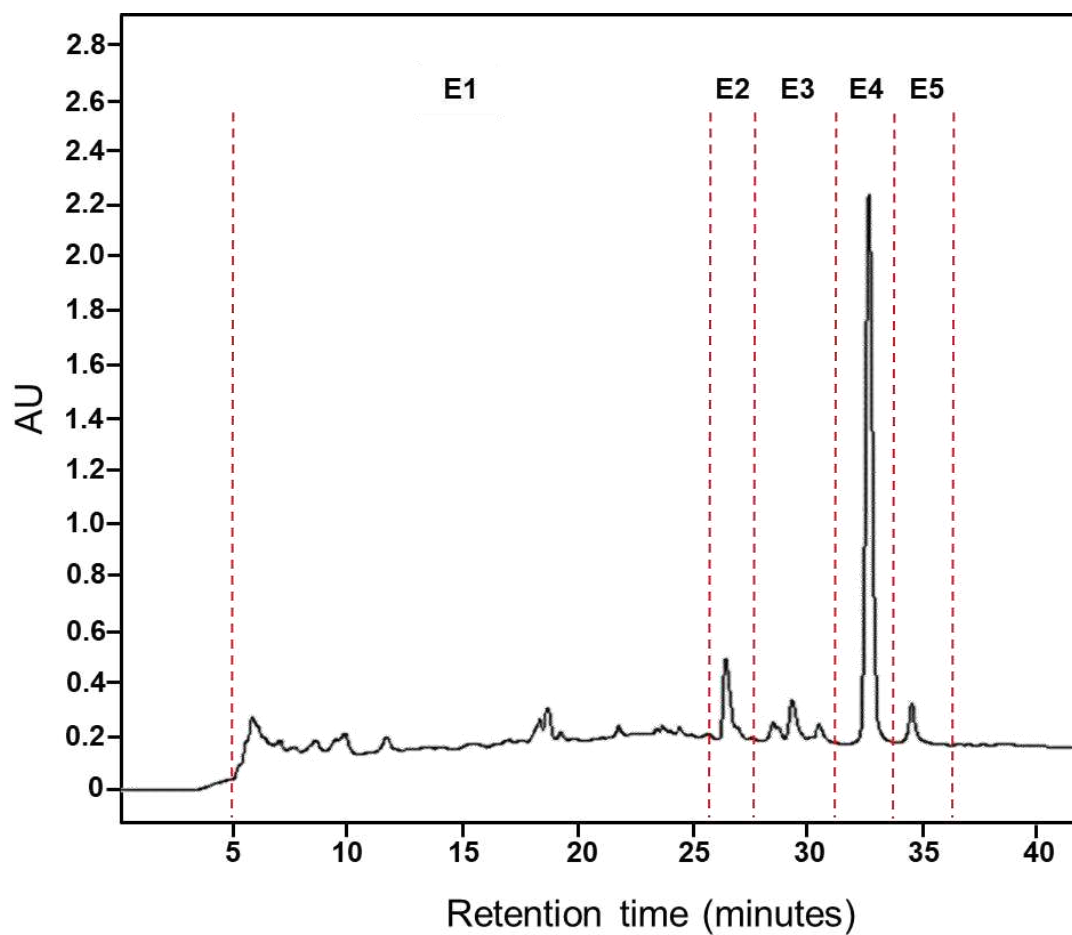
## Supplementary Scheme, Figures and Tables:

Acidic lipid extract from bovine lung									Si-VLC								
Fraction	A	B	C	D	E	F	G	H	I	J	K	L	M	N	O	P	Q
Solvent system	100% PE	90:10 PE:EA	80:20 PE:EA	60:40 PE:EA	40:60 PE:EA	20:80 PE:EA	100% EA	25:75 MeOH:EA	100% MeOH								
weight (mg)	3.1	4.5	459.1	404	285.8	70.1	29.5	21.6	344.6	753.3	95.7	85.3	175.5	136.3	54.7	27.4	17.9
% AC5 activity	116.5	125	100.5	80	73	48.5	84	87.5	102.5	44.5	11	1	30	50	44.5	38	25
% AC3 activity					376	372											

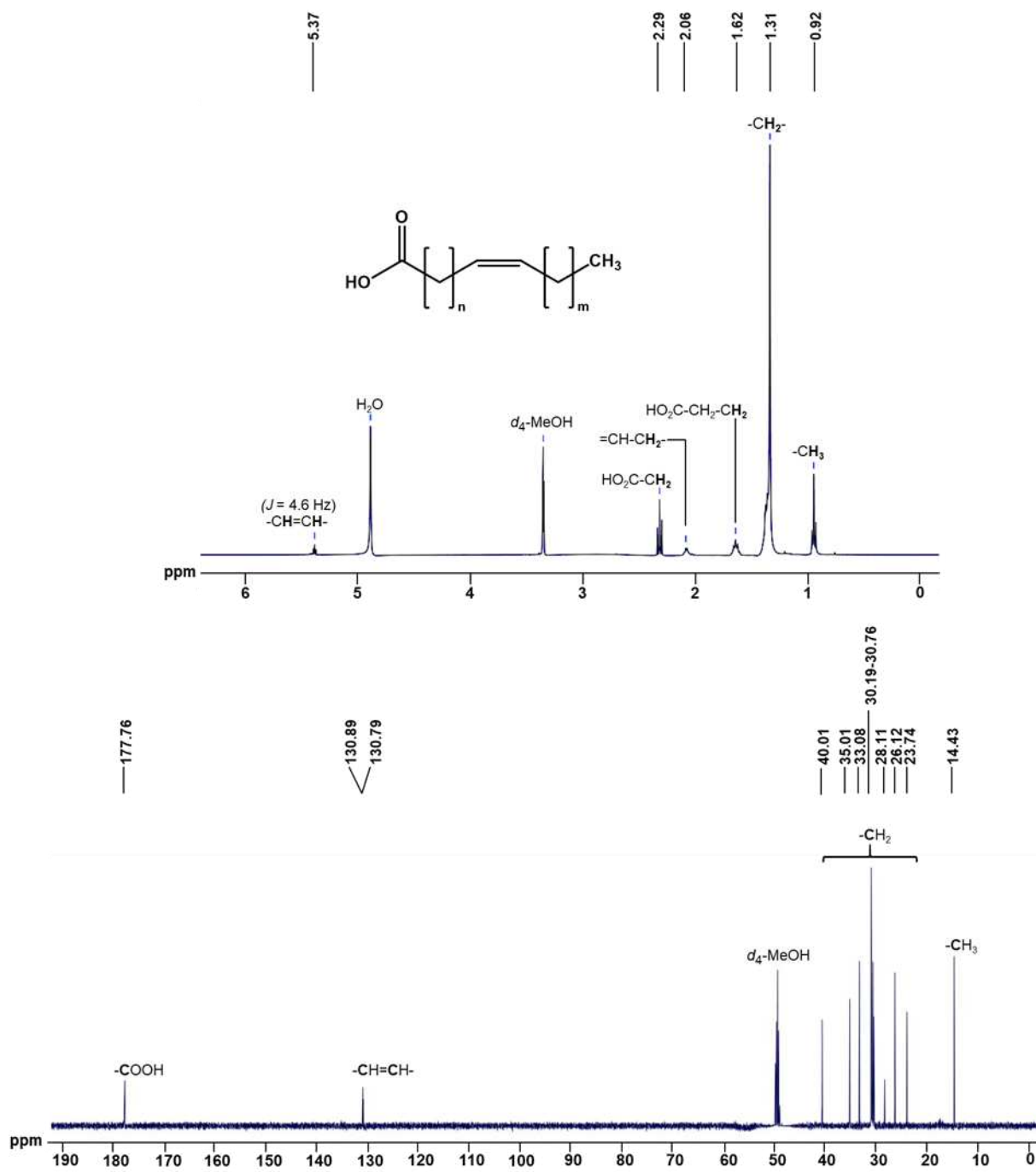
  

40 mg RP18-HPLC					
Fraction	E-1	E-2	E-3	E-4	E-5
weight (mg)	7.5	5.4	6.8	3.9	0.5
% AC5 activity	129	96	142	157	162
% AC3 activity	389	411	153	208	257

**Fractionation Scheme.** Si-VLC: Silica-Vacuum Liquid Chromatography, RP-HPLC: Reversed phase-High-performance liquid chromatography, EA: Ethyl acetate, PE: petroleum ether, MeOH: Methanol. % AC3 and AC5 activities compared to 300 nM G $\alpha$ s stimulation (= 100 %; values are means of two experiments carried out in triplicates. Fractions were tested at 1  $\mu$ g/10  $\mu$ L assay. Basal AC5 and 300 nM G $\alpha$ s activities were 0.05 nmol and 2.1 and for mAC3 0.02 and 0.15 nmol cAMP•mg<sup>-1</sup>•min<sup>-1</sup>, respectively.



**Fig. S1. RP-HPLC chromatogram of fraction E. UV-absorbance at 210 nm.**



**Fig. S2. NMR spectra of Fraction E2 in  $d_4$ -MeOH. (Top panel)  $^1\text{H}$ -NMR spectrum. (Bottom Panel)  $^{13}\text{C}$ -NMR spectrum.**

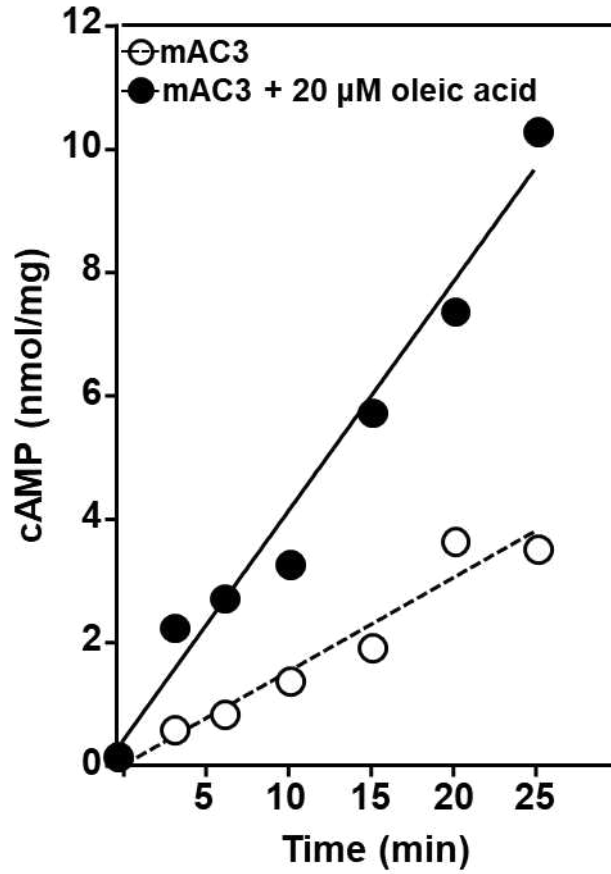


**Fig. S3. Time-dependent stimulation of mAC3 by oleic acid.** mAC3 was incubated with 300 nM Gs $\alpha$   $\pm$  20  $\mu$ M oleic acid at 37°C for the time depicted. Data represent the mean of two independent experiments performed in duplicates.

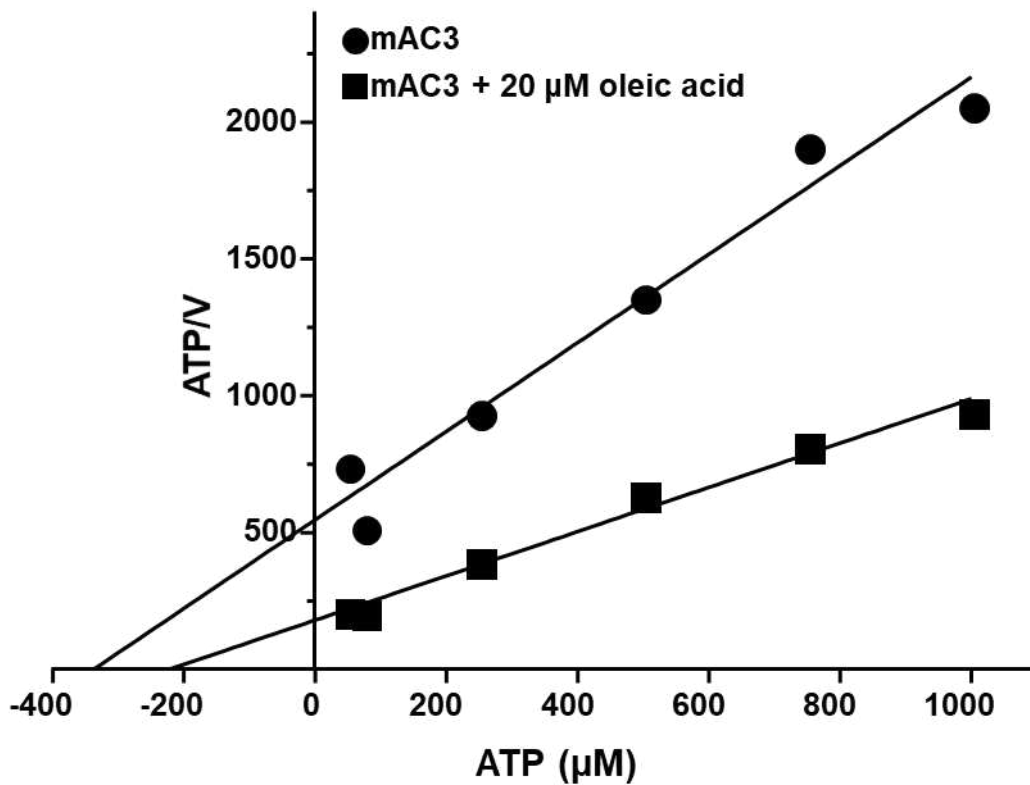


**Fig. S4. Hanes-Woolf plot of mAC3 ± 20 μM oleic acid.** The assay at 37°C, 15 min.  $K_m$  of ATP was 335 and 221 μM ± oleic acid, respectively (not significant).  $V_{max}$  ± oleic acid was 0.62 and 1.23 nmol cAMP•mg<sup>-1</sup>•min<sup>-1</sup>, respectively. Lineweaver-Burk plots and Eddie-Hofstee plots yielded identical data (not shown).

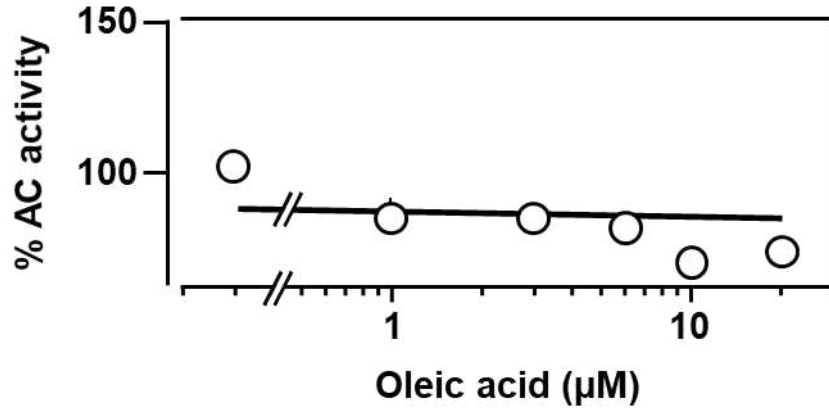


**Fig. S5. Oleic acid has no stimulatory effect on the soluble catalytic dimer.** Basal and 300 nM Gs $\alpha$  activities of the mAC1-C1/mAC2-C2 were  $0.02 \pm 0.003$  and  $0.08 \pm 0.02$  nmol cAMP $\cdot$ mg $^{-1}\cdot$ min $^{-1}$ , respectively. Error bars within the symbol size (n=3).

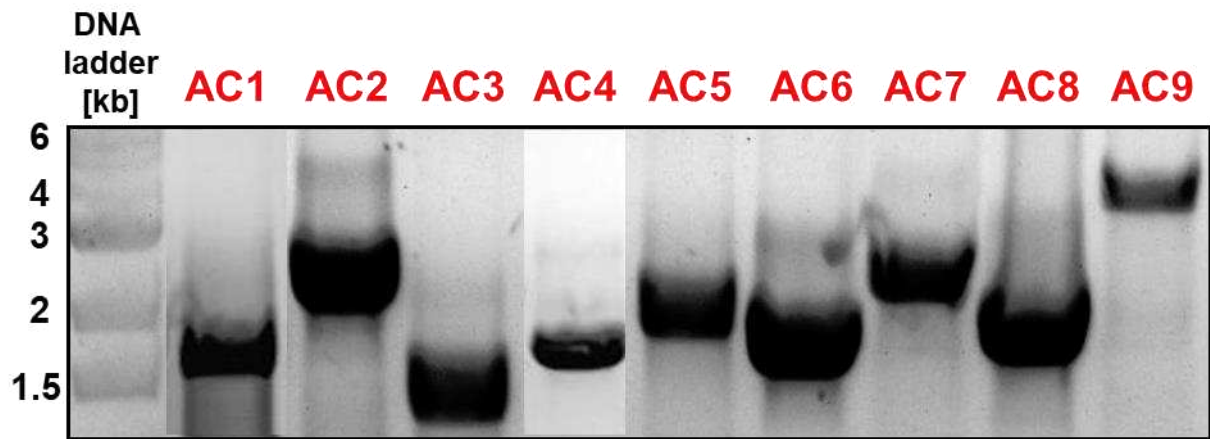


**Fig. S6. Agarose gels of PCR products from HEK293 cells permanently transfected with mAC1-9.** Expected amplicon lengths were 1667, 2266, 1296, 1642, 1864, 1624, 2270, 1730, and 3614 bp for mAC isoforms 1-9, respectively. As controls, the primers pairs for each isoform were tested with DNA isolated from all other eight cell lines, resulting in no bands (not shown). Further, the untransfected HEK293 cells were tested with the primers specific for each isoform, resulting in no bands (not shown; the primer pairs are listed in the experimental section above).

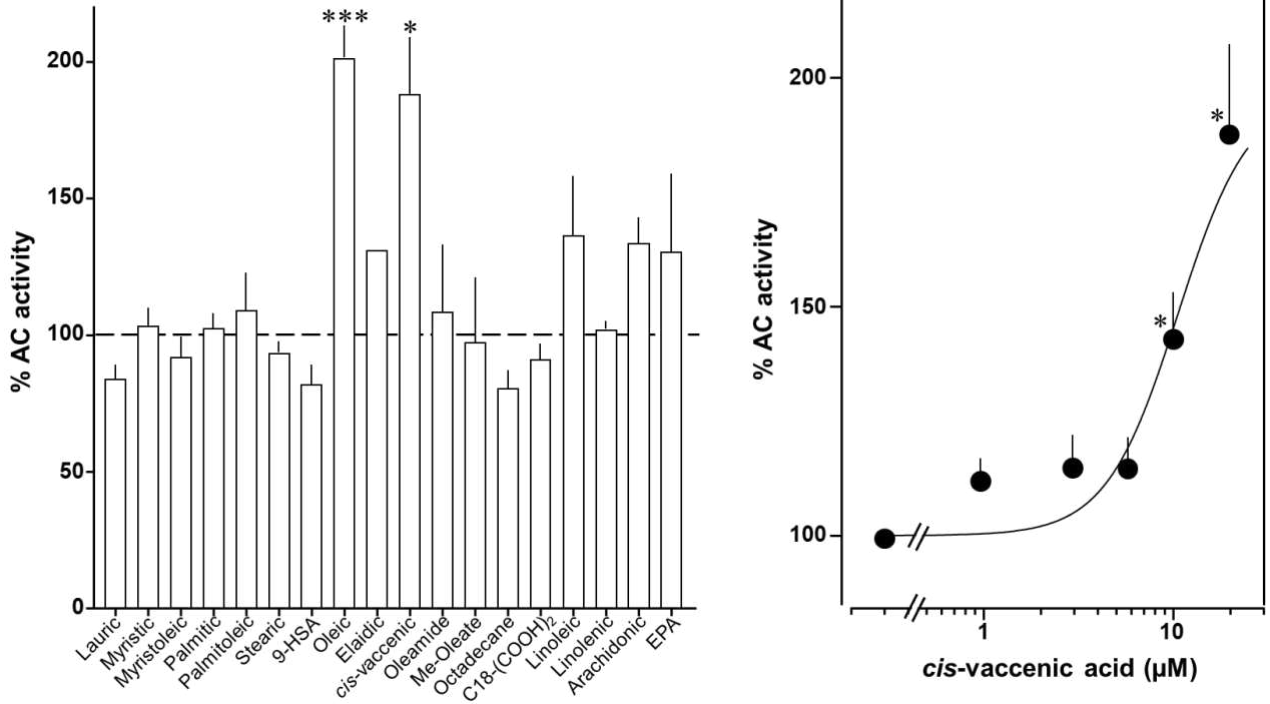


**Fig. S7. Effect of lipids on 300 nM Gs $\alpha$  stimulated mAC2.** (Left) Effect of 20  $\mu$ M lipids on mAC2. (Right) Concentration-response curve of *cis*-vaccenic acid. Basal and Gs $\alpha$ -stimulated activities of mAC2 were  $0.38 \pm 0.04$  and  $2.79 \pm 0.35$  nmol cAMP $\cdot$ mg $^{-1}$  $\cdot$ min $^{-1}$ , respectively. Error bars denote SEM of n=2-7. One-sample *t* test: \**P* < 0.05; \*\*\**P* < 0.001 compared to 100% (300 nM Gs $\alpha$  stimulation).

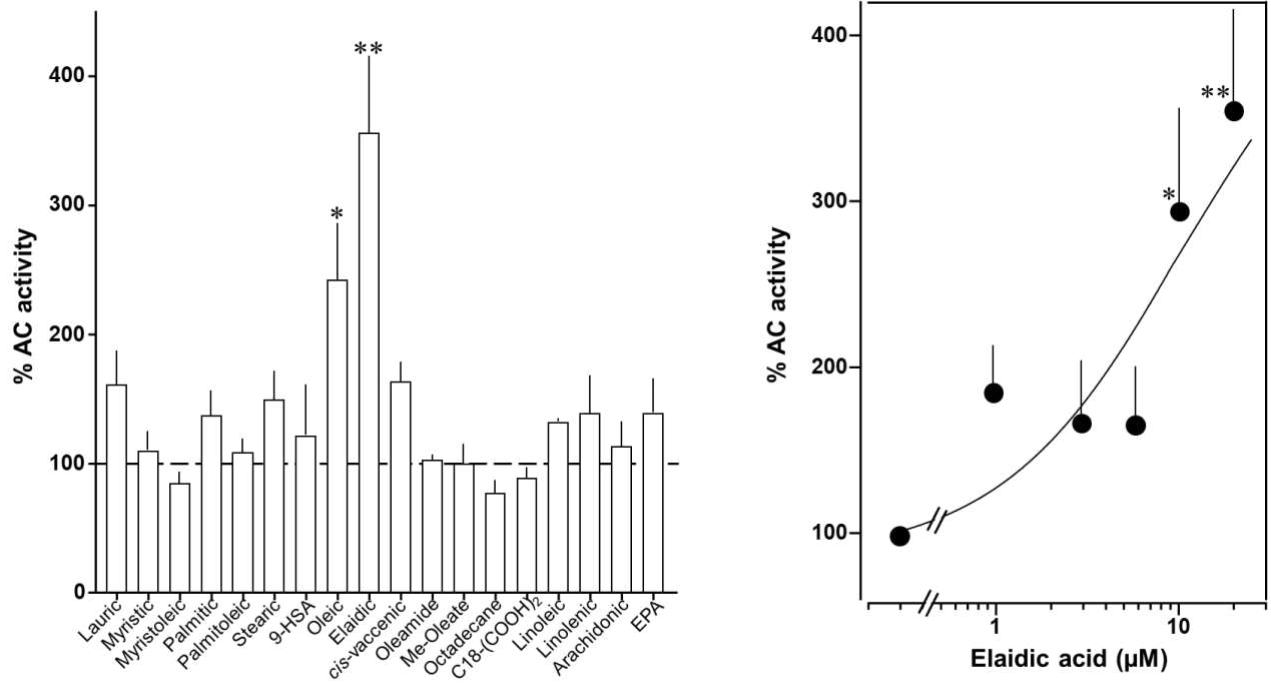


**Fig. S8. Effect of lipids on 300 nM G $\alpha$  stimulated mAC7. (Left)** Effect of 20  $\mu$ M lipids on mAC7. **(Right)** Concentration-response curve for elaidic acid. Basal and G $\alpha$ -stimulated activities were  $0.01 \pm 0.003$  and  $0.06 \pm 0.01$  nmol cAMP $\cdot$ mg $^{-1}$  $\cdot$ min $^{-1}$ , respectively. Error bars denote SEM of n=2-7. One-sample *t* test: \**P* < 0.05; \*\**P* < 0.01 compared to 100% (300 nM G $\alpha$  stimulation).

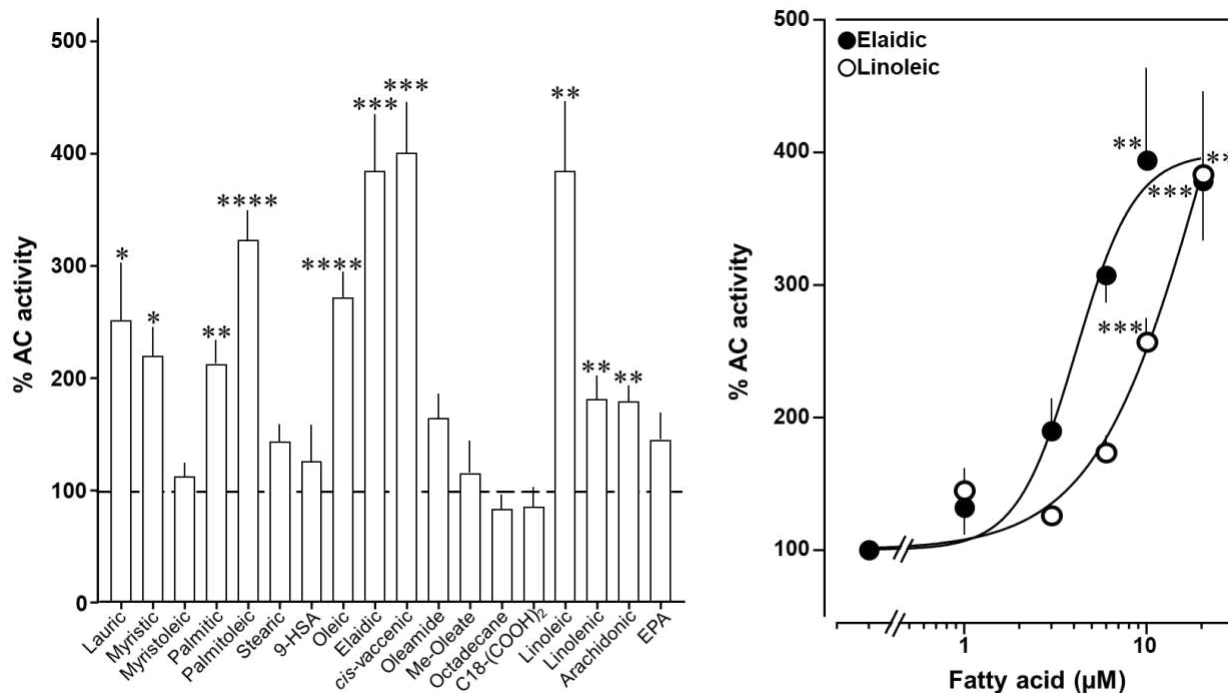


**Fig. S9. Effect of lipids on 300 nM G $\alpha$  stimulated mAC9.** (Left) Effect of 20  $\mu$ M lipids on mAC9. (Right) Concentration-response curves of elaidic and linoleic acids. EC<sub>50</sub> for elaidic acid was 5  $\mu$ M. Basal and G $\alpha$  activities were  $0.07 \pm 0.005$  and  $0.95 \pm 0.06$  nmol cAMP $\cdot$ mg<sup>-1</sup> $\cdot$ min<sup>-1</sup>, respectively. Error bars denote SEM of n=2-15. One-sample *t* test: \**P* < 0.05; \*\**P* < 0.01; \*\*\**P* < 0.001; \*\*\*\**P* < 0.0001 compared to 100% (300 nM G $\alpha$  stimulation).

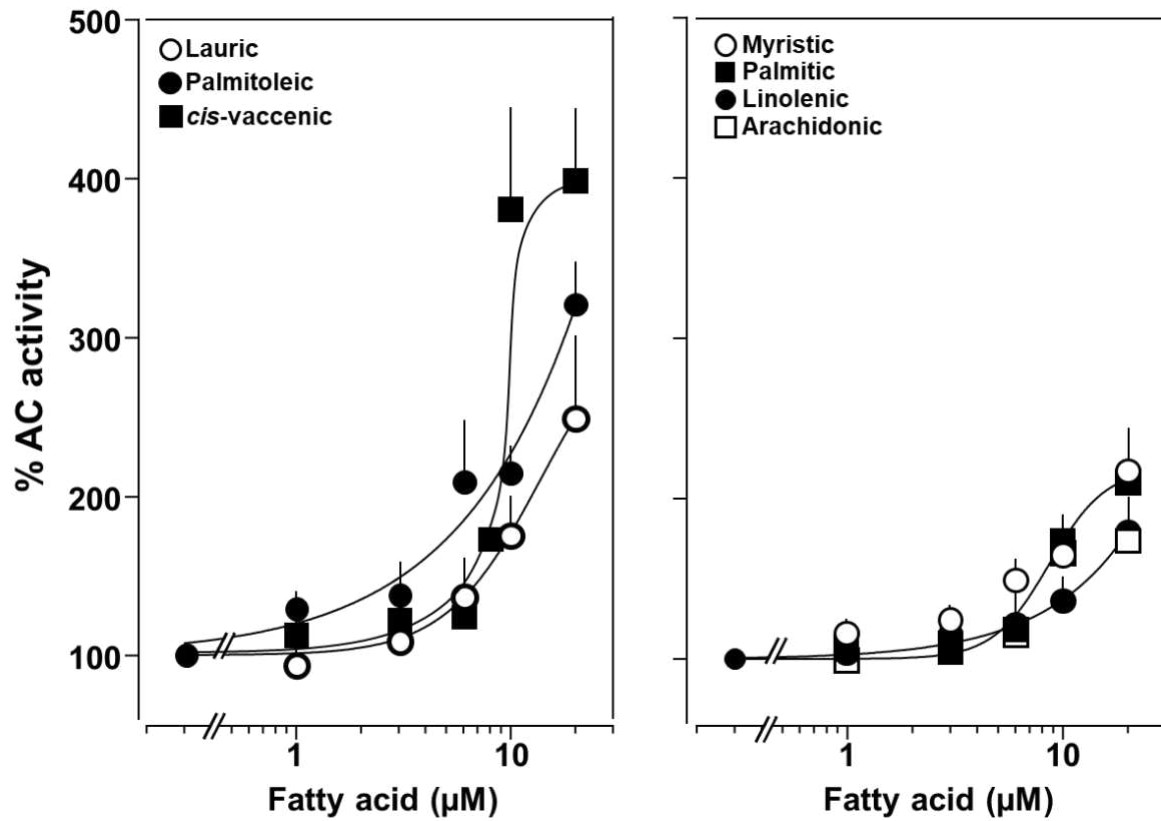


**Fig. S10. Concentration-response curves of fatty acids activating G $\alpha$ -stimulated mAC9.** Basal and G $\alpha$ -stimulated activities were  $0.06 \pm 0.005$  and  $0.92 \pm 0.07$  nmol cAMP $\cdot$ mg $^{-1}\cdot$ min $^{-1}$ , respectively. EC $_{50}$  values for lauric, *cis*-vaccenic, palmitic and arachidonic acids were 13.7, 8.5, 8.6 and 7.5  $\mu$ M, respectively. Error bars denote SEM of n=3-9. Significances were removed for clarity.

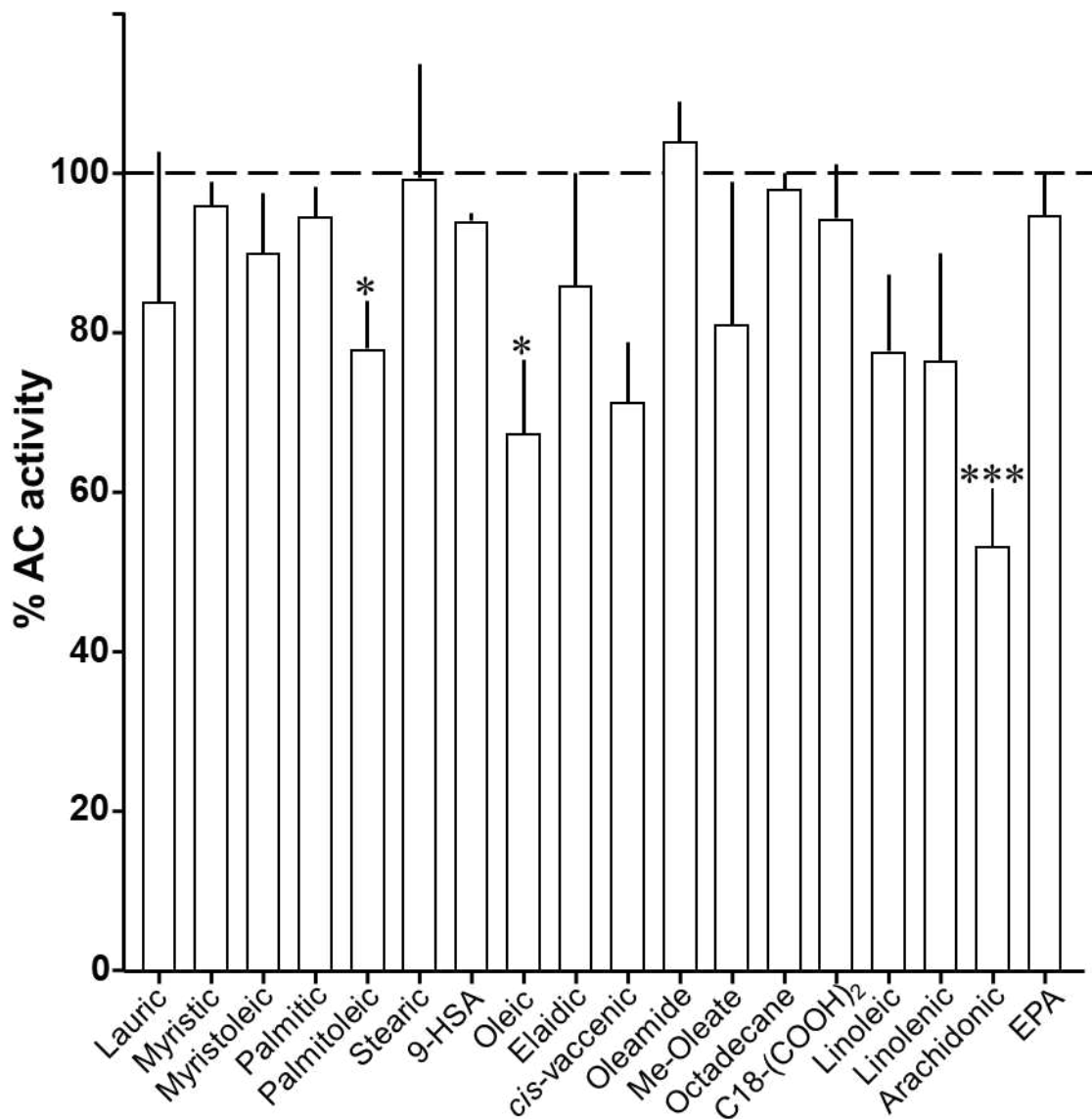


**Fig. S11. Effect of 20  $\mu$ M lipids on 300 nM G $\alpha$  stimulated mAC1.** Basal and G $\alpha$ -stimulated activities were  $0.18 \pm 0.02$  and  $0.46 \pm 0.02$  nmol cAMP $\cdot$ mg $^{-1}$  $\cdot$ min $^{-1}$ , respectively. Error bars denote SEM of n=2-9. One-sample *t* test: \**P* < 0.05; \*\*\**P* < 0.001 compared to 100% (300 nM G $\alpha$  stimulation).

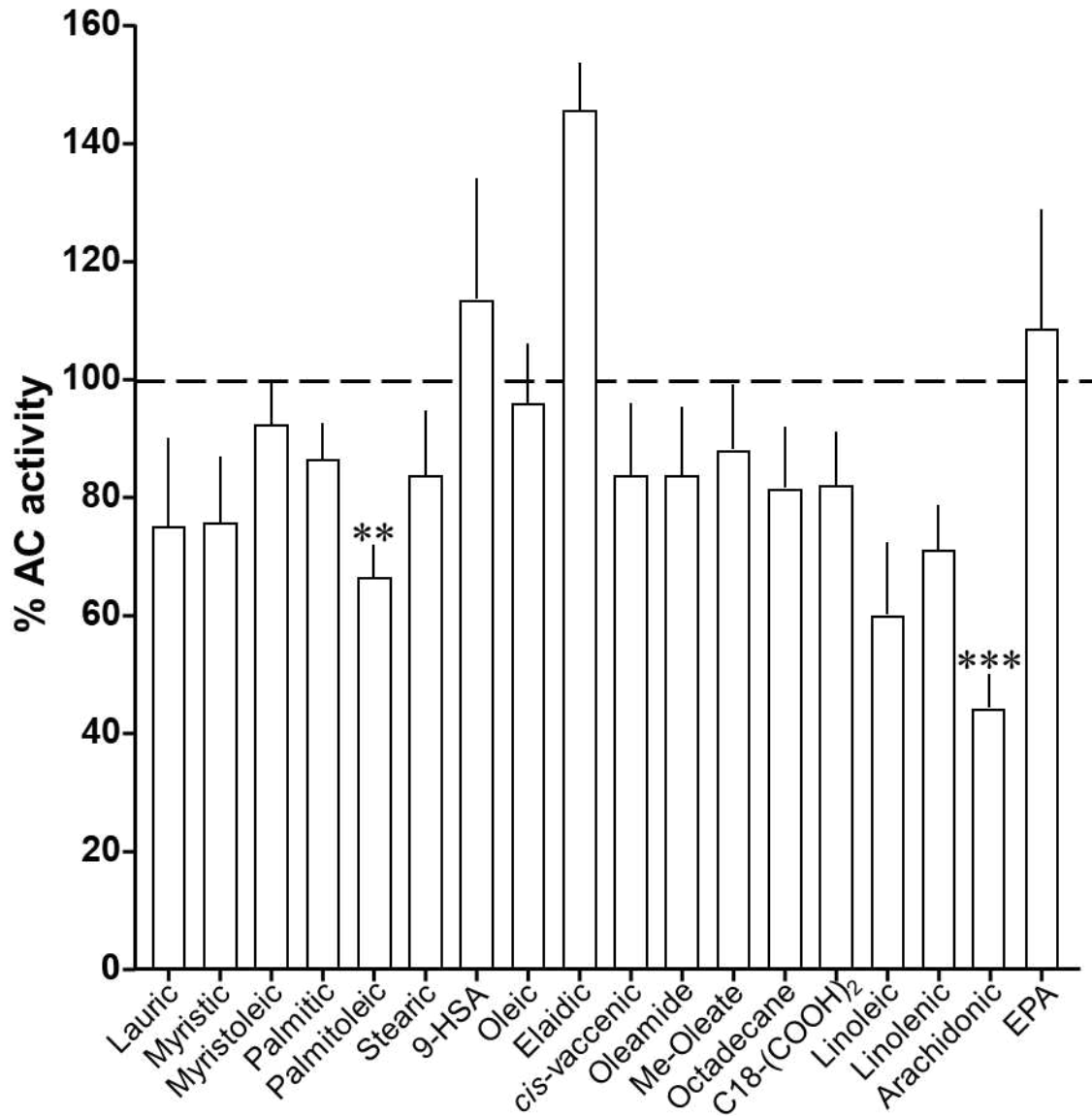


**Fig. S12. Effect of 20  $\mu$ M lipids on 300 nM Gs $\alpha$ -stimulated mAC4.** Basal and Gs $\alpha$ -stimulated activities were  $0.03 \pm 0.003$  and  $0.59 \pm 0.11$  nmol cAMP $\cdot$ mg $^{-1}$  $\cdot$ min $^{-1}$ , respectively. Error bars denote SEM of n=2-6. One-sample *t* test: \*\**P* < 0.01; \*\*\**P* < 0.001 compared to 100% (300 nM Gs $\alpha$  stimulation).

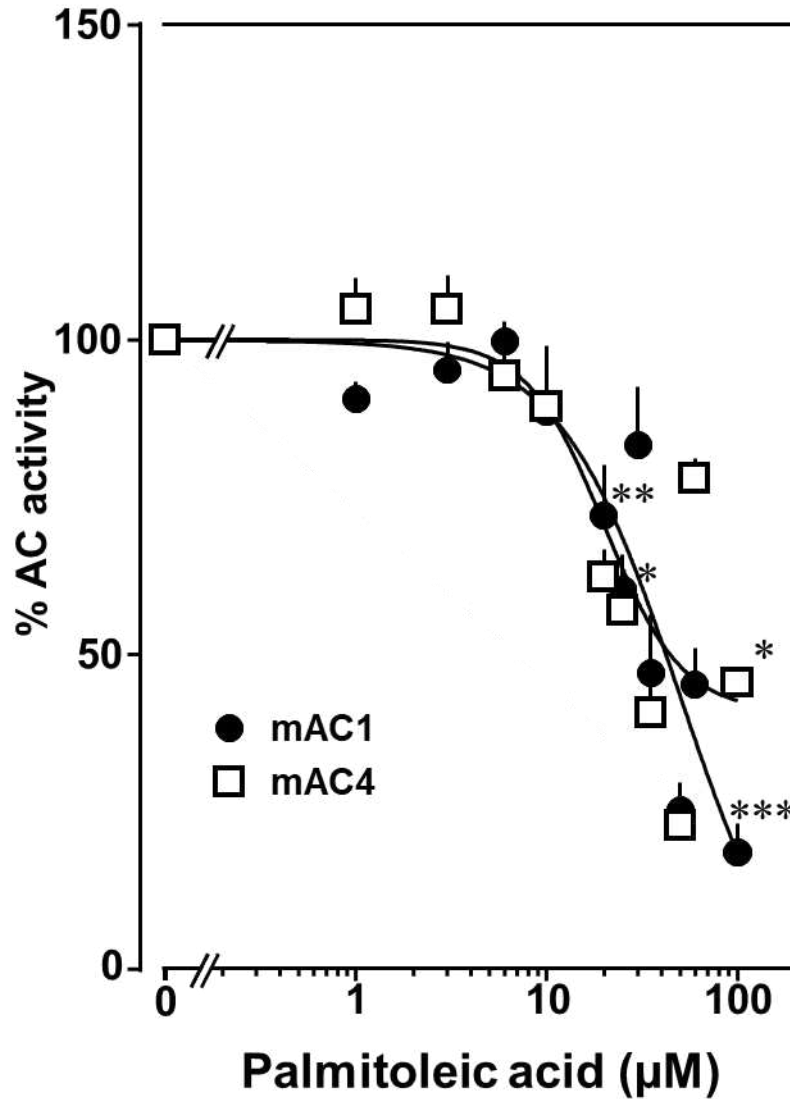


**Fig. S13. Palmitoleic acid inhibits mACs 1 and 4 stimulated by 300 nM G $\alpha$ .** Basal and G $\alpha$ -stimulated activities of mAC1 were  $0.14 \pm 0.01$  and  $0.44 \pm 0.02$  and of mAC4 were  $0.03 \pm 0.002$  and  $0.25 \pm 0.02$  nmol cAMP $\cdot$ mg $^{-1}$  $\cdot$ min $^{-1}$ . IC $_{50}$  for mAC1 and 4 were 49 and 20  $\mu$ M, respectively. Error bars denote SEM of n= 3-6. One-sample *t* test: \**P* < 0.05; \*\**P* < 0.01 \*\*\**P* < 0.001; compared to 100% (300 nM G $\alpha$  stimulation).

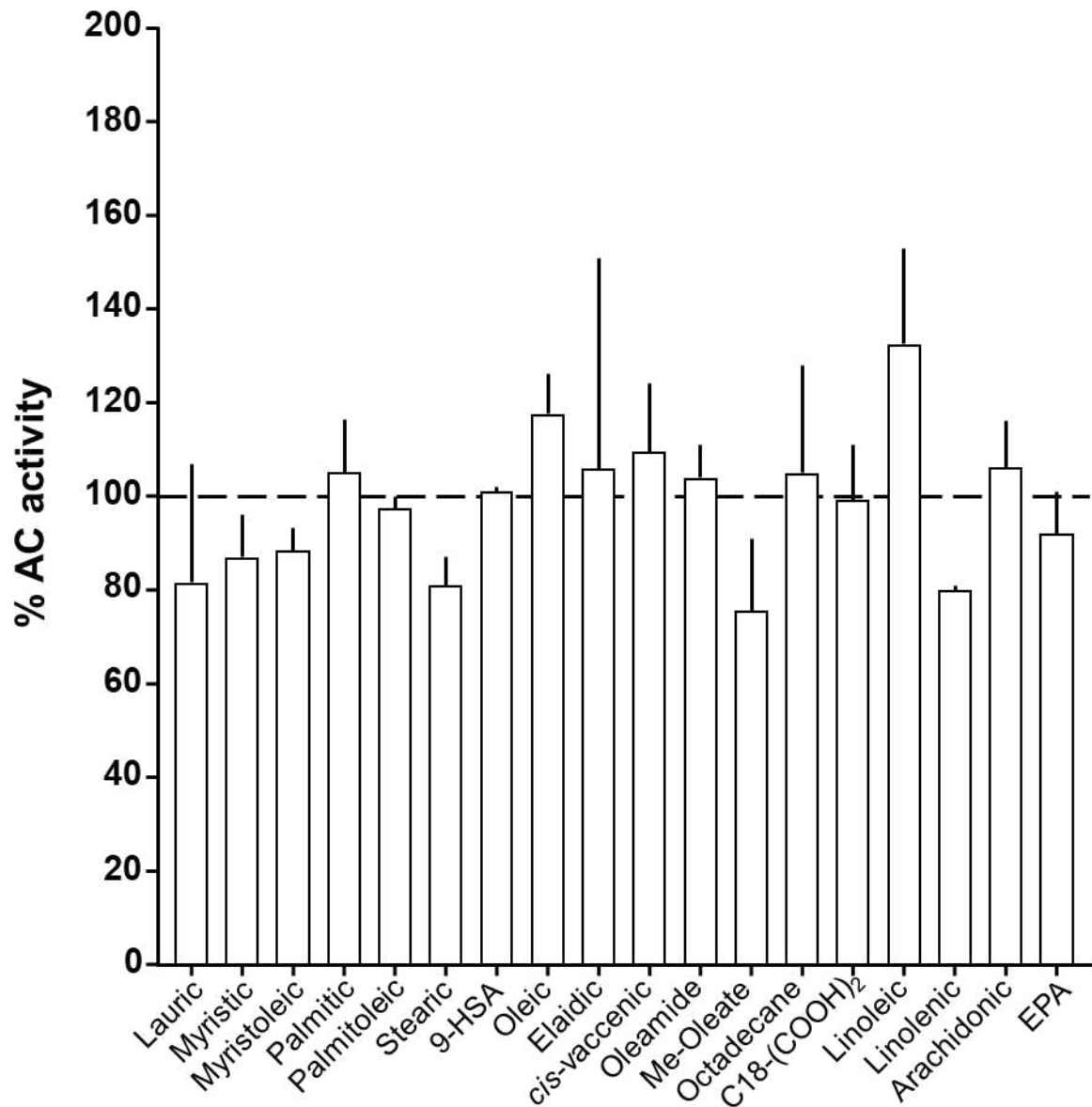


**Fig. S14. Effect of 20  $\mu$ M lipids on 300 nM Gs $\alpha$ -stimulated mAC5.** Basal and Gs $\alpha$  activities were  $0.07 \pm 0.01$  and  $0.46 \pm 0.04$  nmol cAMP $\cdot$ mg $^{-1}\cdot$ min $^{-1}$ , respectively. Error bars denote SEM of n=2-5.

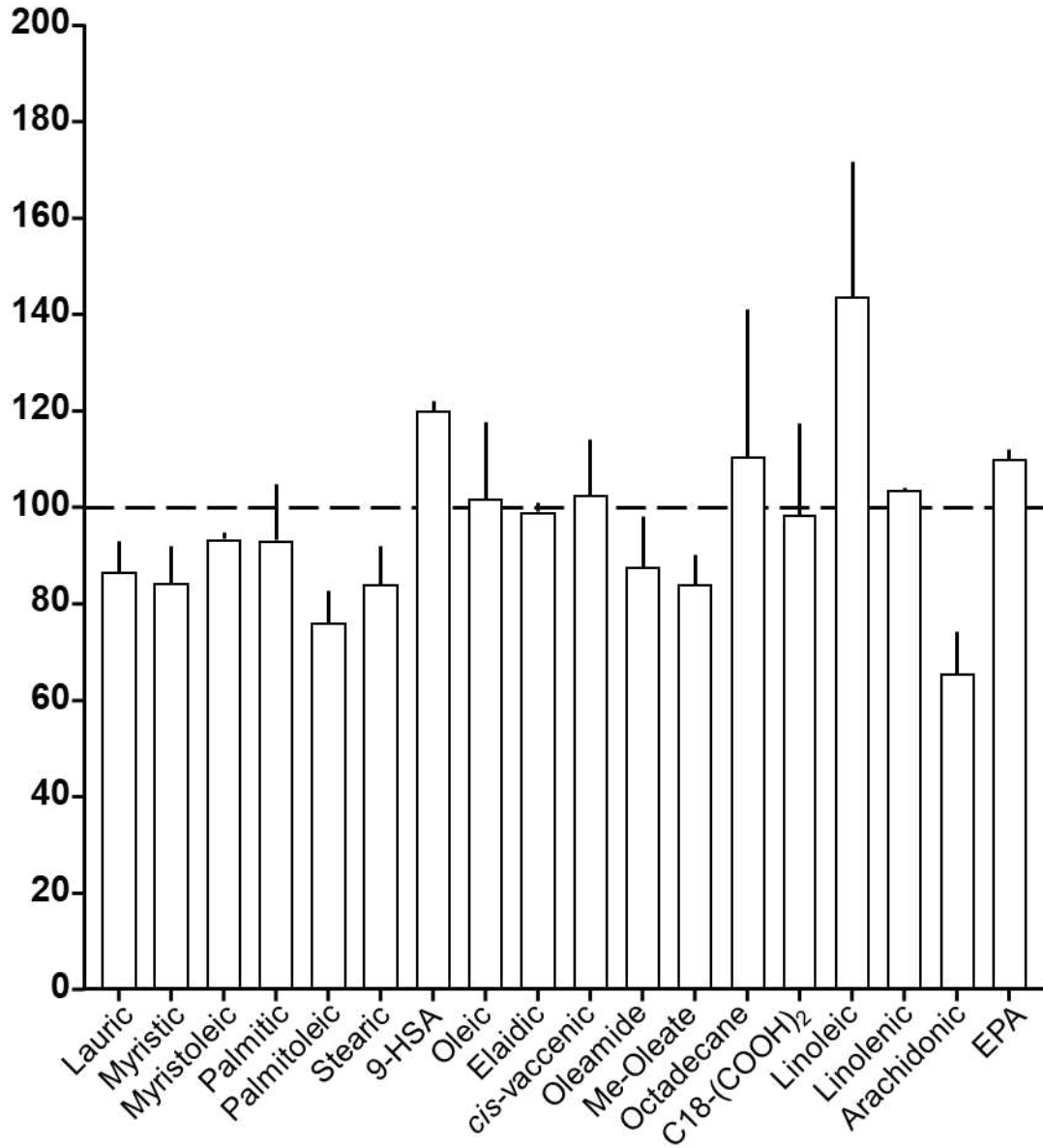


**Fig. S15. Effect of 20  $\mu$ M lipids on 300 nM Gs $\alpha$ -stimulated mAC6.** Basal and Gs $\alpha$  activities were  $0.07 \pm 0.01$  and  $0.50 \pm 0.06$  nmol cAMP $\cdot$ mg<sup>-1</sup> $\cdot$ min<sup>-1</sup>, respectively. Error bars denote SEM of n=2-6.

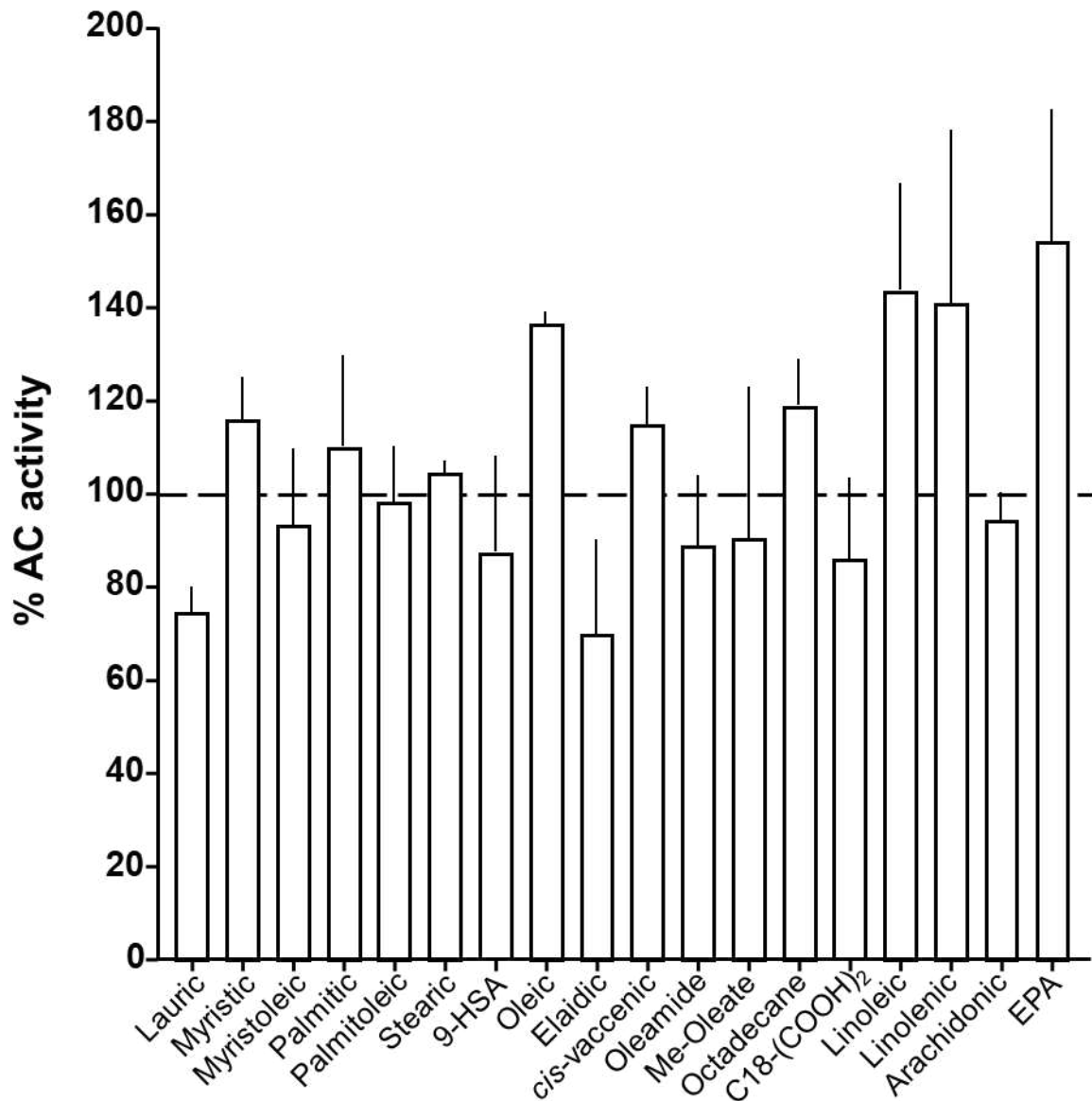


**Fig. S16. Effect of 20  $\mu\text{M}$  lipids on 300 nM  $\text{G}\alpha$  stimulated mAC8.** Basal and  $\text{G}\alpha$  activities were  $0.19 \pm 0.01$  and  $1.04 \pm 0.19 \text{ nmol cAMP}\cdot\text{mg}^{-1}\cdot\text{min}^{-1}$ , respectively. Error bars denote SEM of  $n=2-5$ .

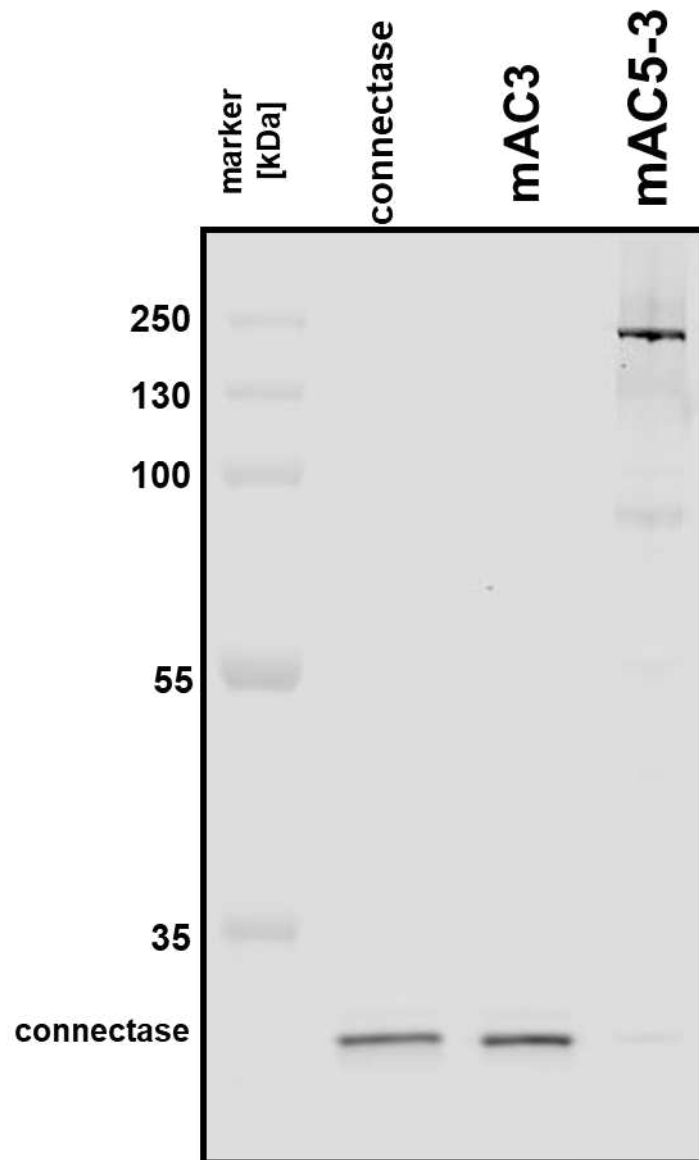


**Fig. S17. Detection of AC5<sub>(membr)</sub>-AC3<sub>(cat)</sub> receptor chimeras.** AC5<sub>(membr)</sub>-AC3<sub>(cat)</sub> [AC5-3] was expressed in HEK293 cells with an N-terminal tag for labeling with the protein ligase Connectase. A membrane preparation was incubated with fluorophore-conjugated Connectase and separated by SDS-PAGE. A fluorescence scan of the gel detects AC5<sub>(membr)</sub>-AC3<sub>(cat)</sub> (right), the reagent (fluorophore-conjugated Connectase) is detected when using HEK293 membrane (middle) or a buffer control (left).

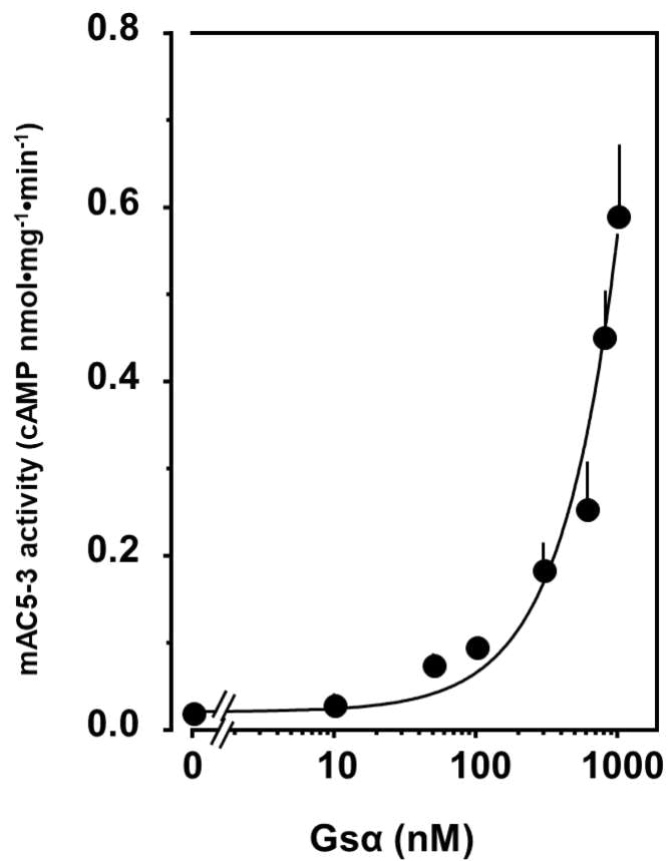


**Fig. S18. Gsa concentration response curve of mAC5-3.** Basal activity for mAC5-3 was 0.02 pmol cAMP·mg<sup>-1</sup>·min<sup>-1</sup>. Error bars denote SEM of n=3, each with two technical replicates.

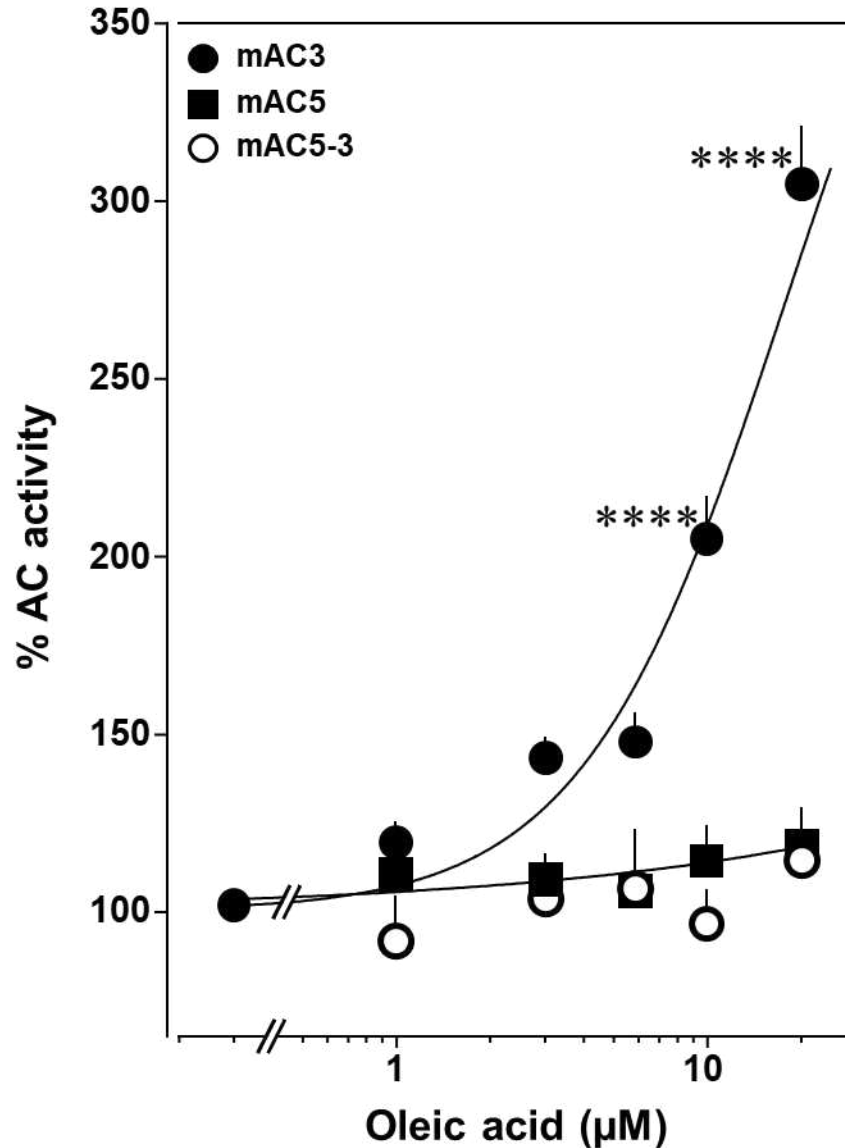


**Fig. S19. Exchange of TM domains abrogates oleic acid effect on mAC3.** Basal and Gs $\alpha$ -stimulated activities of mAC3 were  $0.02 \pm 0.003$  and  $0.11 \pm 0.02$  and of mAC5 were  $0.05 \pm 0.008$  and  $0.53 \pm 0.1$  and of mAC5-3 were  $0.01 \pm 0.004$  and  $0.2 \pm 0.02$  nmol cAMP $\cdot$ mg $^{-1}\cdot$ min $^{-1}$ , respectively. Error bars denote SEM of n= 6-33. One-sample *t* test: \*\*\*\**P* < 0.0001 compared to 100% (300 nM Gs $\alpha$  stimulation).

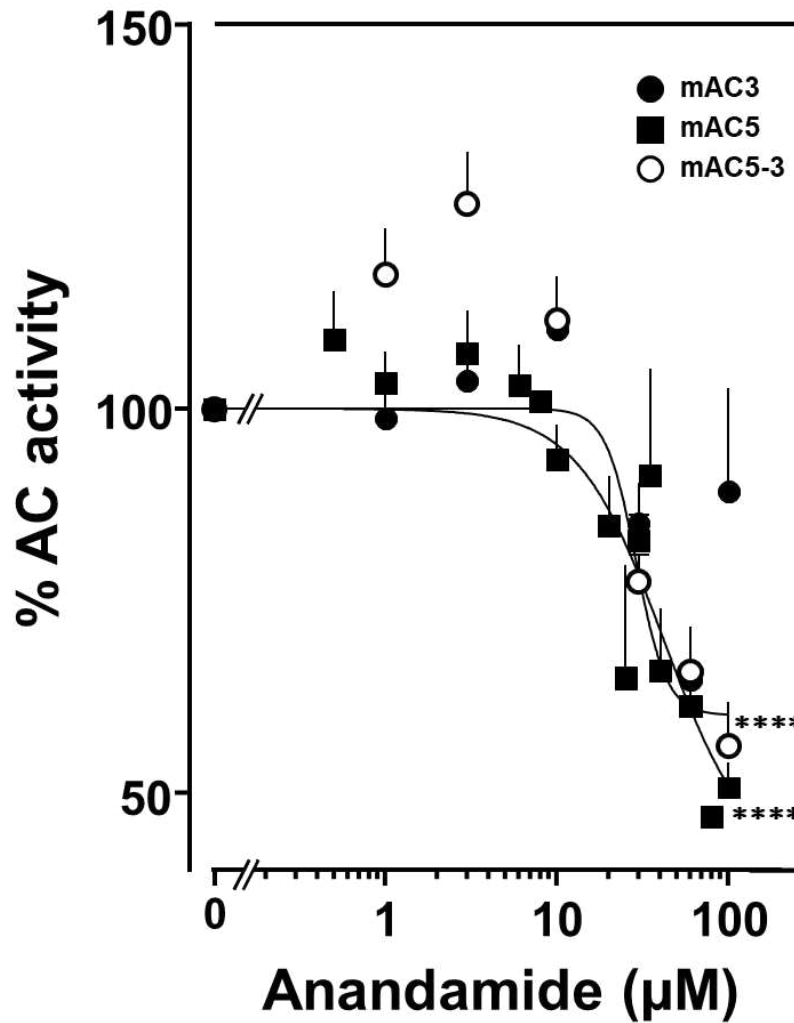


**Fig. S20. Exchange of TM domains transfers anandamide effect on mAC3.** Basal and Gs $\alpha$ -stimulated activities of mAC3 were  $0.02 \pm 0.002$  and  $0.12 \pm 0.02$  and of mAC5 were  $0.05 \pm 0.005$  and  $0.98 \pm 0.12$  and of mAC5-3 were  $0.02 \pm 0.002$  and  $0.22 \pm 0.03$  nmol cAMP $\cdot$ mg $^{-1}\cdot$ min $^{-1}$ , respectively. Error bars denote SEM of n=6-32. One-sample *t* test: \*\*\*\**P* < 0.0001 compared to 100% (300 nM Gs $\alpha$  stimulation).

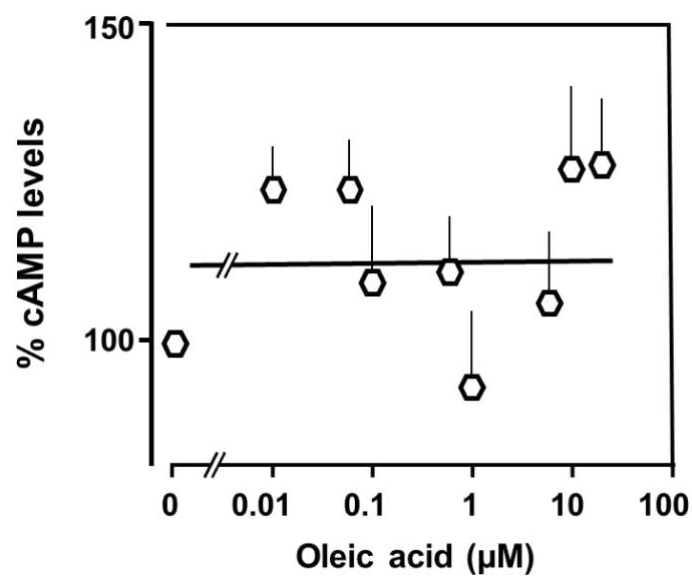


**Fig. S21. Effect of oleic acid on HEK293-mAC5-3 cells.** Cells were stimulated by 2.5 µM isoproterenol (set as 100 %). Basal and isoproterenol stimulated cAMP levels were  $0.17 \pm 0.02$  and  $3.12 \pm 0.55$  pmol cAMP/10000 cells in the presence of 0.5 mM IBMX. Error bars denote SEM of  $n=4$ .

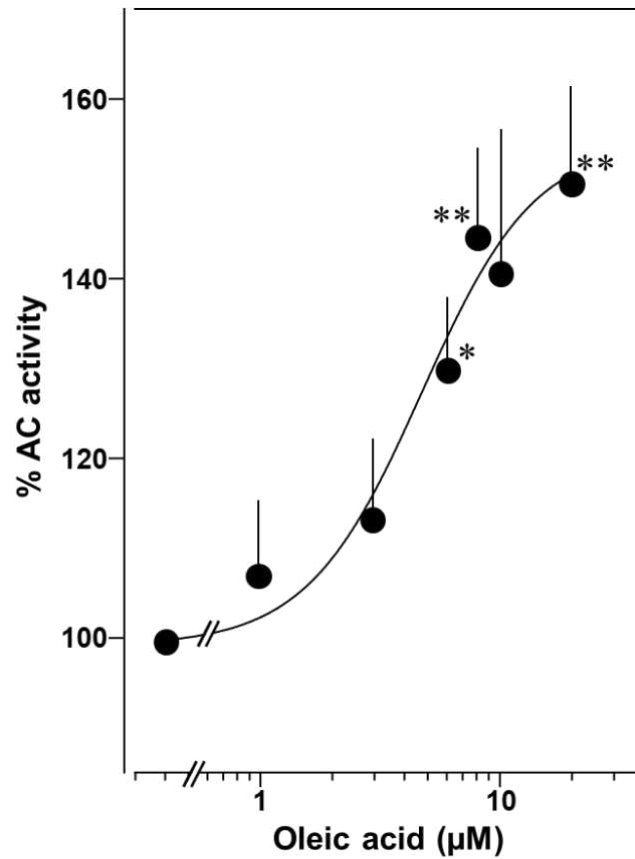


**Fig. S22. Oleic acid concentration-dependently potentiates mAC activity in brain cortical membranes from mouse.** Basal and 300 nM Gs $\alpha$ -stimulated activities were  $0.4 \pm 0.1$  and  $2.7 \pm 0.7$  nmol cAMP $\cdot$ mg $^{-1}\cdot$ min $^{-1}$ , respectively. N= 4-6. One-sample *t* test: \**P* < 0.05; \*\**P* < 0.01 compared to 100% (Gs $\alpha$  stimulation).

---

Tested Compounds

---

Lauric (Dodecanoic) acid

Myristic (Tetradecanoic) acid

Myristoleic ((9Z)-Tetradec-9-enoic) acid

Palmitic (Hexadecanoic) acid

Palmitoleic ((9Z)-Hexadec-9-enoic) acid

Octadecane

1,18-Octadecanedicarboxylic acid

Stearic (Octadecanoic) acid

9-Hydroxystearic acid

Oleic ((9Z)-Octadec-9-enoic) acid

Oleamide ((9Z)-Octadec-9-enamide)

Methyl oleate

Elaidic ((9E)-Octadec-9-enoic) acid

*cis*-vaccenic ((11E)-Octadec-11-enoic) acid

Linoleic ((9Z,12Z)-Octadeca-9,12-dienoic) acid

Linolenic ((9Z,12Z,15Z)-Octadeca-9,12,15-trienoic) acid

Arachidonic ((5Z,8Z,11Z,14Z)-Icosa-5,8,11,14-tetraenoic) acid

Eicosapentaenoic ((5Z,8Z,11Z,14Z,17Z)-Icosa-5,8,11,14,17-pentaenoic) acid

---

**Table S1. List of lipids tested against mAC isoforms.**

	<b>N</b>	<b>Basal activity</b>	<b>300 nM Gsα activity</b>
<b>AC1</b>	5	0.12 ± 0.02	0.39 ± 0.05
<b>AC2</b>	7	0.22 ± 0.05	1.41 ± 0.21
<b>AC3</b>	23	0.02 ± 0.002	0.17 ± 0.03
<b>AC4</b>	4	0.02 ± 0.007	0.19 ± 0.02
<b>AC5</b>	7	0.05 ± 0.01	0.50 ± 0.11
<b>AC6</b>	3	0.06 ± 0.02	0.29 ± 0.05
<b>AC7</b>	7	0.01 ± 0.001	0.05 ± 0.002
<b>AC8</b>	2	0.08 ± 0.02	0.31 ± 0.06
<b>AC9</b>	15	0.09 ± 0.02	0.97 ± 0.15

**Table S2. Basal and Gsα-stimulated activities of mAC isoforms.** Activities are listed as mean ± SEM in nmol cAMP•mg<sup>-1</sup>•min<sup>-1</sup>.

## 4. DISCUSSION and OUTLOOK

Nine mACs with similar architecture are encoded in mammals and catalyze the generation of cAMP from ATP (Dessauer, Watts et al. 2017). The current knowledge on the functional importance of its TM domains is poor. Expression of 1C1:2C2 chimeric protein i.e. no TM domains, resulted in functionally active enzyme, deeming TMs unnecessary (Tang and Gilman 1995). However, many conceivable arguments have drawn the attention to other possible roles aside membrane anchoring. Our group proposed a receptor function for these anchors (Seth, Finkbeiner et al. 2020). In this role, TM domains would receive extracellular input signal (ligand) and transduce it through cytosolic linkers to the catalytic dimer. We showed that components in the serum may bind to the membrane anchors and alter the activity of mACs (Seth, Finkbeiner et al. 2020). To validate this novel function, it was necessary to identify the potential ligands. This would add a new perspective towards mACs regulation, in conjunction with the already established indirect ways of regulation i.e. G-proteins, calmodulin, Ca<sup>2+</sup>, FSK, etc. I embarked on a quest to possibly identify mACs ligands. We initiated our work with the anticipation of finding inhibitory compounds, based on our earlier results (Seth, Finkbeiner et al. 2020). By eliminating proteins and peptide and taking into consideration the hydrophobic nature of the CqsS ligand CAI-1, we expected the ligands to be of lipidic nature. For this, we first used FBS as potential source of ligands. Lipid extraction followed by lipidomic analysis led to identification of GPLs which unexpectedly enhanced mAC activity. A major component of biological membranes, GPLs are known to participate in many signaling processes including GPCRs and ion channels (Mukhopadhyay and Trauner 2023). No previous reports have linked GPLs and mACs. Our study was demonstrated that GPLs can affect various mAC isoforms distinctly, their action being similar to that of FSK. Changing the acyl groups led to remarkable reduction or loss of potency. Besides, GPLs with different head groups showed different efficacies albeit similar potencies. We speculate that GPLs most likely bind to the catalytic dimer. Yet, information about how their biosynthesis and release is linked to cAMP is still unknown.

We then tried to isolate lipids, this time using lung tissue as a starting material. We identified free heme b as a non-specific inhibitor of mammalian as well as bacterial ACs. As a signaling molecule, heme b is known to control the activities of distinct regulators (Mense and Zhang 2006). It was shown previously that heme b and cAMP

are connected (ref. [40-44] in publication II). Interestingly, a heme-binding domain was identified in the soluble isoform of AC with activating effect on its activity (Middelhaufe, Leipelt et al. 2012). We again assume that heme b would bind to the cytosolic catalytic domains. Considering that free heme b levels are elevated in several pathological conditions, we speculate that the effect of heme b on cAMP generation might be of medical relevance. Further studies are mandatory to elucidate the exact mechanism.

Lastly, we reached our primary goal by identifying aliphatic lipids (fatty acids and the endocannabinoid anandamide) as mACs ligands. These lipids were able to specifically enhance mACs 2, 3, 7, and 9 and attenuate mACs 1, 4, 5, and 6, distinct effects which bolster the receptor hypothesis. A ligand for mAC8 could not be identified. Generally, constructing chimeras of full-length mAC isoforms is deemed difficult due to instability and thereby functional inactivity (Seebacher, Linder and Schultz 2001). However, we managed to generate a catalytically active mAC5<sub>TM</sub>-mAC3<sub>cat</sub> chimera which was not affected by the mAC3-enhancing oleic acid and attenuated by the mAC5-inhibiting anandamide, proving that specific lipid-TM domain interaction is necessary for eliciting a response. Fatty acids serve as signaling molecules in numerous physiological processes, e.g. for free fatty acid receptors as well as other receptors (Kimura, Ichimura et al. 2020). As a lipid mediator affecting cannabinoid receptor 1, anandamide was shown to serve key roles in various biological processes in the periphery and central nervous system (Scherma, Masia et al. 2019). Previous studies have demonstrated that free fatty acids can have dual effects i.e. activation and inhibition on ACs activities, which is in agreement with our results (Fain and Shepherd 1975, Orly and Schramm 1975, Ahmad, Alam and Alam 1990, Nakamura, Okamura et al. 2001). Our study, however, is the first to show that these effects can be attributed to the fatty acids' direct binding to specific mACs membrane anchors. Anandamide, on the other hand was shown to inhibit AC activity via direct acting on cannabinoid receptor (Vogel, Barg et al. 1993). Our study revealed that it can also act directly on mACs, specifically attenuating isoforms 1, 5 and 6.

Our studies do not cancel or contradict the already established ways of mAC regulation. On the contrary, it paves the way towards looking for novel mACs regulators that would help to understand its physiological roles. Comprehending the specific role and regulation of an individual mAC isoform is hindered by the complexity and heterogeneity of mAC expression patterns in different cell types. Most importantly,

from the pharmacological perspective, mACs constitute important drug targets. However, it is difficult until now to develop high-affinity inhibitory or stimulatory compounds that would selectively bind to a specific mAC isoform. Here, our work comes into play. It could be possible now to achieve these goals i.e. developing specific binders to study specific mAC roles and regulation and for pharmacological modulation, by targeting the non-conserved mACs membrane anchors. Noteworthy is the proposed cytosolic catalytic action of GPLs which also showed specific effects on mACs. However, our studies are still lacking structural information. Knowledge of the structural basis of mACs-ligand interaction would form the basis for the development of selective and potent mAC isoform activators and inhibitors. It goes without saying that our work has some unresolved questions which mandate further studies.

## 5. REFERENCES

- Ahmad, S. N., S. Q. Alam and B. S. Alam (1990). "Fatty acid incorporation into membranes of dispersed rat submandibular salivary gland cells and their effect on adenylate cyclase activity." Arch Oral Biol **35**(11): 879-883.
- Andersson, R. and K. Nilsson (1972). "Cyclic AMP and calcium in relaxation in intestinal smooth muscle." Nat New Biol **238**(82): 119-120.
- Barzu, O. and A. Danchin (1994). "Adenylyl cyclases: a heterogeneous class of ATP-utilizing enzymes." Prog Nucleic Acid Res Mol Biol **49**: 241-283.
- Bassler, J., J. E. Schultz and A. N. Lupas (2018). "Adenylate cyclases: Receivers, transducers, and generators of signals." Cell Signaling **46**: 135-144.
- Beltz, S., J. Bassler and J. E. Schultz (2016). "Regulation by the quorum sensor from *Vibrio* indicates a receptor function for the membrane anchors of adenylate cyclases." Elife **5**.
- de Rooij, J., H. Rehmann, M. van Triest, R. H. Cool, A. Wittinghofer and J. L. Bos (2000). "Mechanism of regulation of the Epac family of cAMP-dependent RapGEFs." J Biol Chem **275**(27): 20829-20836.
- Dessauer, C. W., V. J. Watts, R. S. Ostrom, M. Conti, S. Dove and R. Seifert (2017). "International Union of Basic and Clinical Pharmacology. Cl. Structures and Small Molecule Modulators of Mammalian Adenylyl Cyclases." Pharmacol Rev **69**(2): 93-139.
- Fain, J. N. and R. E. Shepherd (1975). "Free fatty acids as feedback regulators of adenylate cyclase and cyclic 3':5'-AMP accumulation in rat fat cells." J Biol Chem **250**(16): 6586-6592.
- Fesenko, E. E., S. S. Kolesnikov and A. L. Lyubarsky (1985). "Induction by cyclic GMP of cationic conductance in plasma membrane of retinal rod outer segment." Nature **313**(6000): 310-313.
- Gancedo, J. M. (2013). "Biological roles of cAMP: variations on a theme in the different kingdoms of life." Biol Rev Camb Philos Soc **88**(3): 645-668.
- Hardman, J. G., G. A. Robison and E. W. Sutherland (1971). "Cyclic nucleotides." Annu Rev Physiol **33**: 311-336.
- Heldin, C. H., B. Lu, R. Evans and J. S. Gutkind (2016). "Signals and Receptors." Cold Spring Harb Perspect Biol **8**(4): a005900.
- Iseki, M., S. Matsunaga, A. Murakami, K. Ohno, K. Shiga, K. Yoshida, M. Sugai, T. Takahashi, T. Hori and M. Watanabe (2002). "A blue-light-activated adenylyl cyclase mediates photoavoidance in *Euglena gracilis*." Nature **415**(6875): 1047-1051.
- Khanppnavar, B., V. Mehta, C. Qi and V. Korkhov (2020). "Structure and function of adenylyl cyclases, key enzymes in cellular signaling." Curr Opin Struct Biol **63**: 34-41.
- Khanppnavar, B., D. Schuster, P. Lavriha, F. Uliana, M. Ozel, V. Mehta, A. Leitner, P. Picotti and V. M. Korkhov (2024). "Regulatory sites of CaM-sensitive adenylyl cyclase AC8 revealed by cryo-EM and structural proteomics." EMBO Rep **25**(3): 1513-1540.
- Kimura, I., A. Ichimura, R. Ohue-Kitano and M. Igarashi (2020). "Free Fatty Acid Receptors in Health and Disease." Physiol Rev **100**(1): 171-210.
- Krupinski, J., F. Coussen, H. A. Bakalyar, W. J. Tang, P. G. Feinstein, K. Orth, C. Slaughter, R. R. Reed and A. G. Gilman (1989). "Adenylyl cyclase amino acid sequence: possible channel- or transporter-like structure." Science **244**(4912): 1558-1564.
- Lambert, D. G. (1993). "Signal transduction: G proteins and second messengers." Br J Anaesth **71**(1): 86-95.

- Levin, L. R. and R. R. Reed (1995). "Identification of functional domains of adenylyl cyclase using in vivo chimeras." J Biol Chem **270**(13): 7573-7579.
- Linder, J. U. and J. E. Schultz (2003). "The class III adenylyl cyclases: multi-purpose signalling modules." Cell Signal **15**(12): 1081-1089.
- McDonough, K. A. and A. Rodriguez (2011). "The myriad roles of cyclic AMP in microbial pathogens: from signal to sword." Nat Rev Microbiol **10**(1): 27-38.
- Mehta, V., B. Khanppnavar, D. Schuster, I. Kantarci, I. Vercellino, A. Kosturanova, T. Iype, S. Stefanic, P. Picotti and V. M. Korkhov (2022). "Structure of Mycobacterium tuberculosis Cya, an evolutionary ancestor of the mammalian membrane adenylyl cyclases." Elife **11**.
- Mense, S. M. and L. Zhang (2006). "Heme: a versatile signaling molecule controlling the activities of diverse regulators ranging from transcription factors to MAP kinases." Cell Res **16**(8): 681-692.
- Middelhaufe, S., M. Leipelt, L. R. Levin, J. Buck and C. Steegborn (2012). "Identification of a haem domain in human soluble adenylate cyclase." Biosci Rep **32**(5): 491-499.
- Mukhopadhyay, T. K. and D. Trauner (2023). "Concise Synthesis of Glycerophospholipids." J Org Chem **88**(15): 11253-11257.
- Nakamura, J., N. Okamura, S. Usuki and S. Bannai (2001). "Inhibition of adenylyl cyclase activity in brain membrane fractions by arachidonic acid and related unsaturated fatty acids." Arch Biochem Biophys **389**(1): 68-76.
- Okumura, S., J. Kawabe, A. Yatani, G. Takagi, M. C. Lee, C. Hong, J. Liu, I. Takagi, J. Sadoshima, D. E. Vatner, S. F. Vatner and Y. Ishikawa (2003). "Type 5 adenylyl cyclase disruption alters not only sympathetic but also parasympathetic and calcium-mediated cardiac regulation." Circ Res **93**(4): 364-371.
- Orly, J. and M. Schramm (1975). "Fatty acids as modulators of membrane functions: catecholamine-activated adenylate cyclase of the turkey erythrocyte." Proc Natl Acad Sci U S A **72**(9): 3433-3437.
- Ostrom, K. F., J. E. LaVigne, T. F. Brust, R. Seifert, C. W. Dessauer, V. J. Watts and R. S. Ostrom (2022). "Physiological roles of mammalian transmembrane adenylyl cyclase isoforms." Physiol Rev **102**(2): 815-857.
- Paccani, S. R., F. Finetti, M. Davi, L. Patrussi, M. M. D'Elisio, D. Ladant and C. T. Baldari (2011). "The Bordetella pertussis adenylate cyclase toxin binds to T cells via LFA-1 and induces its disengagement from the immune synapse." J Exp Med **208**(6): 1317-1330.
- Pei, J. and N. V. Grishin (2001). "GGDEF domain is homologous to adenylyl cyclase." Proteins **42**(2): 210-216.
- Pierce, K. L., R. T. Premont and R. J. Lefkowitz (2002). "Seven-transmembrane receptors." Nat Rev Mol Cell Biol **3**(9): 639-650.
- Post, S. R., H. K. Hammond and P. A. Insel (1999). "Beta-adrenergic receptors and receptor signaling in heart failure." Annu Rev Pharmacol Toxicol **39**: 343-360.
- Qi, C., S. Sorrentino, O. Medalia and V. M. Korkhov (2019). "The structure of a membrane adenylyl cyclase bound to an activated stimulatory G protein." Science **364**(6438): 389-394.
- Rogel, A., J. E. Schultz, R. M. Brownlie, J. G. Coote, R. Parton and E. Hanski (1989). "Bordetella pertussis adenylate cyclase: purification and characterization of the toxic form of the enzyme." EMBO J **8**(9): 2755-2760.
- Sadana, R. and C. W. Dessauer (2009). "Physiological roles for G protein-regulated adenylyl cyclase isoforms: insights from knockout and overexpression studies." Neurosignals **17**(1): 5-22.

- Scherma, M., P. Masia, V. Satta, W. Fratta, P. Fadda and G. Tanda (2019). "Brain activity of anandamide: a rewarding bliss?" Acta Pharmacol Sin **40**(3): 309-323.
- Schultz, J. E. (2022). "The evolutionary conservation of eukaryotic membrane-bound adenylyl cyclase isoforms." Front Pharmacol **13**: 1009797.
- Seebacher, T., J. U. Linder and J. E. Schultz (2001). "An isoform-specific interaction of the membrane anchors affects mammalian adenylyl cyclase type V activity." Eur J Biochem **268**(1): 105-110.
- Seth, A., M. Finkbeiner, J. Grischin and J. E. Schultz (2020). "G $\alpha$  stimulation of mammalian adenylate cyclases regulated by their hexahelical membrane anchors." Cell Signal **68**: 109538.
- Sunahara, R. K., C. W. Dessauer, R. E. Whisnant, C. Kleuss and A. G. Gilman (1997). "Interaction of G $\alpha$  with the cytosolic domains of mammalian adenylyl cyclase." J Biol Chem **272**(35): 22265-22271.
- Sutherland, E. W. and T. W. Rall (1958). "Fractionation and characterization of a cyclic adenine ribonucleotide formed by tissue particles." J Biol Chem **232**(2): 1077-1091.
- Syrovatkina, V., K. O. Alegre, R. Dey and X. Y. Huang (2016). "Regulation, Signaling, and Physiological Functions of G-Proteins." J Mol Biol **428**(19): 3850-3868.
- Tang, W. J. and A. G. Gilman (1995). "Construction of a soluble adenylyl cyclase activated by G $\alpha$  and forskolin." Science **268**(5218): 1769-1772.
- Taylor, C. W. (1990). "The role of G proteins in transmembrane signalling." Biochem J **272**(1): 1-13.
- Tesmer, J. J. and S. R. Sprang (1998). "The structure, catalytic mechanism and regulation of adenylyl cyclase." Curr Opin Struct Biol **8**: 713-719.
- Vogel, Z., J. Barg, R. Levy, D. Saya, E. Heldman and R. Mechoulam (1993). "Anandamide, a brain endogenous compound, interacts specifically with cannabinoid receptors and inhibits adenylate cyclase." J Neurochem **61**(1): 352-355.
- Walsh, D. A., J. P. Perkins and E. G. Krebs (1968). "An adenosine 3',5'-monophosphate-dependant protein kinase from rabbit skeletal muscle." J Biol Chem **243**(13): 3763-3765.
- Yen, Y.-C., Y. Li, C.-L. Chen, T. Klose, V. J. Watts, C. W. Dessauer and J. J. G. Tesmer (2024). "Structure of adenylyl cyclase 5 in complex with G $\beta\gamma$  offers insights into ADCY5-related dyskinesia." Nature Structural & Molecular Biology.
- Ziegler, M., J. Bassler, S. Beltz, A. Schultz, A. N. Lupas and J. E. Schultz (2017). "Characterization of a novel signal transducer element intrinsic to class IIIa/b adenylate cyclases and guanylate cyclases." FEBS J **284**(8): 1204-1217.